Quantitative Imaging Biomarkers in the Assessment of Patients with Pulmonary Hypertension:

The Role of Computed Tomography (CT) and Magnetic Resonance Imaging (MRI)

Dr Sobitha Sathianandan MBBS Bsc MRCP

National Heart and Lung Institute, Imperial College London

Thesis submitted for the Degree of Doctor of Medicine by Research [MD(Res)]

Submitted June 2022

Statement of Originality

I confirm that the content of this thesis is the product of my own work and that any assistance received has been acknowledged and other sources referenced.

Copyright Declaration

The copyright of this thesis rests with the author. Unless otherwise indicated, its contents are licensed under a Creative Commons Attribution-Non-Commercial 4.0 International Licence (CC BY-NC). Under this licence, you may copy and redistribute the material in any medium or format. You may also create and distribute modified versions of the work. This is on the condition that: you credit the author and do not use it, or any derivative works, for a commercial purpose. When reusing or sharing this work, ensure you make the licence terms clear to others by naming the licence and linking to the licence text. Where a work has been adapted, you should indicate that the work has been changed and describe those changes. Please seek permission from the copyright holder for uses of this work that are not included in this licence or permitted under UK Copyright Law.

Acknowledgements

Firstly, I would like to thank my supervisors: Dr. John. Wort, Prof. Simon. Padley and Dr. Laura. Price for their guidance throughout this process. In addition, Dr. Tom. Semple, for his time, invaluable input and essentially being an additional supervisor. I would also like to thank Dr. Kostas. Dimopoulos for his help with Chapter 4 and giving me a better grasp of statistics and Dr. Heba. Neshat for her help with this chapter too. To my fellow Clinical Research Fellow, Dr. Bhavin. Rawal, thank you for taking the time to perform some of the CT measurements in this project and providing me with company and moral support during the research period. I would also like to thank Dr. Mike. Wilde, my clinical supervisor whilst working as a Clinical Research Fellow, for introducing this opportunity and his support.

I am grateful to the extended Pulmonary Hypertension Team at the Royal Brompton Hospital for welcoming me during my time there, educating me in various aspects of pulmonary hypertension and helping with the logistics of this research project. Also, the MRI team at Wimpole Street (particularly Sergio, James, Dan, and Valerie) for their time and expertise in enabling the research MRI studies and the Bioxydyn team for their collaboration in the postprocessing of the scans and helping me make sense of the results (Prof. Geoff. Parker, Dr. Marta. Tibiletti and Dr. Jo. Naish).

I am indebted to and humbled by the selflessness of the patients who agreed to take part in the prospective study whilst facing a new and life-changing diagnosis. The best part of the research process was undoubtedly getting to know you all and the privilege of hearing your personal and medical journeys whilst travelling to and from the research scans.

Finally, my family. To my parents, thank you for your sacrifices so we could have opportunities. Dad, your words of encouragement still drive me and Mum, it's your ongoing support that makes everything possible. Also, to my sisters for being there throughout, my husband for his enduring patience and love and to my daughter, I'm sorry for all the missed bedtimes and playtimes, thank you for your understanding and unconditional love.

Abstract

The use of computed tomography (CT) and magnetic resonance imaging (MRI) in pulmonary hypertension (PH) is expanding and already plays an important role in its diagnosis, classification, and prognostication. With recent advances in CT and MRI, there is growing interest in quantitative, imaging-based biomarkers that can be used in the evaluation of pulmonary hypertension (PH).

This thesis seeks to examine the role of existing and novel CT and MRI derived imaging biomarkers in the assessment of disease severity, treatment response and prognosis in patients with PH.

CT is readily available in clinical practice and allows assessment of the pulmonary vasculature alongside the parenchyma, cardiac and mediastinal structures. The role of CT in two groups of PH patients was retrospectively analysed. In Chapter 3, CT derived measurements in a cohort of patients with severe group 3 PH (due to lung diseases and/or hypoxia) treated with sildenafil did not relate to disease severity or treatment response. In Chapter 4, CT based measurements of pulmonary artery morphology and calcification in a cohort of patients with Eisenmenger Syndrome appeared to reflect the chronicity of PH in these patients as opposed to its severity.

The pathophysiology of PH primarily involves vascular remodelling of the smaller pulmonary arterioles with progressive resistance to blood flow and subsequent increase in pulmonary vascular resistance, mean pulmonary arterial pressure and right ventricular afterload(1). Imaging of these more distal pulmonary arterioles may therefore provide a more sensitive measure of PH severity and treatment response as they are also the site of action of available treatment options.

In Chapter 5, a pilot study of a novel MRI technique (Oxygen-Enhanced MRI) in a cohort of patients with pulmonary arterial hypertension and chronic thromboembolic pulmonary hypertension showed it is feasible, can demonstrate abnormalities related to gas exchange in PH and detect changes following treatment.

Table of Contents

Statement of Originality and Copyright Declaration 2

Acknowledgements 3

Abstract 4

Table of Contents 5

List of Figures 8

List of Tables 11

Abbreviations 14

Chapter 1: Introduction 19

1.1 Pulmonary Circulation and Gas Exchange *19*

1.2 Pulmonary Hypertension *22*

1.3 The Role of Imaging in PH *44*

1.4 Novel Quantitative MRI Measures in PH *53*

1.5 Hypothesis, Aims and Objectives *57*

Chapter 2: Methods 58

2.1 Background *58*

2.2 Chapters 3 and 4: Retrospective CT based studies *58*

2.3 Chapter 5: Oxygen-Enhanced MRI *64*

2.4 Other investigations and recorded variables *68*

2.5 Statistical analysis *70*

Chapter 3: Quantitative CT findings in group 3 pulmonary hypertension treated with Sildenafil 72

3.1 Introduction *72*

3.2 Study Rationale *85*

3.3 Hypothesis, Aims and Objectives *86*

3.4 Methods *87*

3.5 Results *89*

3.6 Discussion *99*

3.7 Conclusion *101*

Chapter 4: Pulmonary artery morphology and calcification on Computed Tomography in Eisenmenger Syndrome 102

4.1 Introduction *102*

4.2 Study Rationale *106*

4.3 Hypothesis, Aims and Objectives *107*

4.4 Methods *107*

4.5 Results *108*

4.6 Discussion *114*

4.7 Conclusion *116*

Chapter 5: A novel quantitative MRI derived biomarker: Dynamic Oxygen Enhanced MRI. Is there a role for it in the assessment of Pulmonary Hypertension? 117

5.1 Introduction *117*

5.2 Study Rationale *119*

5.3 Hypothesis, Aims and Objectives *119*

5.4 Methods *120*

5.5 Results *121*

5.6 Discussion *134*

5.7 Conclusion *138*

Chapter 6: Final Discussion and Conclusion 139

6.1 Discussion *139*

6.2 Conclusion *143*

Bibliography 144

Appendices 164

i. Participant Information Sheet 164

ii. Informed Consent Form 169

iii. Patient Experience Questionnaire 170

List of Figures:

Chapter 1: Introduction

1.1 A schematic of the pulmonary circulation and systolic pressures within it. 22

1.2 Pathophysiology and progression of pulmonary arterial hypertension. 31

Chapter 2: Methods

2.1 Measurement of the PA and aortic diameter to calculate PA:Ao ratio. 60

2.2 Measurement of pulmonary trunk volume. 61

2.3 Pulmonary artery in-situ thrombus and calcification. 62

2.4 Quantification of pulmonary artery calcification using a modified Agatston score on Terarecon iNtuition browser and software. 63

2.5 Volume rendered tomogram from a patient with Eisenmenger Syndrome. 64

2.6 Measuring RV and LV diameter to calculate RV:LV ratio. 65

2.7 Schematic of Study Design. 67

Chapter 3: Quantitative CT findings in group 3 pulmonary hypertension treated with Sildenafil

3.1 Pathogenesis of pulmonary hypertension in chronic obstructive pulmonary disease. 75

3.2 Features favouring a pulmonary arterial hypertension versus group 3 pulmonary hypertension phenotype based on physiological testing and computed tomography morphology. 87

3.3 Underlying Chronic Lung Disease Diagnosis. 92

3.4 Boxplot of change in 6-minute walk distance following treatment with Sildenafil. 94

3.5 Boxplot of baseline % predicted FEV1 and FVC in responders (n=4) vs non-responders (n=20) by World Health Organisation functional class criteria. 98

Chapter 4: Pulmonary artery morphology and calcification on Computed Tomography in Eisenmenger Syndrome

4.1 Mechanisms involved in the development of Eisenmenger Syndrome. 103

4.2 Trans-axial CT sections demonstrating PA dilatation, intra-mural calcification, and calcified in-situ thrombus. 106

4.3 Scatter plots to show correlation of age with PA diameter and trunk volume. 110

4.4 Scatter plot showing correlation of age with distance from pulmonary bifurcation to most distal pulmonary artery calcification. 113

4.5 Scatter plots to show degree of agreement in measurement of pulmonary artery trunk volume and distance from pulmonary bifurcation to the most distal calcification between 2 independent reviewers. 114

Chapter 5: A novel quantitative MRI derived biomarker: Dynamic Oxygen Enhanced MRI. Is there a role for it in the assessment of Pulmonary Hypertension?

5.1 Classification of patient's pulmonary hypertension diagnosis. 123

5.2 Haemodynamic measurements at right heart catheterisation pre and post treatment. 124

5.3 Enhancement fraction (EF) maps for a normal subject, patient with IPAH and CTEPH. 126

5.4 Scatter plot of age and EF. 126

5.5 Baseline parameter maps for T1, ΔPO2 and WIT in a normal subject, patient with IPAH and CTEPH. 127

5.6 Parameter maps from a participant with CTEPH. 128

5.7 Dynamic Oxygen Enhanced - MRI parameter maps for a patient with chronic thromboembolic pulmonary hypertension at baseline and post-treatment. 132

5.8 Overall patient experience of study MRI scan. 134

5.9 Interval at which patients would be happy to have scan repeated. 135

List of Tables:

Chapter 1: Introduction

1.1 Haemodynamic definitions of PH. 24

1.2 Clinical classification of Pulmonary Hypertension from the 6th World Symposium on Pulmonary Hypertension 2018. 26

1.3 Classification of genes linked to pulmonary arterial hypertension by level of evidence that they play a causal role in the development of the disease. 32

1.4 Echocardiographic probability of pulmonary hypertension based on tricuspid regurgitation velocity. 37

1.5 Echocardiographic signs suggestive of pulmonary hypertension used in addition to tricuspid regurgitation velocity measurement to assess probability of pulmonary hypertension. 38

1.6 Risk stratification in pulmonary arterial hypertension. 45

1.7 MRI derived predictors of mortality and treatment failure. 54

Chapter 2: Methods

2.1 Eligibility criteria. 66

2.2 Summary of statistical tests used. 72

Chapter 3: Quantitative CT findings in group 3 pulmonary hypertension treated with Sildenafil

3.1 Features of an exhausted circulatory versus ventilatory reserve. 79

3.2 Current and proposed haemodynamic definitions of group 3 Pulmonary Hypertension. 80

3.3 Randomised controlled trials with sildenafil in lung disease. 82

3.4 Eligibility Criteria. 89

3.5 Baseline patient demographics. 91

3.6 Baseline CT characteristics. 92

3.7 Change in haemodynamics at right heart catheterisation following treatment with sildenafil. 93

3.8 Spearman's rank correlation of baseline CT and RHC variables. 94

3.9 Pre versus post-treatment CT measurements. 95

3.10 Comparison of baseline variables in responders (Meeting ≥ 1 of criteria) versus non-responders. 96

3.11 Breakdown of criteria met by responders to treatment with sildenafil. 97

3.12 Comparison of baseline variables in responders versus non-responders to sildenafil treatment by WHO functional class criteria. 97

3.13 Comparison of baseline CT measurements in responders versus non-responders based on meeting ≥ 1 response criteria. 99

Chapter 4: Pulmonary artery morphology and calcification on Computed Tomography in Eisenmenger Syndrome

4.1 Summary of Patient Demographics. 109

4.2 Spearman's rank correlation of age with measures of PA dilatation. 110

4.3 Comparison of patient demographics in those with PA calcification and those without. 111

4.4 Spearman's rank correlation of age with measures of PA calcification. 112

4.5 Intraclass correlation coefficient to assess reliability of novel CT measurements. 114

Chapter 5: A novel quantitative MRI derived biomarker: Dynamic Oxygen Enhanced MRI. Is there a role for it in the assessment of Pulmonary Hypertension?

5.1 Baseline patient demographics and clinical information. 122

5.2 Comparison of baseline Oxygen Enhanced - MRI measurements in patients with group 1 and 4 PH. 129

5.3 Spearman's rank correlation coefficients between dynamic OE-MRI imaging parameters and standard clinical measurements. 130

5.4 Comparison of baseline and post-treatment dynamic Oxygen Enhanced - MRI parameters. 131

List of Abbreviations:

ACHD	Adult congenital heart disease
ASD	Atrial septal defect
AVSD	Atrio-ventricular septal defect
BMPR2	Bone morphogenetic receptor 2
BNP	Brain natriuretic protein
cGMP	Cyclic guanosine monophosphate
CHD	Congenital heart disease
CI	Confidence interval
CLD	Chronic lung disease
CMR	Cardiac magnetic resonance imaging
CO	Cardiac output
COPD	Chronic obstructive pulmonary disease
CPET	Cardiopulmonary exercise testing
CPFE	Combined pulmonary fibrosis and emphysema
CT	Computed tomography
CTPA	Computed tomography pulmonary angiogram
CTD	Connective tissue disease
CTD-PAH	PAH associated with CTD
CTEPH	Chronic thromboembolic pulmonary hypertension
DCE-MRI	Dynamic contrast enhanced magnetic resonance imaging
DECT	Dual energy computed tomography

DL	Total lung diffusing capacity
DLCO	Diffusing capacity of the lung for carbon monoxide
D_m	Alveolar – capillary membrane diffusing capacity
DPG	Diastolic pressure gradient
EDV	End diastolic volume
EF	Enhancement fraction
ERA	Endothelin receptor antagonist
ERS	European Respiratory Society
ES	Eisenmenger syndrome
ESC	European Society of Cardiology
E-10	Emphasis 10
FAC	Fractional area change
FD-MRI	Fourier decomposition magnetic resonance imaging
FEV1	Forced expiratory volume in 1 second
FVC	Forced vital capacity
GOLD	Global initiative for chronic obstructive lung disease
HR	Hazards ratio
HRCT	High resolution computed tomography
ICC	Intraclass correlation coefficient
IIP	Idiopathic interstitial pneumonia
ILD	Interstitial lung disease
IPAH	Idiopathic pulmonary arterial hypertension
IPF	Idiopathic pulmonary fibrosis

IQR	Interquartile range
IR-HASTE	Inverse recovery half fourier acquisition turbospin echo
KCO	Carbon monoxide transfer co-efficient
LAA%	Low attenuation area percent
LAM	Lymphangioleiomyomatosis
LCH	Langerhan's cell histiocytosis
LTOT	Long term oxygen therapy
mPAP	Mean pulmonary arterial pressure
MRI	Magnetic resonance imaging
NO	Nitric oxide
OE-MRI	Oxygen enhanced magnetic resonance imaging
OHS	Obesity hypoventilation syndrome
OR	Odds ratio
OSA	Obstructive sleep apnoea
PA	Pulmonary artery
PAP	Pulmonary artery pressure
PA: Ao	Main pulmonary artery to aorta ratio
PAH	Pulmonary arterial hypertension
PaO_2	Partial pressure of oxygen
PAWP	Pulmonary arterial wedge pressure
PCWP	Pulmonary capillary wedge pressure
PBV	Perfused blood volume
PDE5i	Phosphodiesterase 5 inhibitor

PE	Pulmonary embolus
PFTs	Pulmonary function tests
PH	Pulmonary hypertension
PO_2	Partial pressure oxygen
PVOD	Pulmonary veno-occlusive disease
PVR	Pulmonary vascular resistance
Q_p/Q_s	Ratio of pulmonary blood flow to total systemic blood flow
RA	Right atrium
RAA	Right atrial area
RAP	Right atrial pressure
RBH	Royal Brompton Hospital
RCT	Randomised controlled trial
RHC	Right heart catheterisation
RV	Right ventricle
RV EF	Right ventricular ejection fraction
RVSP	Right ventricular systolic pressure
RV:LV	Right ventricle to left ventricle ratio
RVOT	Right ventricular outflow tract
SSc	Systemic sclerosis
TAPSE	Trans-annular plane systolic excursion
TGF	Transforming growth factor
TI	Inversion time
T1	Longitudinal relaxation time

TLCO	Transfer factor for carbon monoxide
TRV	Tricuspid regurgitation velocity
ufbSSFP	Ultrafast balanced steady state free procession
V_c	Pulmonary alveolar capillary blood volume available for gas transfer
VE/VCO_2	Ventilatory equivalent for carbon dioxide
VO_2	Oxygen consumption
V/Q	Ventilation/Perfusion
V/Q SPECT	Ventilation/Perfusion single photon emission tomography
VSD	Ventricular septal defect
WHO	World Health Organisation
WIT	Wash in time
WSPH	World symposium on pulmonary hypertension
WU	Wood units
6MWD	Six-minute walk distance
%CSA<5	Percentage of total cross-sectional area of vessels <5mm^2 normalised by lung area
ΔPO_2	Oxygen enhancement as change in partial pressure of oxygen

Chapter 1: Introduction

1.1 Pulmonary Circulation and Gas Exchange

1.1.1 Normal Pulmonary Circulation

The primary role of the pulmonary circulation is gas exchange. It achieves this through delivery of deoxygenated blood from the right ventricle to the alveolar gas exchange surfaces. The structure of the normal pulmonary vasculature is designed to ensure a high compliance, low resistance network that provides a large surface area for gas exchange (2). The pulmonary circulation can accommodate the entire cardiac output (CO) of 4-6L per minute, maintaining high blood flow at low intravascular arterial pressure to prevent alveolar damage and pulmonary oedema (1,3–6).

Pulmonary vascular resistance (PVR) is approximately one tenth that of the systemic circulation (≤3 wood units in healthy subjects) and the pulmonary arteries are the site of the greatest contribution to resistance despite having thinner walls with less vascular smooth muscle and reduced basal tone (secondary to a high level of endogenous vasodilators and low production of vasoconstrictors) compared to systemic arteries (4,6).

Intravascular pressure in the pulmonary circulation is also much lower with a mean pulmonary arterial pressure (mPAP) of approximately 15-20mmHg (6,7).

The relationship between these haemodynamic parameters is expressed by the following equation (where PAWP [pulmonary arterial wedge pressure] is an indirect measure of left atrial pressure at right heart catheterisation):

PVR = (mPAP-PAWP)/CO

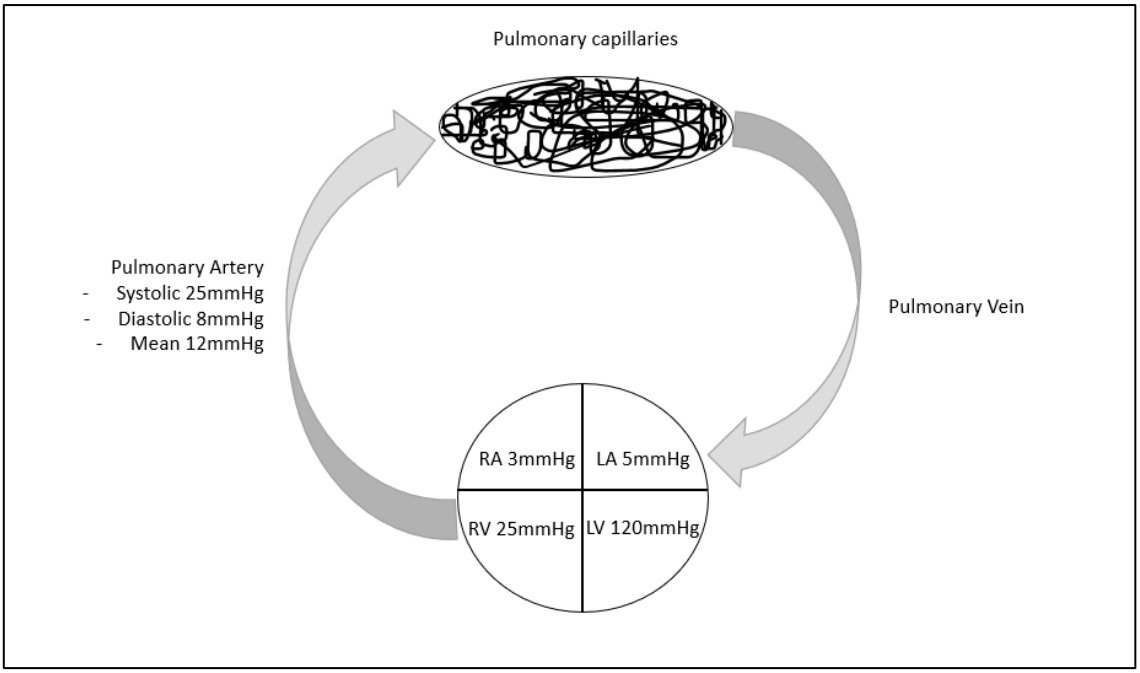


Figure 1.1: A schematic of the pulmonary circulation and systolic pressures within it. [RA: right atrium, LA: left atrium, RV: right ventricle, LV: left ventricle].

1.1.2 Gas Exchange

The main processes involved in gas exchange are:

1. Ventilation
2. Diffusion
3. Perfusion

Gas exchange was conventionally thought to occur in the pulmonary capillaries. However, pre-capillary gas exchange has been clearly documented (8–10) with studies showing that oxygenation begins in pre-capillary arterioles with oxygen saturation levels increasing exponentially with decreasing vessel diameter and up to 50% of total oxygen uptake occurring before red cells enter the alveolar capillaries (11).

Gas transfer across the alveolar capillary membrane is determined according to (Fick's) laws of diffusion:

Rate of diffusion $\propto$ [surface area x concentration difference]/ thickness of membrane.

In pulmonary diseases, alterations in the ventilation and perfusion ratio and impaired oxygen diffusion from the alveoli can occur secondary to a range of pathophysiology.

1.1.3 The Pulmonary Arteries

The main pulmonary artery divides into the right and left main branches which further divide to supply each lobe before entering the lung. Within the lung, each lobar artery subdivides into branches corresponding to the bronchial tree and culminates in arterioles and capillaries that cover 85-90% of the alveolar surface (12). At this level, an extremely thin membrane of 1 µm separates the alveolar gas and blood compartments allowing gases to diffuse efficiently between them (13,14). The close proximity of the pulmonary arteries and airways underscores the relationship between ventilation and perfusion that defines the normal function of the lung (4).

The large pulmonary arteries are classified as elastic, with the media comprised mainly of elastic fibres and some smooth muscle. As vascular diameter decreases, these elastic arteries give rise to vessels with increased smooth muscle content. However, the walls are still thinner than their systemic counterparts. The pulmonary arterial wall also comprises collagen and advential fibroblasts, a longitudinal elastic lamina (which allows for expansion during inspiration) and an intima composed of endothelial cells (4).

Whereas systemic arteries dilate in response to hypoxia, the pulmonary vessels demonstrate vasoconstriction. This acute response is the lung's intrinsic mechanism for matching perfusion to ventilation and optimising systemic oxygen delivery (15). To an extent, even sustained hypoxic pulmonary vasoconstriction is reversible on returning to normal oxygen concentrations (4). However, if hypoxia is maintained over a prolonged period as occurs in chronic lung disease, the vasoconstriction can be followed by remodelling of the vasculature and leads to an increase in PVR and mPAP (15).

1.2 Pulmonary Hypertension

1.2.1 Definition and Classification

Pulmonary hypertension (PH) was initially defined following the first World Symposium on Pulmonary Hypertension (WSPH) in 1973 as a mean pulmonary arterial pressure (mPAP) ≥ 25mmHg at rest, measured on right heart catheterisation (RHC) (16). PH is further defined as pre or post capillary depending on the pulmonary arterial wedge pressure (PAWP) measured at RHC. Table 1.1 summarises the different haemodynamic definitions of PH and the clinical groups which fall within them.

Definitions	Characteristics	Clinical Groups

Table 1.1: Haemodynamic definitions of PH (17). [mPAP: mean pulmonary arterial pressure, PAWP: pulmonary arterial wedge pressure, DPG: diastolic pressure gradient, PVR: pulmonary vascular resistance, WU: wood units].

Analysis of RHC studies in healthy individuals has shown a normal mPAP at rest of 14.0±3.3mmHg; two standard deviations above this would suggest mPAP > 20mmHg as above the upper limit of normal (7). The clinical significance of a mPAP between 20 and 25mmHg remains unclear.

Following the 6th WSPH in 2018, recommendations have been made that the definition of PH should expand to include pulmonary vascular resistance (PVR) of ≥ 3 wood units (WU) in the presence of a mPAP > 20mmHg (18). It was felt that this definition used a more evidence-based cut-off for mPAP and the inclusion of the PVR criteria would help select pulmonary vascular disease (secondary to intrinsic structural changes of the pulmonary arteries) as

opposed to raised mPAP secondary to increased cardiac output (CO) or raised PAWP and left heart disease (post capillary PH).

The new proposed definition of pre-capillary PH would therefore be “concomitant presence of mPAP >20 mmHg, PAWP ≤ 15 mmHg and PVR ≥3 WU” (18). The European Society of Cardiology/European Respiratory Society guidelines used in clinical practice have not yet changed to encompass the new definition and prospective trials are required to evaluate treatment options in this group.

PH is clinically classified into five groups encompassing conditions with similar clinical, pathological, haemodynamic characteristics and treatment strategies (Table 1.2) (19). The research studies within this thesis relate to patients within Group 1, 3 and 4 PH which are discussed in more detail below.

Idiopathic **Heritable** **Drugs and toxins induced** **Associated with:** • **Connective tissue disease** • **Human immunodeficiency virus infection** • **Portal hypertension** • **Congenital heart disease** • **Schistosomiasis** **PAH long term responders to calcium channel blockers** **PAH with overt features of venous/capillaries involvement** **[Pulmonary veno-occlusive disease and/or pulmonary capillary haemangiomatosis]** **Persistent PH of the new born syndrome**
PH due to heart failure with preserved LVEF **PH due to heart failure with reduced LVEF** **Valvular heart disease disease** **Congenital/acquired cardiovascular conditions leading to post-capillary PH**
Obstructive lung disease **Restrictive lung disease** **Other lung disease with mixed restrictive and obstructive pattern** **Hypoxia without lung disease** **Developmental lung disorders**
Chronic thromboembolic pulmonary hypertension **Other pulmonary artery obstructions**
Haematological disorders **Systemic disorders and metabolic disorders** **Others** **Complex congenital heart disease**

Table 1.2: Clinical classification of Pulmonary Hypertension from the 6th World Symposium on Pulmonary Hypertension 2018 (18). [PAH: pulmonary arterial hypertension, PH: pulmonary hypertension, LVEF: left ventricular ejection fraction].

1.2.2 Group 1 – Pulmonary arterial hypertension

Pulmonary arterial hypertension (PAH), Group 1, describes a group of PH patients characterised haemodynamically at RHC by the presence of pre-capillary PH [mPAP ≥ 25mmHg, PAWP ≤ 15mmHg and a PVR > 3 WU] in the absence of other causes of pre-capillary PH such as lung disease and chronic thromboembolic pulmonary hypertension (CTEPH) (17).

Within this group lie the idiopathic form of PAH, PAH associated with connective tissue disease and congenital heart disease. These are the patient groups that have been studied in Chapters 4 and 5 of this thesis.

1.2.2.1 Idiopathic pulmonary arterial hypertension (IPAH)

IPAH is a disease in which there is no family history or identified risk factor for PAH. Data from the National Audit of Pulmonary Hypertension (20,21) show the median age at diagnosis for IPAH is 60 years old with a female preponderance (65% females).

1.2.2.2 Pulmonary arterial hypertension associated with connective tissue disease (CTD-PAH)

PAH is a well-known complication of connective tissue disease (CTD), with the limited variant of systemic sclerosis(SSc) being the most commonly associated with PAH in Europe and the USA(17). The prevalence of haemodynamically proven pre-capillary PH in large cohorts of SSc patients ranges from 5 to 12% (17). PAH is also reported in mixed CTD, systemic lupus erythematosus and more rarely in Sjogren syndrome, inflammatory idiopathic myopathies and rheumatoid arthritis (22).

CTD-PAH has a similar pathogenesis to IPAH. However, group 2-5 PH can also occur in CTD. For example, secondary to left heart involvement, interstitial lung disease, chronic thromboembolic disease and pulmonary vascular disease affecting the post capillary venules (pulmonary veno-occlusive disease) (23). Careful determination of the predominant mechanism is required to ensure appropriate treatment is given.

PAH is a leading cause of death in SSc and is associated with a worse prognosis than IPAH(24).

1.2.2.3 Pulmonary arterial hypertension associated with adult congenital heart disease

PAH associated with adult congenital heart disease (ACHD) represents a heterogenous group of patients and includes the following (17 25):

1. Eisenmenger's Syndrome (discussed further in Chapter 4)

2. PAH associated with prevalent systemic to pulmonary shunts (left to right shunt through a moderate defect)
3. PAH with small/coincidental defects (atrial septal defects < 2cm and ventricular septal defects <1cm)
4. PAH after defect correction

Congenital heart defects with a large intra or extra cardiac communication allow unrestricted pressure and volume overload of the pulmonary circulation which may result in a typical pulmonary obstructive arteriopathy identical to other forms of PAH (26)(27). The rate of progression of pulmonary arterial disease depends on the size and type of the defect.

1.2.2.4 Pathophysiology of PAH and Right Heart Failure

Whilst the subcategories of PAH differ in their underlying causes, they are all characterised by a combination of:

1. Endothelial dysfunction
2. Excessive pulmonary vasoconstriction
3. Abnormal vascular proliferation
4. Remodelling of endothelial and smooth muscle cells
5. In situ thrombosis (1,28).

These changes primarily affect the small pulmonary arterioles and lead to a loss of cross-sectional area, progressive resistance to blood flow with increased PVR, mPAP and right ventricular (RV) afterload(1).

The pulmonary endothelium is a source of both vasodilators and vasoconstrictors, the balance of which in normal conditions favours a low PVR. With endothelial dysfunction, release of nitric oxide and prostacyclin (vasodilators) is reduced whilst release of endothelin-1 and thromboxane (vasoconstrictors) is augmented causing a shift favouring vasoconstriction that leads to increased PVR(4). These vasoactive mediators are the targets of advanced PH drug therapy.

Endothelial dysfunction and injury can be triggered by a variety of environmental stimuli that arise in the setting of pulmonary hypertension, including: hypoxia, acidosis, oxygen centred free radicals, inflammatory mediators and increased shear forces associated with increased pulmonary blood flow(29).

Vascular remodelling involves endothelial cell proliferation, invasion of the intima by myofibroblast-like cells, enhanced matrix deposition with intimal fibrosis and obstruction of the vascular lumen by plexiform lesions (30). Vascular smooth muscle cell proliferation is also a prominent feature of PAH(31).

Some vasoconstrictors can exert a pro-proliferative action. For example, endothelin-1 stimulates smooth muscle cell proliferation via downstream signalling cascades involving endothelin type A and B receptors(32).

Several growth factors have been implicated in vascular remodelling and PAH. By binding to and activating cell surface tyrosine kinase receptors, growth factors are potent mitogens and chemo-attractants for smooth muscle cells, fibroblasts and endothelial cells, triggering intracellular signalling cascades that result in cellular proliferation, migration and resistance to apoptosis(31). The following growth factors are those most evidenced in PAH:

1. Vascular endothelial growth factor (VEGF) and VEGF receptor 2 (VEGFR-2) - expressed in the plexiform lesions of patients with PAH(33).
2. Basic fibroblast growth factor (bFGF) – alterations in plasma and urine levels of bFGF have been observed in patients with PAH(34).
3. Transforming growth factor alpha (TGFα) – pulmonary expression results in the development of pulmonary hypertension and vascular remodelling in mice(35).
4. TGF-β – this family of cytokine growth factors control many cellular functions; including proliferation, migration, differentiation, and extracellular matrix secretion and deposition (36).
5. Platelet-derived growth factor (PDGF) - acts as a potent mitogen and chemoattractant for smooth muscle cells(37) and pulmonary expression of the PDGF ligand and receptor is increased in patients with severe PAH and PDGF signalling is upregulated in the pulmonary arteries of patients with IPAH(38).

Inflammation plays an important role in PAH (39) and contributes to the formation of plexiform lesions (40). Monocytes, macrophages, T lymphocytes, and dendritic cells are found in plexiform and other vascular lesions of PAH-affected human lungs(41). Increased circulating levels of monocyte chemoattractant protein 1, tumour necrosis factor, IL-1β, and IL-6 have also been found in patients with IPAH(31,42).

Thrombosis is a common feature of PAH and research using calibrated automated thrombography has demonstrated a hypercoagulable phenotype in patients with IPAH (43). Increased levels of fibrinopeptide A (a marker of fibrin generation) and impaired fibrinolysis with increased levels of plasminogen activator inhibitor 1 are seen in IPAH (44), as well as increased activity of von Willebrand factor, which is essential for the interaction between platelets and endothelial cells(44). There may be an increase in platelet aggregation as a result of the imbalance in vasoactive mediators; with higher thromboxane A_2 (pro-aggregatory) levels in PAH and reduced nitric oxide and prostacyclin (which inhibit aggregation)(45).

1.2.2.5 The Right Ventricle (RV)

The RV is a thin-walled structure designed to pump blood through a low pressure and compliant pulmonary vascular system to allow efficient gas exchange to occur. Therefore, the RV is able to accept a large blood volume (pre-load) and pump blood against a low resistance (low afterload)(1).

The RV initially compensates for increased afterload (secondary to raised PVR) with an increase in hypertrophy and contractibility to increase cardiac output (CO) (46,47). With persistently raised PVR, progressive contractile dysfunction occurs, leading to decompensation, dilatation and right heart failure (48).

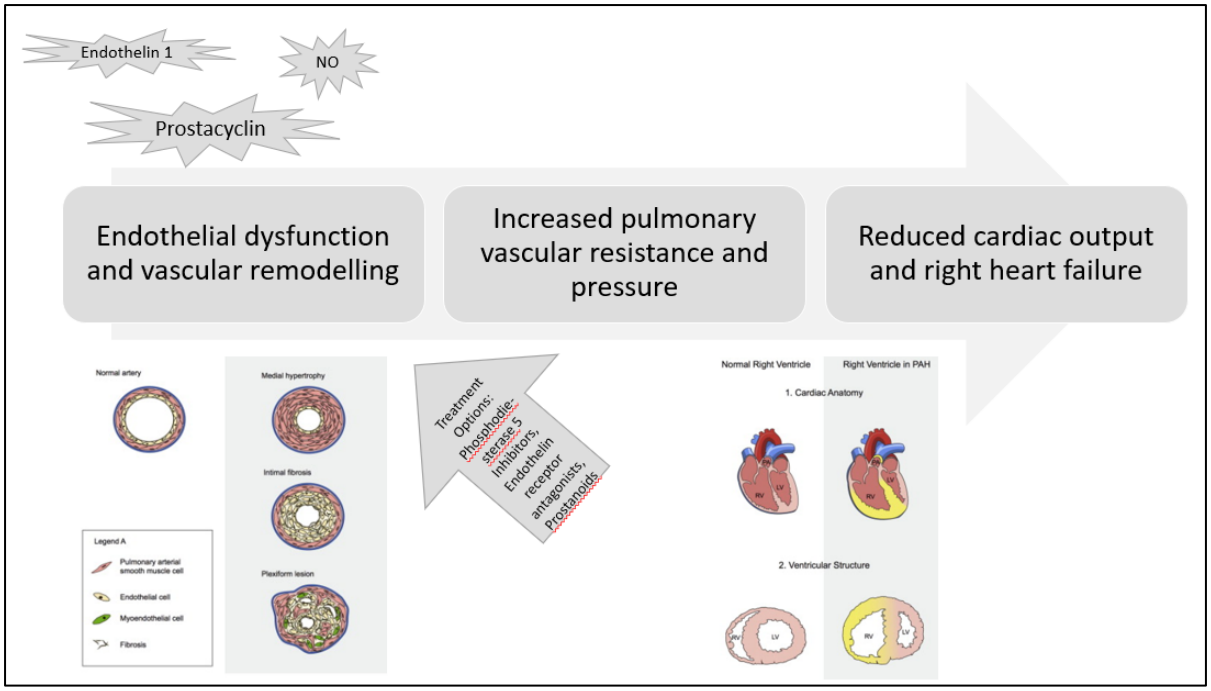


Figure 1.2: Pathophysiology and progression of pulmonary arterial hypertension – Pulmonary arteries undergo vasoconstriction, medial hypertrophy, intimal fibrosis, and inflammation in the adventitia leading to luminal obstruction and increased pulmonary vascular resistance and pulmonary artery pressure. Compensation by the right ventricle results in right ventricular hypertrophy, fibrosis, and remodelling. With decompensation there is reduced cardiac output and right heart failure. (Images reprinted from: Canadian Journal of Cardiology, volume 31, issue 4, Ryan et al, Right Ventricular Adaptation and Failure in Pulmonary Arterial Hypertension, pages 391-406, copyright year 2015, with permission from Elsevier (49)*). [NO: nitric oxide, PAH: pulmonary arterial hypertension, RV: right ventricle, LV: left ventricle].*

The response of the RV in PAH associated with ACHD (in particular, Eisenmenger syndrome) differs and the RV is better adapted to the high pressure through hypertrophy. So, where RV dysfunction is a major contributor to mortality in other patients with PAH, in PAH-ACHD the RV is able to sustain an elevated afterload over a much longer period of time(50).

1.2.2.6 Genetics

It is recognised that there is a genetic predisposition which in combination with other insults, such as oxidative and sheer stresses and inflammation, leads to the primary event of PA endothelial cell dysfunction(46). A mutation in the gene encoding bone morphogenetic protein receptor type 2 (BMPR2) has been identified as the most common predisposing genetic factor and is present in about 75% of familial PAH(51). It is also found in 25% of patients with IPAH(17). However penetrance is low with carriers having a 20% lifetime risk of developing PAH(47). Hereditary PAH may show genetic anticipation, with younger age of onset and death in subsequent generations(52).

144 BMPR2 mutations affecting multiple loci in the gene have been found in patients with PAH(53). BMPs are multifunctional regulators that modulate cell proliferation, differentiation, and apoptosis in different tissues(1). Loss of BMPR2 in pulmonary artery endothelial cells increases susceptibility of the endothelial cells to apoptosis, leading to endothelial dysfunction and the subsequent development of PAH(54).

Table 1.3 summarises the genes implicated in heritable PAH.

Higher level of evidence	Lower level of evidence

Table 1.3: Classification of genes linked to pulmonary arterial hypertension by level of evidence that they play a causal role in the development of the disease(55).

1.2.3 Group 3 – PH due to lung diseases and/or hypoxia

PH secondary to lung disease and chronic hypoxia is classified into Group 3 of the clinical classification. It is a frequent complication of chronic lung disease and is associated with reduced functional status, increased oxygen requirements, impaired quality of life and increased risk of mortality(56).

The most common lung diseases associated with PH are chronic obstructive pulmonary disease (COPD), interstitial lung disease (ILD) and combined pulmonary fibrosis and emphysema (CPFE)(17).

Group 3 PH is discussed in more detail in Chapter 3.

1.2.4 Group 4 – Chronic Thromboembolic Pulmonary Hypertension

Chronic thromboembolic pulmonary hypertension (CTEPH) occurs as a result of pulmonary artery (PA) remodelling following thromboembolism and has been reported with a cumulative incidence of 0.1–9.1% within the first 2 years after a symptomatic pulmonary embolus (PE) event(17). Studies suggest that most cases are identified within 2 years of the index event(57). However, in some cases, patients will not have been aware of previous PEs. Characteristic pathoanatomical findings are intimal irregularity, stenoses with ring, slit or web like forms and pouch defects, tapered vascular stenosis or complete occlusion caused by fibrotic intra-luminal material, occasionally with an overlying thrombus(58). These changes lead to vascular remodelling like that seen in PAH. Diagnosis is based on the following criteria(17), which should be obtained after at least 3 months of effective anticoagulation:

1. PH confirmed by RHC with mPAP ≥ 25mmHg and PAWP ≤ 15mmHg at rest.
2. Mismatch on ventilation/perfusion scintigraphy with at least one large perfusion defect in one segment or 2 sub-segments, or evidence of pulmonary vascular lesions on computed tomography, magnetic resonance imaging or pulmonary angiography.

Risk factors for the development of CTEPH include: signs of right heart strain at the time of initial PE, certain inherited hypercoagulable states (elevated factor VIII levels, factor V leiden mutation, lupus anticoagulant/antiphospholipid antibodies), prior splenectomy, hypothyroidism, inflammatory medical conditions, ventricular-atrial shunts and pacemakers(57).

1.2.5 Epidemiology

The prevalence of PH in the UK is estimated at 97 cases per million(17) with Group 2 and 3 being the most common causes. PH is found in 18-50% of patients assessed for transplantation or lung volume reduction surgery and in up to 83% of those with diastolic heart failure(47).

The prevalence and incidence of PAH in Europe are estimated to be 15-60 cases per million and 5-10 cases per million respectively(59). The prevalence is higher within certain patient groups such as those with systemic sclerosis (9%) and congenital heart disease (5-10%)(47). The incidence of CTEPH is estimated as 4 per 1 million adults(60).

1.2.6 Clinical Presentation of PH

There is often a delay in the diagnosis of PH as symptoms are non-specific. Symptoms are related to progressive RV dysfunction and are initially precipitated by exertion and include shortness of breath, fatigue, angina and syncope. These symptoms predominantly occur due to a failure to increase CO appropriately. Dry cough and exercise induced nausea and vomiting have also been described. Symptoms at rest suggest advanced disease and RV failure(17).

On examination, a left parasternal lift may be felt, and auscultation may reveal a loud pulmonary component of the second heart sound, a third heart sound, pan-systolic murmur of tricuspid regurgitation and diastolic murmur of pulmonary regurgitation. Elevation of the jugular venous pressure, hepatomegaly, ascites, peripheral oedema, and cool peripheries are late signs of PH.

Clinical examination may also suggest the underlying cause such as telangiectasia, digital ulceration and sclerodactyly in scleroderma.

Because dyspnoea is primarily caused by an inability to increase CO as opposed to impaired alveolar gas exchange, oxygen desaturation is often not seen till PAH is very advanced(1). However, in PAH associated with ACHD, cyanosis is often seen secondary to right-left shunting.

1.2.7 Diagnosis

The diagnosis and classification of PH involves a raft of investigations including biochemical markers, echocardiography, pulmonary functions tests, computed tomography (CT), ventilation/perfusion lung scans, cardiac magnetic resonance imaging (CMRI), cardiopulmonary exercise testing (CPET) and RHC. Invasive RHC remains the gold standard for diagnosis. The role of CT and MRI are discussed in more detail in Section 1.3 of this chapter.

1.2.7.1 Blood Tests

Blood tests are helpful in identification of the cause of PH, end organ damage associated with PH and in optimising and monitoring patient management. Biochemistry, haematology, and thyroid function tests are required in all patients. Iron studies, HIV and autoimmune screens are also carried out at diagnosis. Abnormal liver function tests may be a result of high hepatic venous pressure, liver disease and/or a side effect of therapy.

Up to 40% of patients with IPAH have elevated anti-nuclear antibodies in a low titre (1:80)(17). The patten and presence of certain anti-nuclear antibodies will help define connective tissue disease associated with PAH.

Patients with CTEPH should undergo thrombophilia screening, including antiphospholipid antibodies, anticardiolipin antibodies and lupus anticoagulant.

N-terminal pro-brain natriuretic peptide (NT-proBNP) may be elevated in patients with PH and is an independent risk predictor in these patients(17).

1.2.7.2 ECG

An abnormal ECG is more common in severe disease and ECG abnormalities include p pulmonale, right axis deviation, RV hypertrophy and right bundle branch block (17).

1.2.7.3 CXR

CXR may show pulmonary artery dilatation with 'pruning' of the peripheral blood vessels, right atrial (RA) and RV enlargement. Signs suggestive of the cause of PH may be evident such as lung disease or pulmonary venous congestion secondary to left heart disease.

1.2.7.4 Pulmonary function Tests (PFTs)

PFTs help to distinguish the underlying cause of PH. In PAH, there is generally preservation of spirometry, mild to moderate reduction of lung volumes related to disease severity, and a decreased diffusion capacity for carbon monoxide (DLCO). A DLCO of less than 45% is associated with a poor outcome(17).

In clinical practice, DLCO is used as a measure of the efficiency of gas transfer in the lung and measures the ability of the lungs to transfer gas from the alveolar space to the red blood cells in the pulmonary vessels(61). DLCO is described as a series of resistances: the diffusion of the gas across the alveolar-capillary membrane, the transfer into the plasma and across the red cell membrane, and the chemical reaction of the gas with haemoglobin(as summarised by the below equation)(62):

$$1/DL = 1/D_m + 1/\vartheta V_c$$

[DL = total lung diffusing capacity, D_m = alveolar-capillary membrane diffusing capacity, Vc = pulmonary alveolar capillary bed volume available for gas transfer, ϑ = rate of reaction of the gas with the red cell].

In PAH, both D_m and V_c have been shown to be reduced(63,64). The reduction in V_c is likely related to increased PVR, decreased CO and local thrombosis of the vascular bed and the reduced D_m secondary to an increase in alveolar capillary membrane thickness caused by the remodelling, fibrotic and proliferative changes seen in PAH(65). The relative contribution of reduced D_m and V_c to the lower DL seen in PAH is unclear with some studies attributing the impaired DL to a loss of D_m rather than V_c(65–67) and others showing a proportional reduction in both and an interdependence between D_m and V_c in PAH as any change in the vascular bed that reduces V_c would lead to a reduction in D_m through a loss of surface area available to gas exchange(65).

1.2.7.5 Echocardiography

Echocardiography is used as a screening tool for PH and to estimate the systolic PA pressure and effects of PH on the heart. However, when treatment of PH is considered, it alone is not sufficient to support a treatment decision.

The estimation of systolic PA pressure is based on the peak tricuspid regurgitation velocity (TRV) taking into account right atrial pressure (RAP) as described by the simplified Bernoulli equation(17).

The echocardiographic probability of PH was derived from data in normal adults and consolidated using the combination of TRV with other echocardiographic findings associated with PH (Tables 1.4 and 1.5)(17,68). A peak TRV of ≤2.8m/s with absence of any additional echocardiographic features suggests a low echocardiographic probability of PH and TRV > 3.4m/s suggests high probability regardless of other echocardiographic features.

Peak TRV (m/s)	Presence of other echocardiographic PH signs	Echocardiographic probability of PH
≤ 2.8 or not measurable	No	Low
≤ 2.8 or not measurable 2.9-3.4	Yes No	Intermediate
2.9-3.4 > 3.4	Yes Not required	High

Table 1.4: Echocardiographic probability of pulmonary hypertension based on tricuspid regurgitation velocity [from the ESC/ERS guidelines(17) *and recommendations of the 6th world symposium on pulmonary hypertension*(68)*]. (TRV: tricuspid regurgitation velocity, PH: pulmonary hypertension).*

The ventricles	Pulmonary artery	Inferior vena cava and right atrium
Right ventricle/left ventricle basal diameter ratio > 1.0	Right ventricular outflow doppler acceleration time < 105 msec and/or mid-systolic notching	Inferior vena cava diameter > 21mm with decreased inspiratory collapse
Flattening of the interventricular septum	Early diastolic pulmonary regurgitation velocity >2.2m/sec	Right atrial area (end-systole) > 18cm^2
	Pulmonary artery diameter >25mm	

Table 1.5: Echocardiographic signs suggestive of pulmonary hypertension used in addition to tricuspid regurgitation velocity measurement to assess probability of pulmonary hypertension [from the ESC/ERS guidelines(17) *and recommendations of the 6th world symposium on pulmonary hypertension*(68)*].*

1.2.7.6 Ventilation/Perfusion Single Photon Emission Tomography (V/Q SPECT)

A V/Q SPECT scan is predominantly used to look for CTEPH as it is more sensitive when compared with CT pulmonary angiogram (CTPA). A normal or low probability V/Q scan effectively excludes CTEPH with a sensitivity of 90-100% and specificity of 94-100%(17). In PAH, the scan may be normal or show small, peripheral unmatched and non-segmental perfusion defects(69).

1.2.7.7 Abdominal Ultrasound scan

Abdominal ultrasound scan may confirm portal hypertension but not formally exclude it. The use of contrast agents and addition of a colour doppler examination may improve diagnostic accuracy(17).

1.2.7.8 Cardiopulmonary Exercise Testing (CPET)

CPET can be useful in assessing patients with unexplained dyspnoea and evaluating the cardiopulmonary limitations and pulmonary vascular involvement in these patients. Hence aiding diagnosis of PH. Lower peak oxygen uptake, higher ratio of minute ventilation to carbon dioxide production and reduced end-tidal carbon dioxide tension obtained during CPET indicate an increasing likelihood of pulmonary vascular disease(70). CPET may also be considered to quantify the degree of exercise limitation and to estimate prognosis after diagnosis of PH(68). Measures of exercise capacity have been shown to predict survival and clinical outcome in patients with moderate to severe PAH(71).

1.2.7.9 Right Heart Catheterisation (RHC)

RHC is the gold-standard for diagnosis and classification of PH. It is required to confirm PAH and CTEPH prior to treatment, assess the haemodynamic severity and monitor treatment response/disease progression.

A balloon tipped PA catheter is passed from a peripheral vein through the RA and RV into the PA. Measurements are taken in the RA, RV and PA. The catheter is advanced until the balloon tip occludes or wedges into a small PA. In this position, the catheter can measure the reflected pressure coming backward from the end-diastolic left ventricular pressure, the left atrium, through the pulmonary veins and capillaries to the PA. This is termed the PAWP(1).

CO is measured using thermodilution or the direct Fick method. Thermodilution is the preferred method as it can provide reliable measurements even in patients with low CO and/or severe tricuspid regurgitation. However, it may be inaccurate in patients with intra-cardiac shunts. The direct Fick method requires direct measurement of oxygen uptake, a technique that is not widely available. The indirect Fick method uses estimated values of oxygen uptake and is acceptable but less reliable(17).

PVR and transpulmonary pressure gradient are derived variables calculated from RHC measurements.

Patients with suspected IPAH, hereditary PAH or drug-induced PAH undergo vasoreactivity testing with administration of inhaled nitric oxide or intravenous epoprostenol during RHC. A positive response is defined as a reduction of the mPAP by ≥ 10 mmHg to an absolute value of ≤ 40 mmHg (without a fall in CO) (17) and is seen in up to 10% of patients (72). These patients often respond well to treatment with high dose calcium channel blockers.

1.2.8 Treatment

Treatment of PH can be divided into general, supportive measures that are common to all groups and specific vasodilator therapy which is only recommended in groups 1, 4 and 5.

1.2.8.1 General Measures

- Physical activity and supervised rehabilitation
- Infection prevention – influenza and pneumococcal vaccination
- Psychosocial support
- Consideration of oral anticoagulants (lifelong for CTEPH), diuretics, and digoxin
- Oxygen therapy if PaO2 <8kPa
- Treatment of anaemia and iron deficiency(17).

1.2.8.2 Vasodilator Therapy

At the time of the last National Audit of Pulmonary Hypertension(21), there were 4871 patients on active therapy in Great Britain. Patients initiated on these therapies should be closely monitored with re-assessment (including RHC) at 3-4 months to assess response to therapy.

1.2.8.2.1 Calcium channel blockers

Patients with PAH and a positive vasoreactivity test at RHC are treated with high dose calcium channel blockers such as nifedipine, diltiazem and amlodipine. If at 3-4 months, patients show an inadequate response, additional PAH therapy should be initiated.

1.2.8.2.2 Endothelin receptor antagonists (ERA)

Endothelin-1 is a potent vasoconstrictor with a proliferative effect on vascular, smooth muscle cells(73). There are 2 receptor isoforms, endothelin receptor A (ET_A) and B (ET_B). ET_A is found mainly on pulmonary artery smooth muscle cells and ET_B on vascular endothelium. Activation of ET_A causes vasoconstriction and proliferation of vascular smooth muscle cells whilst the ET_B receptors are involved in the clearance of endothelin-1, particularly in the vascular beds of the lungs and kidney, and may induce vasodilation via release of nitric oxide and prostacyclin from the endothelial cells(73).

Ambrisentan is a selective ET_A receptor antagonist which in two large, multicentre, clinical trials, ARIES-1 and -2(74), showed improved six minute walk distance (6MWD), longer time to clinical worsening and improved NYHA functional class.

Bosentan and macitentan are non-selective ERAs. Bosentan has shown clinical efficacy in multiple randomised controlled trials (RCTs). The first, BREATHE-1(75), showed an improvement in 6MWD and NYHA functional class and a later study showed improved PVR and significantly delayed time to clinical worsening (76). The liver hepatotoxicity profile has been shown to be more favourable with ambrisentan than bosentan(77)

Macitentan was the latest approved ERA with increased in vivo preclinical efficacy versus existing ERAs resulting from sustained receptor binding and tissue penetration properties(73). The SERAPHIN (78) trial enrolled a total of 742 patients and indicated that treatment with macitentan decreased the risk of a morbidity/mortality event versus placebo. Secondary endpoints (including change from baseline in 6MWD, NYHA functional class and time to clinical worsening) also showed a dose-dependent effect and only 3.5% of patients experienced elevations of liver transaminases > 3 times the upper limit.

1.2.8.2.3 Phosphodiesterase type 5 (PDE5) inhibitors and guanylate cyclase stimulators

Nitric oxide synthase is responsible for the production of nitric oxide at the endothelial level. Nitric oxide binds to the soluble guanylate cyclase (sGC) and via production of cyclic guanosine monophosphate (cGMP) acts as a vasodilator and inhibitor of cell proliferation. PDE5 degrades cGMP and inhibition of this process with PDE5 inhibitors (sildenafil and tadalafil) has shown both acute and long term beneficial effects in patients with PAH(73).

Sildenafil showed improvements in 6MWD, NYHA functional class and pulmonary haemodynamics (79) with sustained improvements in 6MWD and functional class at 3 years and a 3 year survival rate of 79%(80).

Riociguat, an oral sGC stimulator, has a dual mode of action on the NO-sGC-cGMP pathyway: direct stimulation of sGC and indirect stimulation via sensitisation of sGC to endogenous NO(81). Riociguat significantly improved exercise capacity and secondary efficacy end points (PVR, WHO functional class, NT-proBNP, Borg dyspnoea score and time to clinical worsening)(82).

Riociguat is the recommended therapy in symptomatic patients who have been classified as having persistent or recurrent CTEPH after surgical/ interventional treatment or inoperable CTEPH.

1.2.8.2.4 Prostacyclin analogues and prostacyclin receptor agonists

Prostacyclin signaling is a major pathway in the pathophysiology of PAH. Prostacyclin is mainly produced by endothelial cells and acts with a very short half-life as a potent pulmonary vasodilator as well as having antithrombotic, antiproliferative, antimitogenic and an immunomodulatory effect (73). Different stable prostacyclin analogues are available for the treatment of PAH including epoprostenol, treprostinil and iloprost.

Selexipag is an orally available, selective prostacyclin (IP) receptor agonist. In a pilot RCT in PAH patients already receiving stable ERA and/or PDE5i therapy, selexipag reduced PVR after 17 weeks(83). A further RCT (84) demonstrated that selexipag as monotherapy or in

combination with ERAs and/or PDE-5i was able to reduce by 40% a composite morbidity and mortality endpoint.

1.2.8.2.5 Combination therapy

The benefits of combination therapy, either sequentially or upfront, are increasingly recognised and there has been a move towards this approach. A multi-centre, placebo controlled trial comparing first line monotherapy with tadalafil or ambrisentan with upfront combination therapy with both in treatment naïve patients showed combination therapy resulted in a significantly lower risk of clinical failure events(85). The rationale is to induce additive or synergistic effects of therapies with different mechanisms of action and reduce toxicity(50).

1.2.8.3 Pulmonary Endarterectomy and Balloon pulmonary angioplasty for CTEPH

Pulmonary endarterectomy (PEA) is the treatment of choice for CTEPH and can offer substantial relief from symptoms and near normalisation of haemodynamics with low mortality (≤3.5%) in experienced centres(17). PEA is a substantial operation involving bilateral endarterectomy through the medial layer of the PAs and periods of circulatory arrest in deep hypothermia. General criteria for considering operability include pre-operative WHO functional class of 2-4, patient co-morbidities, pre-operative haemodynamics, surgical accessibility of thrombi in the main, lobar or segmental PAs and the risk benefit ratio of PEA (17)(58). This decision should be made by an experienced multi-disciplinary team.

More recently, balloon pulmonary angioplasty (BPA) has become an option for patients with in-operable CTEPH. BPA is a percutaneous interventional procedure using semi-compliant balloons at low pressures over several sessions to treat vascular CTEPH lesions. The short and medium term clinical and haemodynamic results have been promising(58).

Lifelong anticoagulation is recommended even after successful PEA or BPA. Riociguat is the recommended therapy for patients with persistent PH post intervention, however, off-label use of other drugs approved for PAH may be considered.

1.2.8.4 Lung Transplant

Early referral for lung transplantation should be considered for patients meeting the following criteria (from "Lung Candidate Selection Criteria" compiled by the Cardiothoracic Advisory Group on behalf of NHS Blood and Transplant):

- On maximal medical therapy (including 3 months of parenteral vasodilator therapy), and despite this:
    - WHO functional class 3 or 4
    - Declining 6MWD to < 350m
    - Worsening refractory right heart failure
    - Requirement for continuous intravenous inotropic support
    - Recent RHC showing RAP > 15mmHg and cardiac index <2.0L/min/m^2
- Have a potential survival benefit from transplantation or a potential significant improvement in their quality of life as a result of transplantation
- Have projected post-operative survival >5 years with a quality of life acceptable to the recipient

1.2.9 Disease Monitoring and Risk Stratification

Regular and comprehensive assessment of patients with PAH is strongly recommended to look for any signs of clinical deterioration, response to therapy and progression of PAH. The aim of treatment is to maintain patients in a low risk profile (defined as < 5% estimated 1 year mortality)(17). Patient risk stratification is based upon a series of prognostic markers (Table 1.6).

Prognostic Variables	Estimated 1 year mortality		
	< 5% (Low Risk)	5-10% (Intermediate Risk)	> 10% (High Risk)

Table 1.6: Risk stratification in pulmonary arterial hypertension [From the ESC/ERS guidelines(17)]. ([a]Occasional syncope during brisk or heavy exercise or occasional orthostatic syncope in an otherwise stable patient, [b]Repeated episodes of syncope even with little or regular physical activity). [WHO: World Health Organisation, 6MWD: six-minute walk distance, CPET: cardiopulmonary exercise test, VO_2: oxygen consumption, VE/VCO_2: ventilatory equivalents for carbon dioxide, BNP: brain natriuretic peptide, CMRI: cardiac magnetic resonance imaging, RAA: right atrial area, RAP: right atrial pressure, CI: cardiac index, SVO_2: mixed venous oxygen saturation).

These variables are not always consistent and can fall into different risk categories so the overall clinical assessment should guide therapeutic decisions(17).

1.2.10 Prognosis

Data from the REVEAL registry (a 3000 plus cohort of PAH patients)(86) shows significant heterogeneity in both treatment response and prognosis. Whilst there has been significant improvement in the prognosis of PAH, 5-year survival remains guarded at 56% for IPAH (without any co-morbidities) and 39% for PAH associated with CTD (including scleroderma) [data from the National Pulmonary Hypertension Audit(21)]. IPAH patients with a positive vasoreactivity response at RHC (< 10% of patients (72)) have been shown to have less severe disease (72), respond well to treatment with calcium channel blockers and have a markedly

improved 5-year survival (94% in responders versus 55% in non-responders)(87). Patients with PAH secondary to congenital heart disease have the best prognosis with a 5-year survival of 73%(21).

Early and accurate diagnosis of patients with PH and maintenance of a low risk profile is essential in improving outcomes for patients.

1.3 The Role of Imaging in PH

Imaging plays an important role in the diagnosis, classification and prognostication of PH. Imaging studies have also provided insights into the pathophysiological mechanisms of PH(88). Recent advances in CT and MRI have extended their role and there is growing interest in their future utility.

1.3.1 CT

CT is a commonly used, non-invasive tool in the diagnosis of PH and has the advantages of being easily accessible in daily clinical practice. It can demonstrate lung parenchymal changes with good reproducibility and short acquisition times enabling patients to be scanned with short breath holds. As PH often presents with vague symptomatology, CT suggestion of PH can play an important role in the evaluation of a patient. Several characteristic CT findings have been described which help in screening for PH and some have been demonstrated as prognostic markers.

In CT, a collimated beam is passed through a transverse section of the patient's body and the emergent beam is measured by a semi-circular array of detectors. The X-ray tube and detector array rotate around the patient during data acquisition, so that the plane of interest is scanned from all directions. This gives a large number of attenuation values which are recorded and processed by a computer to produce a digital image of the relevant plane(89).

Whilst CT is a useful tool, its radiation risk is not insignificant and is higher when CT is used to assess haemodynamic alterations related to PH as repetitive CT acquisitions are required in addition to iodine contrast injection which can cause adverse reactions.

1.3.1.1 CT Pulmonary Angiogram (CTPA) and High-Resolution CT (HRCT)

In a CTPA, a bolus of iodinated contrast is administered intravenously (most commonly via the antecubital vein), and the scan is acquired ideally at the point of optimal opacification of the PAs. CTPA provides information on the pulmonary vasculature and the size of the cardiac chambers and can provide clues to the aetiology of PH.

HRCT produces images of the lung parenchyma and identifies structural lung changes and bronchial disease as well as lung infarcts. It can be used to identify the underlying lung disease in group 3 PH and monitor changes in severity.

CT evaluation of patients from the ASPIRE Registry(91) demonstrated that systematic assessment of vascular, cardiac , parenchymal and mediastinal features demonstrated characteristic features of various forms of PH and identified prognostic markers.

1.3.1.1.1 Pulmonary Vasculature

Increased main PA diameter is a well-established feature of PH. Tan et al, showed a transverse PA diameter of >29mm on CT to have a high positive predictive value (97%) for PH (92). Another study used a value of 33mm(93). The PA diameter has also been used to assess the severity of PH, however correlation coefficients between CT derived PA diameter and mPAP on RHC have varied from 0.43 to 0.83(94).

A PA to ascending aorta ratio diameter (PA: Ao) of > 1 has become a widely accepted and reliable sign to identify PH. It has a reported specificity of 92% with a strong correlation seen with RHC derived mPAP (correlation coefficient = 0.74), the negative predictive value was however relatively low (52%)(95). Further multivariate analysis showed it was only confounded by age(95).

Serpiginous vessels within the pulmonary parenchyma are seen in severe PH, particularly Eisenmenger's syndrome and IPAH and are thought to represent neovascularity(96).

In CTEPH, CTPA can demonstrate the distribution of vascular webs, stenosis and mural thrombus, aiding diagnosis, and treatment planning. There are concerns regarding the

sensitivity of CTPA for the diagnosis of CTEPH (97) and therefore it cannot be used to definitively exclude it. Image reformations derived from multidetector row CT have improved detection of thrombo-emboli in distal PAs (down to the fifth order), however few studies have looked at chronic PE and V/Q remains more sensitive for detection of sub-segmental thrombo-emboli(94).

Dilated bronchial artery collaterals or other systemic collateral vessels, demonstrating compensatory perfusion, may also be seen in CTEPH as well as IPAH and PAH associated with ACHD(94).

Right PA distensibility (defined as the change in cross-sectional area of the right PA between diastolic and systolic phase) derived from ECG-gated multidetector CT has been demonstrated to identify PH reliably and correlate with mPAP(98).

1.3.1.1.2 Cardiac evaluation

Signs of right ventricular impairment can be seen on CTPA and include dilatation of the right heart chambers, right ventricular hypertrophy (defined as wall thickness of > 4mm) and displacement of the inter ventricular septum towards the left ventricle. Changes of right ventricular hypertrophy are often best appreciated in the right ventricular outflow tract, likely reflecting the reduced quantity of trabeculation(97).

The ratio of the right ventricle to left ventricle (RV:LV) is used to evaluate the degree of RV dilatation. In acute PE, a ratio of > 1 suggests modest RV dilatation and >1.5, severe(99). An RV:LV ≥ 1 strongly predicted mortality or transplantation in patients with PH secondary to interstitial lung disease(99).

Groves et al showed a moderately good agreement between CT and echocardiographic assessment of the severity of TR and CT grading of TR correlated well with RHC measurements of pulmonary artery pressure(100).

CT can also identify structural abnormalities associated with congenital heart disease.

1.3.1.1.3 Parenchymal changes

Centrilobular ground glass opacities can be seen in patients with IPAH, PAH with systemic sclerosis and PAH associated with ACHD(97). They are also seen in pulmonary veno-occlusive disease (PVOD) in combination with the additional characteristic features of interlobular septal thickening, mediastinal lymphadenopathy and pleural effusions(101). The presence of these findings in combination has been demonstrated to have sensitivity and specificity of 66% and 100% respectively for diagnosing PVOD in patients with PAH(102). These findings can also have an important role in determining treatment of these patients as their presence shows correlation with risk of developing pulmonary oedema after treatment with epoprostenol(103).

Perfusion abnormalities appear as a mosaic perfusion pattern with regions of differing pulmonary attenuation on CT. Low attenuation areas represent decreased perfusion and oligaemia. This can be seen in CTEPH (often limited to a few segmental or subsegmental vessels) and PAH (diffusely distributed) (58)(94).

In PAH, CT features have been shown to predict outcome in treatment naïve patients. These features include RV: LV ratio, right atrial size, interventricular septal position, inferior vena caval (IVC) size, presence of pericardial/pleural effusions, mediastinal lymphadenopathy, and septal lines(91). IVC area and the presence of pleural effusions/septal lines were predictors of outcome independent of pulmonary haemodynamics and WHO functional class, highlighting the prognostic value of CT(91).

1.3.1.2 Dual energy computed tomography (DECT)

DECT scanners allow simultaneous imaging of the lungs and pulmonary vasculature at different kVp by using different X-ray tubes or oscillating kVp systems to produce images of low and high kV spectra(97). Scanning after IV administration of iodinated contrast medium provides iodine maps as a marker of pulmonary blood volume which can be used in the assessment of patients with CTEPH(104). Initial studies showed that lung perfusion studies on DECT were comparable to perfusion scintigraphy and improved detection of small, distal

thrombo-emboli compared with CTPA alone(105). DECT could also illustrate perfusion defects beyond non-occlusive proximal thrombo-emboli(106).

Perfusion imaging with DECT has demonstrated the ability to estimate cardiac output by measuring the transit of contrast(107) and detect PH with high sensitivity and specificity(108).

Routine clinical use of DECT is currently limited by the requirement of expensive specialist CT systems.

1.3.2 MRI

The role of MRI in PH has been expanding and is a promising one, as it can provide both morphological and functional information regarding the heart and lungs (which are both involved in the pathophysiology of PH) without radiation exposure.

MRI works by exposing tissue protons to a strong, external, magnetic field. Tissue protons realign along the plane of the magnetic gradient and from this position can be deflected by applying a radiofrequency pulse. As the protons realign to this position, they emit an electromagnetic signal which is detected by a receiving radiofrequency coil. Signal detection can be confined to a preselected body plane and processing of this data yields a cross-sectional image of the plane of interest(89).

Cardiac MRI is widely used in PH for assessment of RV size, morphology, and function. It also allows non-invasive assessment of blood-flow (including stroke volume, CO and pulmonary arterial distensibility) and therefore provides useful prognostic information both at baseline and at follow-up and serial measurements can be used to assess response to therapy(17).

The use of MRI in pulmonary imaging is more challenging due to the inherent limitations of:

1. Low proton density – resulting in a low signal to noise ratio
2. Multiple air-tissue interfaces – resulting in significant susceptibility artefacts
3. Reduced signal secondary to cardiac and respiratory motion and blood flow (109)(110)(69).

Advances in MRI technology are overcoming these.

1.3.2.1 Cardiac MRI

A standard protocol in the assessment of PH patients includes(111):

1. A lung volume anatomical scan at breath-hold for localising.
2. Volumetric cardiac imaging for qualitative and quantitative assessment of the structure and function of the ventricles.
    - End systolic and diastolic chamber images allow the following measurements to be derived:
        i. End diastolic volume and end systolic volume
        ii. Ejection fraction
        iii. Stroke volume
        iv. Ventricular mass - Right and left ventricular mass can be calculated by segmenting out the myocardium of the right and left ventricles. The ratio of these is termed the ventricular mass index. Saba et al found that this index correlates with mPAP in patients with PH and provided a more accurate estimate than doppler echocardiography which may be a reflection of the right ventricular response to sustained PH over a long period that is not influenced by short-term physiological variables affecting echocardiography such as heart rate, posture, hydration status and oxygen supplementation(112).
    - Inter-ventricular septum – a bowing towards the left is seen in PH due to elevated RV pressure. The inter-ventricular septal curvature derived from cardiac MRI has been shown to correlate with haemodynamic measures from RHC(113) and is an accurate metric for estimation of RV systolic pressure(114).
3. Phase contrast MRI performed at the PA and aorta.
    - This allows quantification of cardiac output, stroke volume and flow profile - moving from the RV to the main PA.
    - Pulmonary arterial flow, velocity and area change can be calculated and have been shown to have clinical value in the assessment of patients with PH(97).
    - Assessment of the flow waveform in major vessels enables calculation of the

pulmonary to systemic flow ratio (Qp:Qs) which is essential in the assessment of patients with suspected congenital heart disease(115).

Black blood imaging is a technique employed to allow for morphological assessment of the boundaries between the lumen and vessel walls of cardiac chambers and vascular structures(111). In healthy subjects, there is high contrast resolution between the fast-flowing blood in the PAs (black) and the PA wall (high signal, white). In PH, the reduction in blood velocity and turbulent flow results in high signal within the PAs. This is termed "black blood flow artefact"(97).

1.3.2.2 Pulmonary MR angiography and perfusion imaging

The limitations of temporal and spatial resolution seen with early MRIs can be countered by the rapid injection of contrast media which allows the pulmonary circulation to be clearly differentiated from the systemic circulation of the pulmonary parenchyma(94). Contrast enhanced MR angiography, commonly using intravenous gadolinium-based contrast (a T1 shortening agent), can be used to acquire high spatial resolution 3D images of the pulmonary vasculature. Time resolved imaging of contrast provides high resolution angiographic assessment of the pulmonary circulation haemodynamics (97). Using a lower spatial, but higher resolution acquisition, the dynamic passage of contrast through the pulmonary parenchyma can be imaged. This is often presented as the peak signal for each voxel, after the original unenhanced dataset has been subtracted, giving a peak perfusion image and is particularly useful in the assessment of CTEPH where it has been shown to have equivalent sensitivity to perfusion SPECT imaging(116). CTEPH and IPAH can be differentiated on MR perfusion imaging as they have focal defects or diffuse reduction in perfusion respectively(117).

Quantitative measures derived from post-processing of dynamic contrast enhanced MRI (pulmonary blood volume, blood flow and mean transit time) allow for longitudinal follow up of perfusion abnormalities in PH(97). Pulmonary blood flow has been show to improve in patients who have had pulmonary endarterectomy(118).

Time resolved imaging with dynamic contrast enhanced perfusion angiography allows for

assessment of left-right heart shunts and collateral bronchial circulation(111).

Late gadolinium imaging uses a T1 weighted inversion recovery sequence performed 10-15 minutes after injection of gadolinium. Normal myocytes enhance early but wash-out as they do not retain gadolinium. Abnormal areas of tissue, such as fibrosis, trap gadolinium and remain enhanced on delayed imaging. Late gadolinium enhancement is seen in the RV insertion points and interventricular septum in patients with PH and is thought to be a result of exposure to mechanical stress. The extent of RV insertion point and interventricular septal late gadolinium enhancement has been shown to correlate with right ventricular function(119).

These techniques have the disadvantages of requiring intravenous contrast, possible allergic reactions and must be used with caution in renal dysfunction.

1.3.2.2.1 MRI with Inhaled contrast agents

MRI techniques using hyperpolarised noble gases like 3He and 129Xe alongside MRI perfusion imaging allow MRI based ventilation and perfusion imaging and assessment of gas transfer in patients with PH (120). Hyperpolarised gas ventilation imaging involves the inhalation of gas prior to a breath-hold image acquisition. MRI scanners need to be configured to work at the frequency of 3He or 129Xe with specific radiofrequency coils required. Spin density images of the gas distribution within the lungs visualise areas of ventilated and non-ventilated lung which can be analysed qualitatively or quantitatively by segmenting out the ventilated areas to calculate percentage of lung volume that is ventilated(120).

129Xe has advantages over 3He including solubility in pulmonary tissues. Once inhaled, it freely diffuses from the airspaces, across the interstitial barrier tissues and into the pulmonary capillaries, with distinct spectral peaks in each of the compartments allowing the extraction of gas exchange and alveolar oxygenation using spectroscopy methods(121).

In patients with PAH, 129Xe MRI demonstrated normal ventilation but markedly decreased gas transfer to the red blood cells with focal defects on imaging that were distinct to those described for idiopathic pulmonary fibrosis and obstructive lung disease(122)(123). 129Xe

MRI when combined with dynamic MR spectroscopy (which reveals cardiogenic variations of 129Xe transfer to the capillary red blood cells) has shown potential in differentiating between pre and post capillary PH(124)(123).

Whilst a promising technique, 129Xe MRI is difficult to apply in clinical practice due to increased cost of additional equipment, more complicated imaging protocol and measurement setup(125).

1.3.2.3 MRI derived prognostic markers in PH

There is growing evidence for the role of MRI, as a reliable, reproducible, and sensitive biomarker for patient follow-up in the context of risk stratification and the assessment of treatment response.

Cardiac MRI derived cardiac output has been shown in several studies as an independent marker of adverse outcome in patients with PAH(111). A decreased stroke volume and RV ejection fraction (and change in RV ejection fraction over time), increased RV end-diastolic volume and decreased LV end-diastolic volume are predictive of a poor prognosis (treatment failure and death at follow-up) (126,127).

Associations between the presence and extent of black blood or pulmonary flow artefact and systolic pulmonary artery pressure, PVR and mortality have been demonstrated(128,129).

In PAH, pulmonary transit times derived from perfusion MRI show a correlation with mPAP, mean right atrial pressure, PVR and are predictive of mortality at univariate analysis with equivalent prognostic value to measurements taken at RHC(130).

MRI derived predictors of mortality and treatment failure
RV ejection fraction
Stoke volume and Cardiac output
RV and LV end diastolic and systolic volume
Pulmonary arterial relative area change
Ventricular mass index
Late gadolinium enhancement of RV insertion point
Pulmonary transit times
Presence and extent of black blood

Table 1.7: MRI derived predictors of mortality and treatment failure(111,116,126–130). *[RV: right ventricle, LV: left ventricle].*

1.4 Novel Quantitative MRI Measurements in PH

Abnormalities in pulmonary perfusion, particularly in the peripheral vascular bed, are a hallmark of PH and the area where many pharmaceutical approaches are targeted. Therefore, visualisation and quantification of blood flow in the pulmonary vascular bed are crucial for diagnosis and treatment monitoring in patients.

As discussed, current techniques, are invasive, involve radiation, contrast media or are limited by their complexity and costs in terms of clinical use in an NHS setting. This can sometimes preclude more intensive monitoring of frailer patients and is not ideal for repetitive investigation of young PH patients. There is therefore a need for new techniques, which can be used in the assessment of these patients.

In the research setting, novel MRI techniques are emerging that would allow quantitative analysis of lung perfusion and could be used pre and post therapy to allow both anatomic and functional assessment of therapies (131). This project investigates one of these novel techniques further: Oxygen Enhanced MRI. This technique has the advantages of being non-invasive, not requiring exposure to ionising radiation and the imaging protocol can be carried out on standard clinical MRI scanners.

1.4.1 Oxygen Enhanced MRI (OE-MRI)

The primary role of the respiratory system is gas exchange, which is an interaction of 3 mechanisms: ventilation, diffusion, and perfusion. Oxygen delivered to the alveoli by alveolar ventilation, diffuses into pulmonary arterial and capillary blood and is carried away by blood flow(130,132).

Use of inhaled molecular oxygen as a contrast agent therefore enables direct analysis of oxygen transfer across the alveolus into the pulmonary vasculature.

OE-MRI was first proposed as a new technique for evaluation of regional ventilation using molecular oxygen as the contrast agent by Edelman and colleagues in 1996. Edelman et al showed that it was possible to qualitatively monitor the delivery of oxygen to lung tissue using a single 2 dimensional image acquired every few seconds (133).

Assessment of regional ventilation in human lungs is important for diagnosis and evaluation of multiple pulmonary disorders. Prior imaging techniques for regional ventilation were predominantly nuclear medicine studies and more recently hyper-polarised noble gas MRI(134). Nuclear medicine studies have limitations due to temporal and spatial resolution, radiation and use of radioactive substances(135). OE-MRI has been demonstrated as an alternative indirect method to visualise lung ventilation in both healthy volunteers and patients with pulmonary diseases(136).

Molecular oxygen contains two unpaired electrons and is weakly paramagnetic. It modulates the MR imaging signals of blood and other fluids through 2 different mechanisms(137): (1) the paramagnetic property of deoxyhaemoglobin and (2) the paramagnetic property of molecular oxygen itself.

Deoxyhaemoglobin is compartmentalised in red blood cells and therefore has minimal effect on spin-lattice interactions causing T1 shortening. It does however shorten T2*, the basis for blood oxygenation level dependent (BOLD) contrast, which has been used to evaluate regional blood flow and tissue oxygenation(137). When oxygen is exchanged between the air in the alveoli and blood in the capillary beds, it does not only couple to haemoglobin but also dissolves as molecular oxygen in the blood and shortens T1 relaxation time due to its paramagnetic properties which can be visualised as an increase in signal intensity on MR

imaging(134). The average oxygen induced shortening of the T1 relaxation time of pulmonary parenchyma is between 7-14%(132).

The multiple tissue-air interfaces in the lung mean poor signal intensity when conventional pulse sequences are used. Therefore various adapted sequences have been developed in OE-MRI which incorporate rapid acquisition time and short echo time such as IR-HASTE (Inversion recovery half fourier-single shot turbo spin echo)(138). This allows an adequate signal to be obtained from lung parenchyma and the small pulmonary vessels(134).

Positive results with OE-MRI have been reported in the evaluation of ventilation and perfusion abnormalities in a range of lung diseases (including cystic fibrosis, ILD, cancer, emphysema and pulmonary embolism(139)(132)(140,141)) when quantitatively or semi-quantitatively compared with standard parameters such as pulmonary function tests, CT and ventilation-perfusion scintigraphy(138).

OE-MRI parameters correlated significantly with FEV1 and DLCO(142–144) suggesting that OE-MRI may be capable of assessing alveolo-capillary gas transfer in addition to degree of airway obstruction(141).

In a study by Löffler et al(145), the posterior slices of the lung showed more homogenous correlation maps and a more pronounced signal intensity enhancement during breathing 100% oxygen which may be due to differences in perfusion of the lungs which is dependent on the hydrostatic pressure(145). Therefore, the signal intensity changes related to shortened T1 relaxation time appear to be dependent on not only ventilation and inhaled oxygen reaching the alveoli, but also its diffusion across the alveolar walls and the perfusion of the surrounding pulmonary vasculature(146).

The role of static OE-MRI has previously been studied in PH. In a cohort of patients with IPAH and CTEPH, there was an overall moderate agreement between OE-MRI and V/Q scans (132). In addition to this, quantitative parameters including mean relative signal enhancement and fraction of non-activated pixels, correlated significantly with the number of diseased lung areas in both V/Q scintigraphy and OE-MRI maps suggesting that these may serve as markers for the severity of PH (132).

1.4.1.1 Dynamic OE-MRI

More recently, studies have been utilising dynamic OE-MRI (monitoring signal changes over time as gas supply is switched between air and 100% oxygen) in an attempt to obtain more physiologically relevant biomarkers of lung function(147). Dynamic OE-MRI can provide spatial and temporal information on regional delivery and uptake of oxygen in the lung. Paramagnetic oxygen molecules dissolve in the tissue water and blood plasma within the lung and increase the lung spin-lattice relaxation rate in proportion to dissolved oxygen concentration and therefore local oxygen partial pressure (PaO_2)(148). By measuring the change in lung spin-lattice relaxation rate between breathing air and elevated levels of oxygen, the change in lung tissue PaO_2 can be quantified and provides a reflection of the efficiency of regional alveolar ventilation, membrane function, and perfusion effects(141)(149).

Ohno et al showed the potential of dynamic OE- MRI for pulmonary functional loss assessment and clinical stage classification in COPD(141). A study in asthmatic patients demonstrated sensitivity of dynamic OE-MRI parameters to disease severity and good one month reproducibility and intra-observer agreement(149). In a cohort of cystic fibrosis patients, significant correlations were seen between dynamic OE-MRI parameters and lung function and CT derived severity scores(150). Dynamic OE-MRI parameters also showed response to treatment with bronchodilator therapies in COPD(147).

1.4.1.2 OE-MRI as a Novel Imaging technique in PH

OE-MRI has shown potential as a novel measure of pulmonary perfusion and has the advantage of being non-invasive and not requiring exposure to ionising radiation. The imaging protocol can be carried out on standard clinical scanners and the only additional equipment required is a simple gas mixing system (costing approximately £300). Another important benefit in patients with PH is that data acquisition does not require long breath-holds.

This technique may therefore present a novel set of imaging biomarkers for aiding diagnosis, assessing treatment response and longitudinal disease monitoring in PH patients, with no

additional risk to patients. Combining it with existing cardiac MRI protocols could provide an optimal tool for monitoring pulmonary perfusion and right heart function.

1.5 Hypothesis, Aims and Objectives

1.5.1 Hypothesis

Quantitative CT and MRI derived imaging biomarkers can predict disease severity, treatment response and mortality in patients with PH.

1.5.2 Aims

To explore the relationships between multiple, quantitative CT and MRI derived measures of pulmonary and pulmonary vascular disease with standard clinical markers of disease severity, treatment response and mortality in PH.

1.5.3 Objectives

- Identify retrospective CT cohorts of PH patients
- Investigate previously described and novel CT measurement techniques in these cohorts and correlate results with accepted markers of clinical disease severity
- Prospectively recruit patients with a new diagnosis of IPAH, CTD-PAH or CTEPH for a pre and post treatment research MRI scan
- Correlate novel MRI derived measures with conventional markers of disease severity and treatment response
- Assess acceptability of novel MRI technique to patients with PH.

Chapter 2: Methods

2.1 Background

The Royal Brompton Hospital (RBH) PH service forms part of the National Pulmonary Hypertension Service in the United Kingdom. It is one of 8 designated specialist centres and has a multi-disciplinary team that provides care for PH patients from initial investigations and confirmation of diagnosis through to long term management and decisions regarding end-of-life care. Patients are mainly from the South of England and Wales and the service has shared care clinics at certain District General Hospitals covering these areas allowing patients specialist care closer to home with the option of being seen as an in or out-patient at RBH when required. RBH is also a tertiary centre for ACHD and therefore looks after a large cohort of patients with PAH associated with ACHD.

Patient recruitment and data collection for the studies that form this thesis have been from the RBH PH service, either retrospectively (Chapters 3 and 4) or prospectively (Chapter 5).

2.2 Chapters 3 and 4: Retrospective CT based studies

2.2.1 Patient recruitment

Both retrospective studies had Institutional Review Board ethics approval.

The RBH PH service has a clinical database of all patients that have been under its care on the Infoflex® digital healthcare system adopted by the trust. This data set includes patient demographics, WHO functional class, patient quality of life score (emPHasis-10), 6MWDs, treatment status, dates of RHC and mortality data.

By performing searches on this database, it was possible to identify patients meeting the criteria for inclusion in both retrospective studies. Data was supplemented by other clinical records where required, e.g., Electronic Patient Records.

2.2.2 CT measurements

Both contrast enhanced (CTPA) and non-contrast enhanced scans of the thorax were analysed. Where only non-contrast scans were available, some measurements described below could not be performed. The studies analysed were not ECG gated. The reviewers (SS [Clinical Fellow in Pulmonary Vascular Disease] and BR [Clinical Fellow in Cardiothoracic Radiology]) were blinded to clinical data and outcomes at the time of CT measurements.

2.2.2.1 Vascular measurements

2.2.2.1.1 PA diameter and PA:Ao ratio

Both contrast and non-contrast enhanced scans were used for measurements. However, where contrast enhanced images were available, these were used in preference. Using mediastinal windows, the axial section where the main PA diameter bifurcated was located. Electronic callipers were used to measure the widest portion of the main PA diameter at this point and the aortic diameter was measured at the same level(151). The PA:Ao diameter ratio was calculated from these measurements (Figure 2.1).

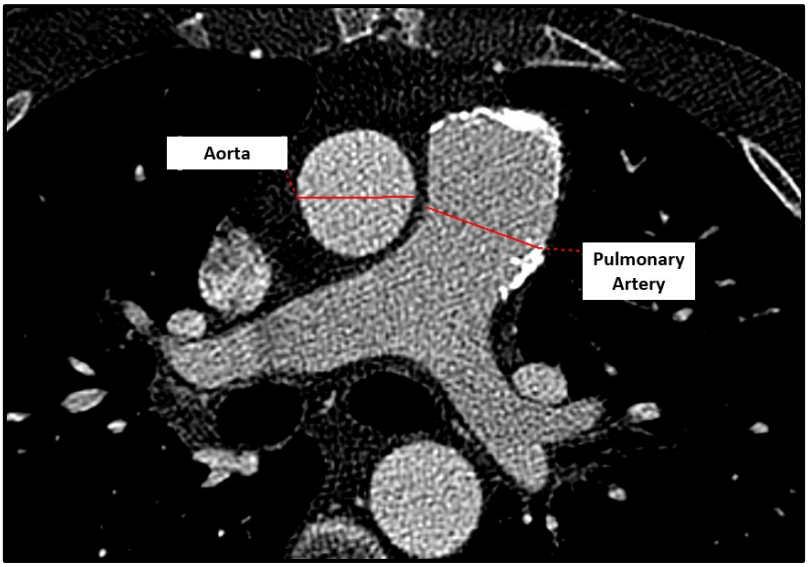


Figure 2.1: Measurement of the PA and aortic diameter to calculate PA:Ao ratio. The PA was measured at its widest point at the bifurcation of the main PA. The Aorta was measured on the same axial level as the PA diameter. The PA:Ao ratio was calculated as PA diameter/Aorta diameter. [PA: pulmonary artery, PA:Ao: pulmonary artery to aorta ratio].

2.2.2.1.2 PA Trunk volume

Using the Intuition Viewer 3D workstation (Aquarius Intuition Viewer, v 4.4.14.254, Terarecon, Durham, NC, USA) the pulmonary trunk was segmented from the level of the pulmonary valve to the bifurcation of the main pulmonary artery and the volume of the isolated pulmonary trunk calculated (Figure 2.2).

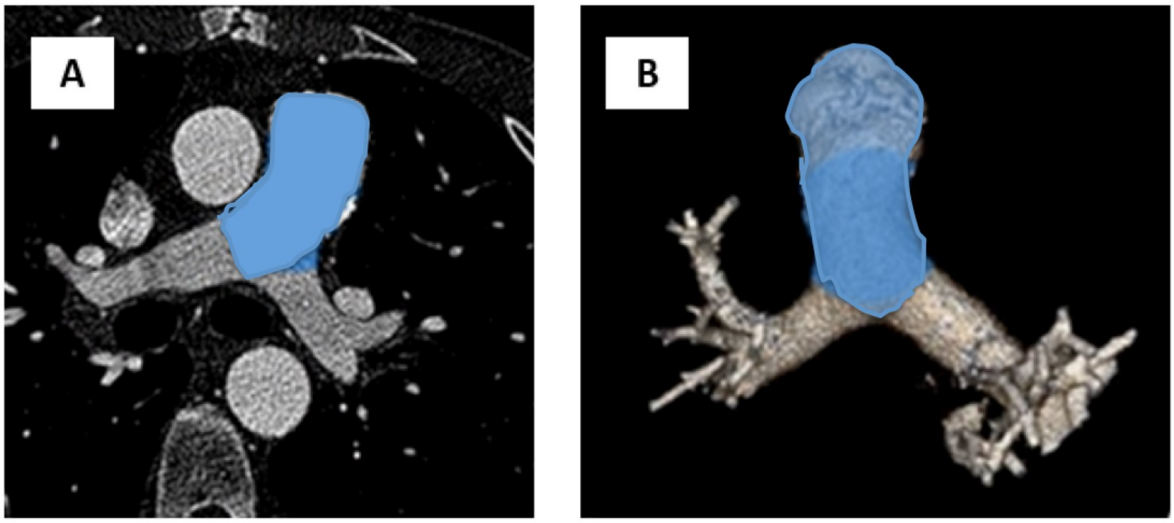


Figure 2.2: Measurement of pulmonary trunk volume. Panel A – The pulmonary trunk was segmented on the axial image from the level of the pulmonary valve to the bifurcation of the main pulmonary artery. Panel B – Using the Intuition Viewer 3D workstation, volume rendered images were used to calculate the pulmonary trunk volume (in blue).

2.2.2.1.3 PA thrombus

The presence of in-situ PA thrombus was documented (Figure 2.3).

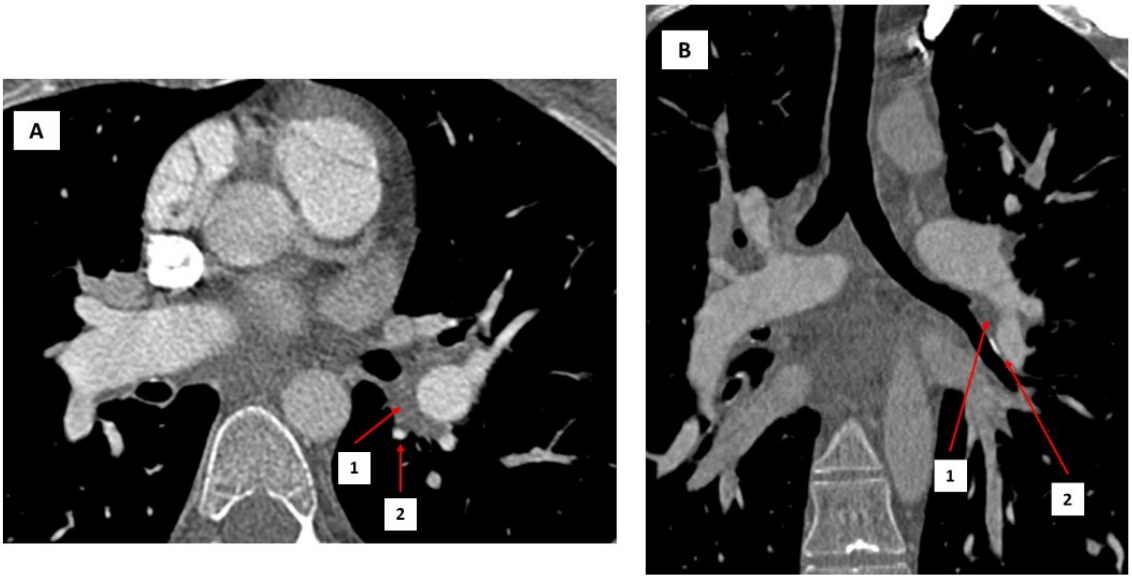


Figure 2.3: Pulmonary artery in-situ thrombus and calcification. Axial (panel A) and coronal (panel B) images demonstrating (1) pulmonary artery in-situ thrombus and (2) calcification within the thrombus.

2.2.2.1.4 PA calcification

The degree of PA calcification was evaluated using a modified Agatston score(152) (as used in assessing coronary artery calcification) where total calcium scores are calculated based on the number, areas and peak Hounsfield units of the calcific lesions detected (Figure 2.4). This was done using the Intuition Viewer 3D workstation. Whilst the use of the Agatston score is established in the assessment of coronary artery calcification, its use in pulmonary arteries is novel.

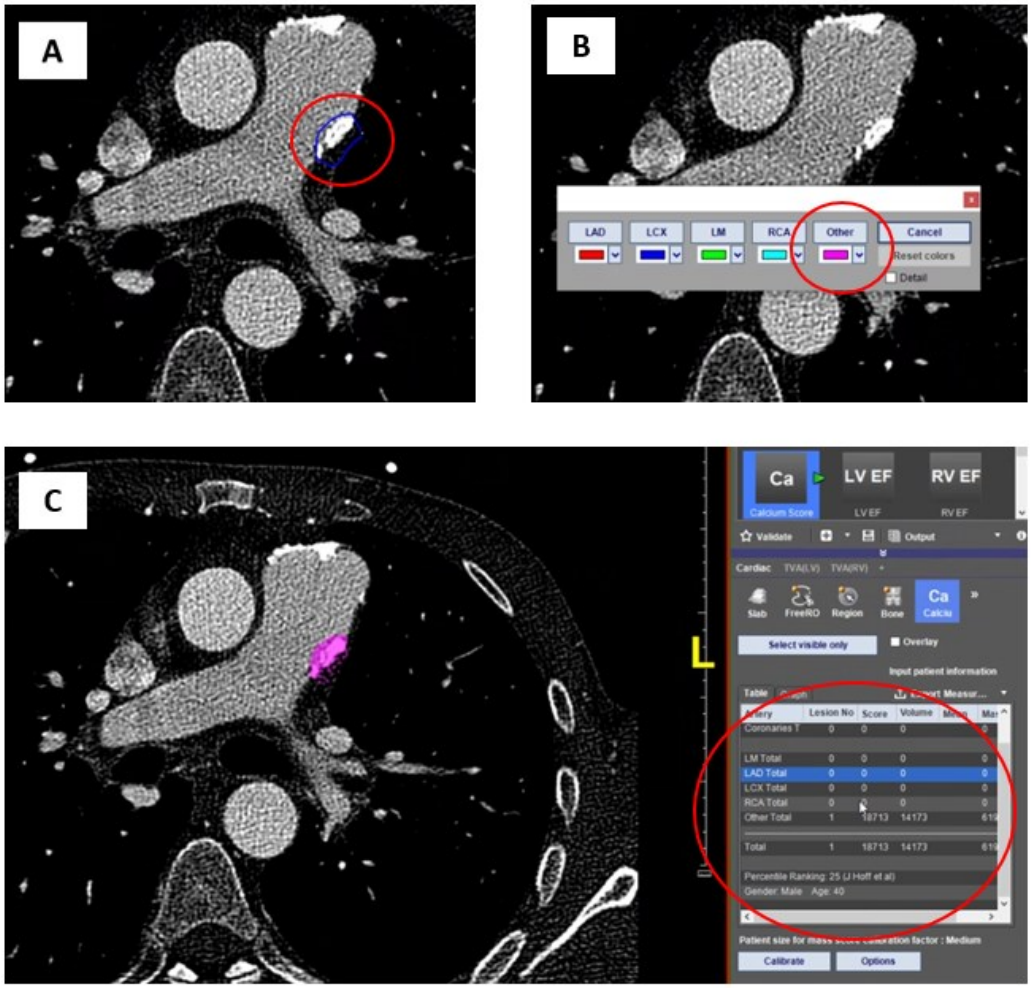


Figure 2.4: Quantification of pulmonary artery calcification using a modified Agatston score on the Intuition Viewer 3D workstation. Panel A – An area of calcification in the pulmonary arteries was manually identified. Panel B – This was used to systematically identify other areas of calcification in the pulmonary arteries. Panel C – The calcium score, volume and mass were calculated.

The distance between the pulmonary bifurcation and the most distal calcification was measured on curved planar reformatted images using the Intuition Viewer 3D workstation (Figure 2.5).

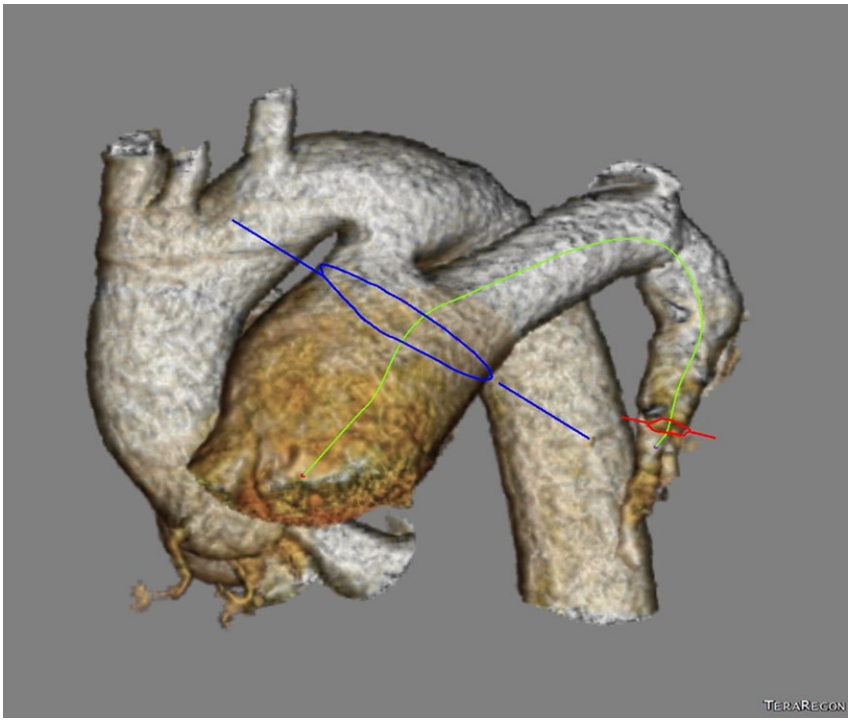


Figure 2.5: Volume rendered tomogram from a patient with Eisenmenger Syndrome (secondary to a large patent ductus arteriosus). The curved plane is shown in green with measurement from the pulmonary bifurcation (blue marker) to the most distal focus of pulmonary arterial calcification (red marker).

2.2.2.2 Cardiac Measurements

2.2.2.2.1 RV diameter and RV:LV ratio

The RV and LV diameter were measured at their widest point (between the ventricular and interventricular endocardial walls) (153) at the mid-ventricular level on the same axial CT image and the RV:LV ratio calculated (Figure 2.6).

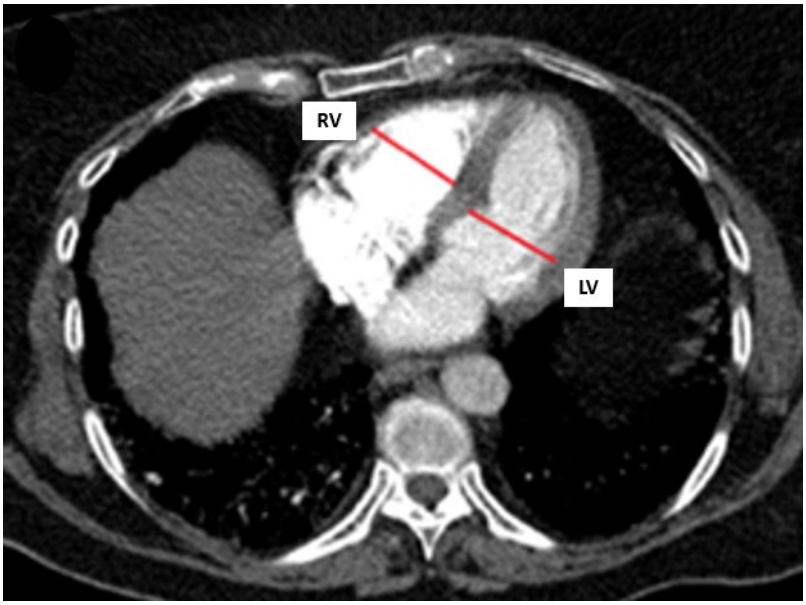


Figure 2.6: Measuring RV and LV diameter to calculate RV:LV ratio. The largest diameter of the RV and LV were measured at the mid-ventricular level. The RV:LV ratio was calculated as RV diameter/LV diameter. [RV: right ventricle, LV: left ventricle].

2.2.2.3 Parenchymal lung disease: Emphysema and Fibrosis

The extent of emphysema and fibrosis was scored using a modified version of the method used in the COPDGene study(154). Both right and left lung were considered together and by systematically examining the lungs in 3 zones (upper zone above the carina, mid zone between carina and inferior pulmonary veins, lower zone below the inferior pulmonary veins), a visual score of extent was given to the nearest 5%.

2.3 Chapter 5: Oxygen Enhanced MRI

2.3.1 Patient recruitment

This study obtained a favourable ethics opinion from the London-Bromley REC and HRA/ HRCW approval (REC reference number: 18/LO/1369). Funding for the study was secured from a NIHR Imperial BRC grant.

Recruitment was prospective and started in November 2018. New patients referred to the RBH PH service who went on to have a confirmed diagnosis of IPAH, PAH associated with CTD

or CTEPH were approached for recruitment into the study. Table 2.1 demonstrates the eligibility criteria for participation. All patients were provided with patient information sheets regarding the study and gave informed, written consent prior to participation (Appendix I and II).

Inclusion Criteria:	• Confirmed new diagnosis of IPAH, PAH associated with CTD, or CTEPH following current gold standard investigations • Age >18 • Informed consent to participate
Exclusion Criteria:	• Standard contra-indications to MRI as per NHS MRI Safety Questionnaire • Co-existent lung disease • Not fit for transfer to MRI • Lack of capacity and inability to consent • Patient judged inappropriate for involvement in study by clinical team e.g., secondary to emotional burden of recent diagnosis

Table 2.1: Eligibility criteria.

Patients consenting to take part went on to have a research MRI scan prior to initiation of treatment. Patients usually have a short admission at RBH to complete diagnostic investigations and start on therapy. The research scans were carried out during this period to avoid delays in patients staring therapy.

The research MRI scan was in addition to standard of care investigations and did not play any part in treatment decisions. Patients also went on to have a repeat research MRI at the time of their 3-6-month follow-up appointment at RBH.

Patients were asked to complete a patient experience questionnaire following their scan (Appendix III). Figure 2.7 demonstrates the study schematic.

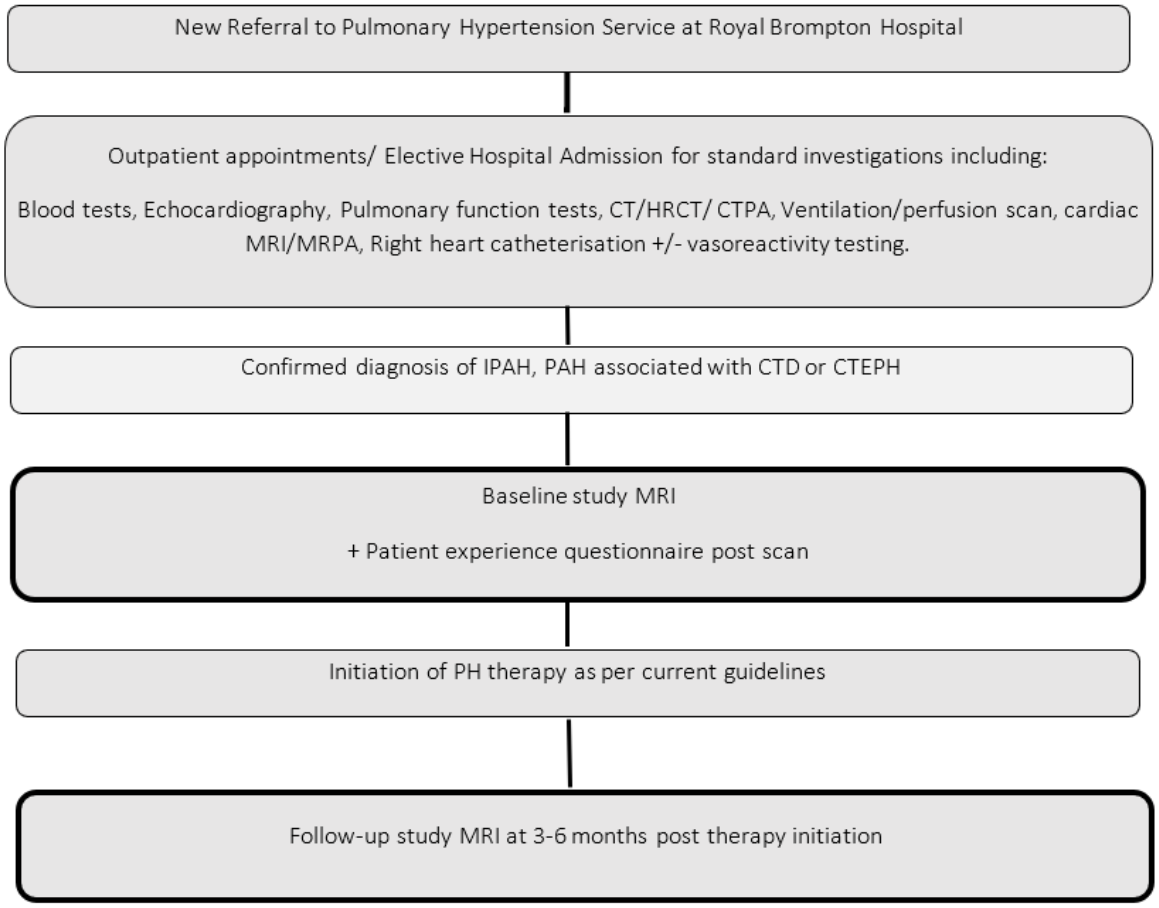


Figure 2.7: Schematic of Study Design.

2.3.2 Research MRI protocol

MRI scans were performed on a 1.5T MRI scanner (Siemens Aera). Scans were anonymised at the point of acquisition with each patient being given a link-anonymised trial identification number.

2.3.2.1 Summary of the study MRI protocol

1. Localisers
2. Breath hold T2 BLADEs for anatomy/morphology (non-cartesian reconstruction motion insensitive sequence). 3 acquisitions and breath holds each lasting 12 seconds with a radiographer-controlled pause between each.

3. IR-HASTE (Inverse recovery half fourier acquisition turbospin echo) based mapping – an established method of T1 mapping with variable inversion time. 5 minutes of free breathing on bottled air.
4. Dynamic oxygen enhanced protocol – repeat of IR-HASTE images but with changing oxygen administration (5 mins bottled air - 5mins 100% oxygen - 5 mins bottled air) using a low flow gas mixer.
5. Post processing (discussed below).

The total scan duration is approximately 30 mins.

2.3.2.2 OE-MRI Acquisition

During the scan, subjects breathed alternatively medical air (21% oxygen) and 100% oxygen via non-rebreathing mask (Intersurgical Ltd., Wokingham, UK) at a flow rate of 15 L/min. Baseline lung T1 measurements were made whilst breathing bottled medical air, using a set of multi-slice inversion-recovery single-shot turbo spin-echo sequence (IR-HASTE), with 6 inversion times (TI) (TI = 22/50/300/1100/2000/5000 ms). There were 5 repetitions for each TI, and 6 coronal slices in each acquisition. Slice thickness was 1 cm and the gap between slices was 1 cm. This was followed by 120 dynamic acquisitions with a TI of 1100 ms, during which the gas supply was switched from medical air to 100% O_2 at the 20th acquisition and back to medical air at the 90th acquisition.

Other scanning parameters included: repetition time (TR) 6000 ms, effective echo time (TE) 9.3 ms, and pixel size 3.52 mm × 3.52 mm. Images were acquired during free breathing with no breath-holding, respiratory or cardiac triggering.

2.3.2.3 Image post processing

The post-processing of the MRI scans has been in collaboration with researchers from Bioxydyn Ltd. Research sequences, software agreements, data sharing agreements and research licences were put in place. Link-anonymised images were transferred via a confidential platform.

2.3.2.4 OE-MRI image analysis

For each TI and each slice acquired, a single frame was chosen by an operator. The criteria applied for the selection were: (1) repeatable expiratory position, (2) lack of clear movement artefacts. These images were then co-registered using advanced normalisation tools (ANTs)(155) and a baseline T1 map was estimated fitting the data to a 3 parameters inversion recovery equation.

All images from the dynamic sequence were then registered to the targets with TI of 1100ms. Lungs were manually segmented by the same operator. Slices with minimal lung tissue or artefacts were not segmented. In the lung mask, the signal curves under air breathing were converted to dynamic T1 curves using the baseline T1 maps (149). The dynamic T1 curves were then converted to dynamic changes in the partial pressure of O2 dissolved in the tissue water and plasma of the lung(149). The signal was fitted to a mono-exponential recovery curve, to extract the oxygen wash-in time and the change in partial pressure of oxygen (ΔPO_2). Additionally, an enhancement fraction (EF) was calculated (the fraction of the region presenting with oxygen enhancement, max = 1, min = 0). Values were summarised at a whole lung level and expressed as medians and homogeneity across the imaged lung expressed via interquartile range.

2.4 Other investigations and recorded variables

The below investigations and variables were acquired as standard of care in the clinical assessment of these PH patients and are validated research end points with recognised correlations to prognosis and survival.

2.4.1 Right heart catheterisation (RHC)

RHCs were performed as per ESC/ERS guidelines(17) with haemodynamic measurements obtained at rest. PH was defined as a mean pulmonary arterial pressure (mPAP) ≥25mmHg. Cardiac output (CO) was measured using the indirect Fick method. PVR was calculated as PVR=(mPAP–PCWP)/CO.

2.4.2 Pulmonary function tests (PFTs)

PFTs were carried out and predicted values calculated using American Thoracic Society/ERS criteria(156). Measurements included spirometry, single-breath diffusion capacity for the lung for carbon monoxide (DLCO) and carbon monoxide transfer co-efficient (KCO).

2.4.3 Echocardiography

Images were acquired using a 3MHz frequency harmonic phased-array transducer. Doppler echocardiography was performed as per the American Society of Echocardiography recommendations(157,158).

2.4.4 Brain natriuretic peptide (BNP)

BNP was performed using a commercially available assay (normal value <20ng/L).

2.4.5 Six-minute walk distance (6MWD)

6MWD tests were carried out by the PH Specialist Nurses as per ATS guidelines(159).

2.4.6 EmPHasis 10 (E-10)

The emPHasis-10 is a short, simple questionnaire for assessing health related quality of life in PH(160).

2.4.7 WHO functional class

WHO functional class defines the severity of symptoms in PH and how they impact on activities of daily living:

Class 1 – No symptoms of PH on exercise or at rest.

Class 2 - No symptoms at rest but uncomfortable and short of breath with normal activity (e.g., climbing a flight of stairs, shopping, or making the bed).

Class 3 - May not have symptoms at rest but activities greatly limited by shortness of breath, fatigue, or near fainting.

Class 4 - Symptoms at rest and severe symptoms with any activity. Signs of right heart failure.

2.4.8 Cardiac MRI (CMR)

CMR was performed using a 1.5 Tesla scanner (Sonata, Siemens, Erlangen, Germany) at the RBH site.

2.4.9 Cardiopulmonary Exercise Testing (CPET)

CPET was performed on either a cycle ergometer or treadmill according to a modified Bruce protocol(161).

2.5 Statistical analysis

Statistical analysis was performed using IBM SPSS Statistics 27.

Data has been summarised as frequency (%) for categorical variables. For continuous variables, mean ± SD or median (range) have been used as appropriate.

The level of statistical significance was set at 5% (probability value [p] < 0.05).

Table 2.2 summarises the statistical tests used in the following chapters. When there were lower frequencies of data available (<20), non-parametric tests were used as it is harder to be sure that the underlying distribution is normal and non-parametric tests are more conservative making a significant result more convincing.

Data Type	Distribution	Independent/Paired	Groups	Test
Categorical	-	-	2	Pearson chi squared test Fishers exact test (if n<5 in any category)
Continuous	Parametric	Independent	2	2 samples independent T-Test
	Parametric	Paired	2	Paired T-Test
	Parametric	Independent	>2	ANOVA (one way analysis of variance)
	Non- parametric	Independent	2	Mann-Whitney (Wilcoxon rank sum test)
	Non- parametric	Paired	2	Wilcoxon signed rank test
	Non- parametric	Independent	>2	Kruskal- Wallis test

Table 2.2: Summary of statistical tests used.

The relationship between 2 continuous variables was assessed with Spearman rank correlation coefficients (r_s) with $r_s = 0$ indicating no correlation, -1 a perfect negative correlation and +1 a perfect positive correlation. The strength of correlation (irrespective of whether – or +) was defined as:

- > 0.7 to 1 - strong
- > 0.4 – 0.7 – moderate
- > 0.1 - 0.4 – small
- ≤ 0.1 – trivial.

The reliability of continuous measurements taken by two independent reviewers was assessed using intraclass correlation coefficients with a two-way mixed effect model measuring consistency. The degree of reliability was interpreted as(162):

- < 0.5 – poor
- 0.5 – < 0.75 – moderate
- 0.75 – < 0.9 – good
- ≥ 0.9 – excellent.

The relationship between an outcome and one or more risk factors was assessed using logistic and Cox regression.

Chapter 3: Quantitative CT findings in group 3 pulmonary hypertension treated with Sildenafil

2.6 Introduction

2.6.1 Group 3 PH

PH secondary to lung disease and chronic hypoxia is classified into group 3 of the clinical classification. It is a frequent complication of chronic lung disease and is associated with reduced functional status, increased oxygen requirements, impaired quality of life and increased risk of mortality(56).

The most common lung diseases associated with PH are chronic obstructive pulmonary disease (COPD), interstitial lung disease (ILD) and combined pulmonary fibrosis and emphysema (CPFE)(17).

The prevalence of group 3 PH varies according to the severity and type of underlying lung disease and how PH is defined and diagnosed. Mild to moderate PH (defined as mPAP ≥ 25 to < 35mmHg) is reported to have a prevalence of 30-70% in COPD and 47-90% in CPFE(163). However, severe PH (defined as mPAP ≥ 35mmHg or ≥ 25mmHg with low cardiac output [cardiac index <2.5L/min]) in lung disease is much rarer with an estimated prevalence of 5-13%(163).

The severe PH group are suspected to have significant vascular abnormalities with evidence of a diminished circulatory reserve rather than a diminished ventilatory reserve leading to exertional dyspnoea disproportionate to pulmonary function tests, low carbon monoxide diffusion capacity, and rapid decline of arterial oxygenation upon exercise(164).

Suggested theories for severe PH in chronic lung disease (CLD) are(164,165):

1. Chronic parenchymal disease triggering progressive vascular remodelling.
2. PH appearing independently to the underlying CLD.

2.6.1.1 COPD

In COPD, severe group 3 PH is often not associated with the degree of airflow obstruction but with marked hypoxaemia and a disproportionately low diffusing capacity of the lung for carbon monoxide (DLCO) (17,163).

The development of PH in COPD is thought to be a combination of alveolar hypoxia with resultant vasoconstriction and vascular remodelling, destruction of the pulmonary vascular bed and compression of alveolar vessels in hyperinflated emphysematous lungs(163). Additional factors that may contribute include tissue destruction with emphysema, increased viscosity due to polycythaemia, and worsening acidosis(166).

An overlap between group 1 (PAH) and 3 PH has been suggested with co-existent lung and idiopathic pulmonary vascular disease. In the REVEAL (Registry to Evaluate Early and Long-term PAH Disease Management) study up to 17% of PAH diagnoses had coexistent COPD(167). The development of severe PH in some patients with COPD is thought to involve a distinct phenotype related to vessels rather than airways(168).

Variability in the response of the pulmonary circulation to hypoxia is seen in both healthy individuals and those with COPD (169,170), suggesting that some patients are more sensitive to hypoxia and exhibit a greater increase in mPAP and PVR during a hypoxic challenge(168). A 5-HTT gene polymorphism may also determine the severity of PH in hypoxaemic patients with COPD(171).

PH in COPD is a strong predictor of mortality with an inverse relationship between pulmonary vascular haemodynamics (mPAP and PVR) and survival(164). The 5-year survival rate for COPD with mPAP >25mmHg is reported as 36%, with pulmonary haemodynamics being a stronger predictor of survival than the lung function variables (FEV1 and TLCO)(172).

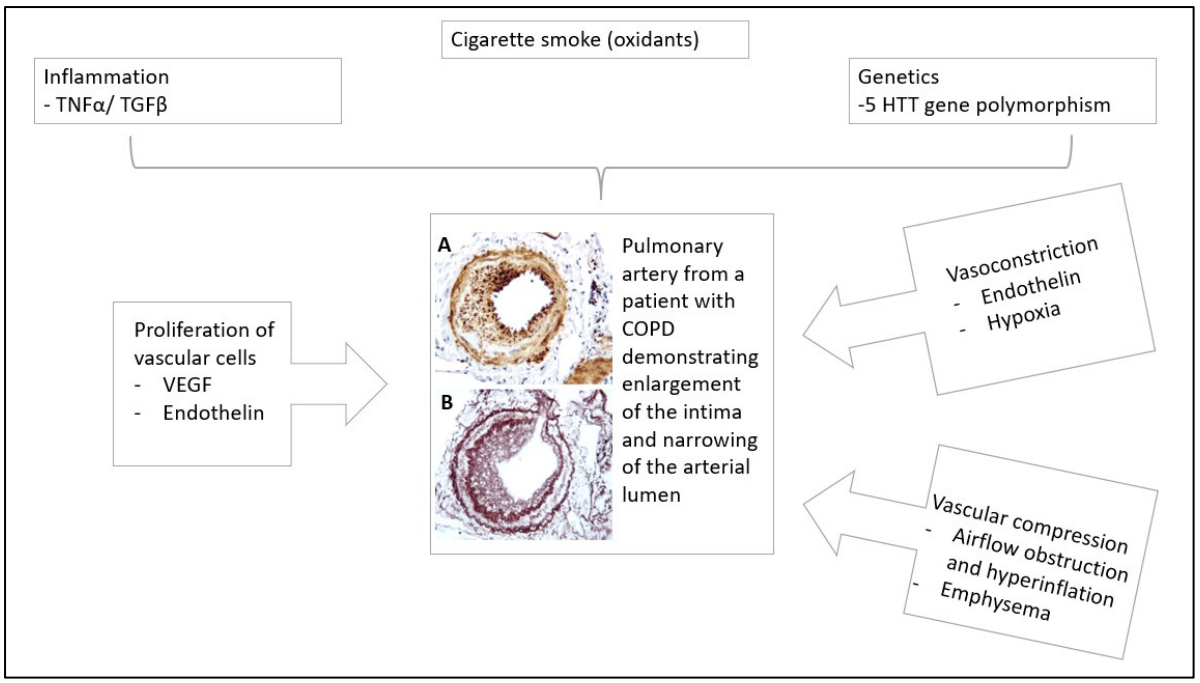


Figure 3.1: Pathogenesis of pulmonary hypertension in chronic obstructive pulmonary disease. A combination of factors including abnormal production of mediators that control vasoconstriction, vasodilatation and vascular cell proliferation lead to abnormal vascular remodelling and pathology (163,173)*. These changes are like those seen in pulmonary arterial hypertension. A: Immunostaining with monoclonal antibody against α-smooth muscle actin, showing proliferation of smooth-muscle cells in the intima, B: Orcein stain demonstrating increased deposition of elastic fibres in the intimal layer. (Image of pulmonary artery reproduced with permission from the European Respiratory Journal, volume 21, issue 5, Barbera et al, Pulmonary hypertension in chronic obstructive pulmonary disease, pages 892-905, 2003).*

2.6.1.2 Idiopathic pulmonary fibrosis (IPF) and other idiopathic interstitial pneumonias (IIPs)

In IPF, a mPAP ≥ 25mmHg has been reported in 8-15% of patients at initial work up, with a greater prevalence reported in advanced (30-50%) and end-stage (>60%) disease(56). A longitudinal study of patients with IPF suggested that mPAP increases by 1.8mmHg per year(174) with a more rapid progression seen in late-stage patients. PH is also associated with an increased risk of acute exacerbations and mortality in advanced IPF(175) with a 2 – 3 fold increase in mortality reported(176). The prognosis of IPF with PH is worse than that of IPAH(177).

Minimal correlation has been demonstrated between the severity of PH and lung function impairment or the extent of fibrosis on CT(56), suggesting it is not just the destruction of the pulmonary vascular bed by progressive fibrosis that leads to the development of PH and that other mechanisms including vascular remodelling are involved(178). Distinct gene signatures have been observed in patients with pulmonary fibrosis and severe PH with these patients showing increased expression of genes related to myofibroblast proliferation and vascular remodelling and patients with no PH strongly expressing pro-inflammatory genes(179).

2.6.1.3 CPFE

CPFE is defined by the simultaneous presence of upper lobe emphysema and fibrosis in the lower lobes on chest CT(56). Patients with CPFE are particularly prone to development of PH with an estimated prevalence of 30-50% and 1 year survival of 60%(180). Often, normal or mildly abnormal lung volumes and the absence of airflow obstruction are accompanied by a markedly impaired diffusion capacity, significant hypoxaemia and PH(56).

2.6.1.4 Sleep disordered breathing and Hypoxia associated PH

Obstructive sleep apnoea (OSA) is common worldwide and the estimated prevalence rates have dramatically increased over the last 2 decades with relative increases of 14 to 55% depending on the subgroup(181). The prevalence of pulmonary hypertension in OSA ranges from 17 to 53% (181) and is generally mild with mPAP ranging from 21.9 - 40.3mmHg(56,181).

More severe PH is seen in patients with obesity hypoventilation syndrome (OHS) or overlap syndrome (combination of OSA and COPD) and is associated with right ventricular failure and poor outcomes(182–184).

2.6.2 Group 5 disorders overlapping with Group 3 PH

Sarcoidosis, langerhan's cell histiocytosis (LCH) and lymphangioleiomyomatosis (LAM) are classified as systemic disorders within group 5 of the PH classification (PH with unclear and/or

multi-factorial mechanisms). These conditions effect the lung and therefore can also overlap with the group 3 PH phenotype.

The prevalence of PH in sarcoidosis ranges from 5.7% to 74%(185) and has a reported 5-year survival of 50–60% (186,187). The underlying pathophysiology of PH associated with sarcoidosis is complex and PH can occur in patients with both minimal and extensive parenchymal disease(56) and the severity of PH does not correlate well with the degree of pulmonary fibrosis (188). The following mechanisms have all been attributed to the development of PH in sarcoidosis:

1. Destruction of the distal capillary bed by fibrotic processes and the resultant chronic hypoxaemia(187).
2. Extrinsic compression of central pulmonary vessels by lymphadenopathy or mediastinal fibrosis(189).
3. Granulomatous vascular involvement that leads to pulmonary veno-occlusive like lesions(190,191).
4. Pulmonary vasoconstriction by vasoactive factors(192).
5. Post capillary PH due to specific left heart disease or pulmonary vein compression by fibrosing mediastinitis(186).
6. Porto-pulmonary hypertension secondary to liver sarcoidosis (193).

Pulmonary LCH is a smoking related lung disease characterised by airflow obstruction, granulomatous inflammation, parenchymal nodules and cysts(194). The prevalence of PH in advanced pulmonary LCH is reported as 92-100% (195,196). The severity of PH does not appear to be related to the degree of airflow obstruction and a diffuse, proliferative pulmonary artery vasculopathy is seen (often in areas of the lung unaffected by parenchymal lesions)(196). A fibrotic, venous obliteration and capillary dilatation resembling pulmonary veno-occlusive disease (PVOD) has also been observed(197).

LAM is a rare condition characterised by proliferation of abnormal smooth muscle cells (LAM cells) predominantly around airways, blood vessels and lymphatics leading to the development of diffuse pulmonary cysts(194)(198). PH in LAM is generally mild to moderate and associated with the degree of pulmonary parenchymal involvement and lung function impairment(56,198). Other mechanisms thought to contribute to the development of PH in

LAM include dysregulation of pathways (involved in the atypical proliferation of LAM cells) leading to endothelial dysfunction, chronic hypoxic vasoconstriction and pulmonary artery wall infiltration by LAM cells (198).

2.6.3 PH in CTD-ILD

Patients with CTD-ILD (systemic sclerosis [SSc] in particular) can have multifactorial PH. They are prone to both isolated PAH and significant parenchymal lung disease ± left heart disease(56). Patients with both pulmonary fibrosis and PH have a particularly high mortality risk(199). Patients with pre-capillary PH and minimal fibrosis (often based on pulmonary function tests as opposed to degree of fibrosis on HRCT) are usually classified as having PAH whereas those with more advanced ILD are included in group 3(56). However, there is likely an overlap with some patients having features of both groups.

2.6.4 Detection and Assessment of Group 3 PH

Non-invasive screening tools for the presence of PH include serum biomarkers, lung function tests and echocardiography. It is important that a diagnosis of PH is not made during an acute exacerbation of the underlying CLD, but under stable conditions(56).

Brain natriuretic protein (BNP) or N-terminal pro-BNP are elevated in severe group 3 PH but have less sensitivity and specificity for moderate PH and may be confounded by co-existent left heart disease(56).

A lower DLCO, reduced exercise capacity and more impaired gas exchange than expected based on ventilatory impairment are seen in both ILD and COPD(56). Exercise testing can help to discriminate between an exhausted breathing reserve caused by airflow limitation and an exhausted circulatory reserve caused by PH in patients with COPD (Table 3.1) (165).

Features of exhausted circulatory reserve	Features of exhausted ventilatory reserve
Reduced oxygen pulse	Normal oxygen pulse
Mixed venous oxygen saturation at lower limit	Mixed venous oxygen saturation above lower limit

Table 3.1: Features of an exhausted circulatory versus ventilatory reserve(164)*. [CO: cardiac output, PaCO2: partial pressure of carbon dioxide in arterial blood].*

Echocardiography remains the most widely available non-invasive diagnostic tool for assessment of PH in lung disease, however it's accuracy (in determining peak tricuspid regurgitation velocity to estimate the right ventricular systolic pressure) in patients with advanced lung disease is low. It has been suggested that using additional PH signs on echocardiography (including RAA, early diastolic pulmonary regurgitation velocity, FAC, RV:LV ratio and eccentricity index) can help risk stratify ILD patients for the presence of severe PH(200). However, patients requiring definitive assessment of their PH should be referred to an expert PH centre for further assessment with RHC which remains the gold standard for diagnosis of group 3 PH(17). However, this is only appropriate if confirmation of PH and its severity will have an impact on management of the patient. It is recommended that RHC is performed in patients with CLD in the following scenarios(164,201):

1. Lung transplant assessment.
2. Clinical worsening and progressive exercise limitation or gas exchange abnormalities disproportionate to ventilatory impairment.
3. An accurate prognostic assessment is critical.
4. Suspected severe PH on non-invasive assessment and patient a candidate for further PH specific therapy or clinical trials being considered.

2.6.4.1 RHC and Haemodynamic definitions in Group 3 PH

Due to exaggerated changes in intrathoracic pressures during the breathing cycle in patients with lung disease, it is recommended that an average measurement of mean pressures is

taken over several breaths (without a breath hold) at RHC(56). Table 3.2 summarises the current haemodynamic definitions used in group 3 PH and those proposed following the 6th WSPH(56) to improve accuracy of diagnosis.

Terminology	Haemodynamics (at right heart catheterisation)	
	Current Definition	**Proposed Definition**
CLD **without** PH	mPAP <25 mmHg	mPAP <21 mmHg, or mPAP 21–24 mmHg with PVR <3 WU
CLD **with** PH	mPAP ≥25 mmHg	mPAP 21–24 mmHg with PVR ≥ 3 WU, or mPAP 25–34 mmHg
CLD **with severe** PH	mPAP >35 mmHg, or ≥25 mmHg with low cardiac output (cardiac index <2.5L/min)	mPAP ≥ 35 mmHg, or mPAP ≥ 25 mmHg with low cardiac index < 2.0L/min

Table 3.2: Current and proposed haemodynamic definitions of group 3 Pulmonary Hypertension(17,56). *[CLD: chronic lung disease, PH: pulmonary hypertension, mPAP: mean pulmonary arterial pressure, PVR: pulmonary vascular resistance, WU: wood units].*

2.6.5 Treatment of Group 3 PH

The mainstays of treatment in group 3 PH are optimisation of the underlying lung disease and long-term oxygen therapy (LTOT). LTOT has been shown to stabilise (when used for >15 hours/day) or decrease (when used for >18 hours/day) mPAP in mild to moderate PH associated with COPD but results in severe PH have been less encouraging(163,202). LTOT is recommended to maintain a PaO_2 >8 kPa(202). Ambulatory oxygen is considered when there is evidence of symptomatic benefit and correctable desaturation on exercise(17).

In patients with OHS and overlap syndrome, treatment with non-invasive ventilation has demonstrated improvements in gas exchange, sleepiness, pulmonary haemodynamics, right ventricular function and exercise capacity after 3–6 months (182–184). Similar improvements in gas exchange and haemodynamics were also seen in patients with restrictive thoracic diseases and associated PH treated with non-invasive ventilation(203).

Treatment of group 3 patients with PAH specific therapy, such as sildenafil, remains controversial with mixed results in trials. Studies have shown improvements in exercise tolerance(204) and haemodynamics(205) with some even suggesting a survival benefit(177).

However, there are also concerns that these therapies cause impaired gas exchange due to inhibition of hypoxic pulmonary vasoconstriction which contributes to ventilation-perfusion matching in patients with chronic lung disease(206,207). There is also limited data regarding their efficacy long term.

Analysis of data from the COMPERA registry(177) demonstrated that a cohort of patients with ILD and PH treated with pulmonary vasodilators, mostly phosphodiesterase 5 inhibitors (PDE5i), showed improvements in 6MWD and functional class comparable to those with IPAH. Whilst overall survival in the ILD group was poor (14% at 5 years), those with a response to treatment tended to have a better survival. A similar observation was made in patients with COPD(205).

There is growing interest into treating selected group 3 PH patients with PAH specific therapy within research and specialist centre settings and the current ESC/ERS guidelines(17) state that "patients with suspected PAH in addition to their lung diseases (characterised by mild lung parenchymal abnormalities, symptoms insufficiently explained by lung mechanical disturbances and a haemodynamic 'PAH phenotype', i.e. severe PH with high PVR and low CO) may be treated according to the recommendations for PAH, keeping in mind the potential implications of the co-existing lung disease on symptoms and response to therapy". In these patients, sildenafil is often used as the first line agent.

2.6.5.1 Sildenafil

Sildenafil is an orally active, selective, phosphodiesterase 5 inhibitor (PDE5i) and prevents PDE5 from degrading cyclic guanosine monophosphate (cGMP) which is a vasodilator and inhibitor of cell proliferation(73). It has been shown to prevent and reverse the development of PH through improvement of vasodilation and inhibition of vascular pulmonary remodelling(208). The most common side effects are due to its vasodilatory effects on the capillary smooth muscle in other parts of the body and include headache, flushing, nasal congestion, and epistaxis. Its use alongside nitrates is contraindicated due to a synergic induction of hypotension(208). Table 3.3 summarises some of the studies looking at sildenafil use in group 3 PH to date.

First author (year)	Subjects n	Inclusion criteria	Study design	Diagnosis of PH	Baseline haemodynamics	Baseline PFTs	Therapy	Duration	Primary end-point result	Other outcomes
Rao (2011)	33	GOLD III–IV	RCT	Echo: sPAP >40 mmHg	sPAP 52.7±11.9 mmHg	FEV_1 32.5±11.1%	Sildenafil 20 mg 3 times daily	12 weeks	6MWD, increased 190 m	Decrease in sPAP
Blanco (2013)	60	COPD with PH by RHC or echo	RCT	RHC: mPAP ⩾25 mmHg; echo: sPAP ⩾35 mmHg	sPAP 42±10 mmHg, mPAP 31±5 mmHg	FEV_1 32±11%	Sildenafil 20 mg or placebo 3 times daily and	3 months	Exercise endurance time, no change	No change in 6MWD, peak V'_{O_2}, QoL or oxygenation
Vitulo (2016)	28	COPD with PH by RHC	RCT (2:1)	RHC: mPAP >35 mmHg (if FEV_1 <30%), mPAP ⩾30 mmHg (if FEV_1 ⩾30%)	mPAP 39±8 mmHg, CI 2.4±0.5 $L{\cdot}min^{-1}{\cdot}m^{-2}$, PVR 7±2.6 WU	FEV_1 54±22%, D_{LCO} 33±12%	Sildenafil 20 mg 3 times daily	16 weeks	PVR, decreased 1.4 WU	Improved CI, BODE scores and QoL; no effect on gas exchange
Han (2013)	119	IPF with echo available (66% of the whole cohort)	RCT	Echo: RVSD	Not available	FVC 57%, D_{LCO} 26%	Sildenafil 20 mg 3 times daily	12 weeks	6MWD, less decline in patients with RVSD on sildenafil	Improvement in QoL in patients with RVSD

Table 3.3: Randomised controlled trials with sildenafil in lung disease – Adapted from: Randomised controlled trials with pulmonary arterial hypertension targeted therapy in lung disease, Pulmonary hypertension in chronic lung disease and hypoxia, World symposium on pulmonary hypertension series, S.D. Nathan et al(56)*.*

Use of sildenafil in COPD with PH has demonstrated improvements in haemodynamics (decrease in PVR at follow-up RHC)(209). However, there is a lack of evidence that this translates into improvements in exercise tolerance or symptoms(210,211). Open label studies with sildenafil in IPF have shown improvements in 6MWD(211) and the STEP-IPF study also demonstrated a positive effect on quality of life compared with the placebo arm(212). In patients with IPF and a predicted $DI_{CO} \leq 35\%$, sildenafil in combination with nintedanib did not provide a significant benefit as compared with nintedanib alone(213). There is currently no significant evidence to support the use of sildenafil or other PAH directed therapies in CPFE(56).

2.6.5.2 Other PAH specific therapies

Beneficial pulmonary haemodynamic effects in COPD patients with PH have been seen with bosentan (214). Inhaled prostanoids were shown to reduce mPAP and PVR while largely maintaining gas exchange in this group also(215). However, larger trials are required.

In IIPs, the ARTEMIS study(216) looking at ambrisentan in IPF and the RISE-IIP trial(217) evaluating the effect of riociguat in IIPs were both terminated early due to increased risk of disease progression with hospitalisations and mortality respectively. In IPF, bosentan was well tolerated but failed to improve time to occurrence of lung fibrosis worsening in a phase III trial (BUILD-3)(218). Negative results were also seen with macitentan with no improvements in pulmonary function tests, time to disease worsening or death(219).

In a recent multi-centre trial of inhaled Trepostinil in patients with ILD and RHC proven PH, an improvement in exercise capacity from baseline (as evidenced by a 31m increase in 6MWD compared to placebo) was documented(220).

Evidence for treatment of PH in sarcoidosis with PAH specific therapy remains inconclusive. An RCT looking at the effect of Bosentan in 35 patients showed an improvement in mPAP but no change in functional class, quality of life or 6MWD(221).

In patients with LCH, evidence regarding treatment with PAH therapies has been mixed. With some reporting the development of pulmonary oedema as seen with PVOD(196). However a more recent study showed improved haemodynamics and a trend to improved survival without oxygen worsening or pulmonary oedema(222).

2.6.6 The role of CT in Group 3 PH

CT is an important imaging modality in pulmonary diseases and is commonly used for diagnosis and phenotyping as well as follow-up, during exacerbations and assessment pre-operatively and for lung transplantation. It is readily available in clinical practice and the new generation of multidetector CT scanners allows acquisition of the whole lung in one breath hold with a sub-millimetric slice thickness(223). CT enables assessment of the pulmonary vasculature alongside the parenchyma and there are several CT findings associated with PH as discussed in Chapter 1.

2.6.6.1 CT Findings in Group 3 PH

2.6.6.1.1 PA diameter and PA to Aorta Ratio

Both the absolute PA diameter and its ratio to the diameter of the ascending aorta have been shown to correlate with mPAP in patients with PAH (93,224). PA diameter is usually defined as the widest diameter measured on axial CT images, on inspiratory acquisition, at bifurcation level and the aorta diameter measured on the same image is used to give the PA to aorta ratio (PA:Ao). The cut-off values used to detect PH are: PA diameter ≥ 29 mm and PA:Ao > 1(223). A PA:Ao > 1 is highly specific for PH and may be more reliable than PA diameter alone as it is less affected by factors such as patient size and stage of the cardiac cycle(95).

In COPD, a correlation between the mPAP and diameter of the main PA truncus has been demonstrated which remains when the main PA diameter is normalised by the diameter of the ascending aorta (PA:Ao)(223). The PA:Ao has also been shown to be linked to an increased risk of exacerbations, lower 6MWD and mortality(223).

Ando et al demonstrated a significant decrease in PA:Ao ratio after the initiation of pulmonary vasodilator therapy in COPD-PH(225).

In IPF, absolute PA diameter is not as accurate a sign of PH, however, an increased PA:Ao ratio of greater than 1 remains a reliable indicator and increased segmental artery diameter may also signal PH in IPF(178). A composite score of the PA:Ao ratio on CT and RV systolic pressure on echocardiography was significantly predictive of PH and better than either test in isolation(226).

2.6.6.1.2 Right ventricle to Left Ventricle Ratio (RV:LV)

The RV to left ventricular diameter ratio (RV:LV) has been shown to predict the presence of PH in patients with PAH(227)(228). A study by Bax et al (99) showed that a RV:LV ratio ≥ 1 in patients with ILD was strongly associated with mortality, a higher PVR at RHC and remained an independent predictor of mortality after adjusting for ILD severity and a diagnosis of IPF.

2.6.6.1.3 Parenchymal Disease

Emphysema and parenchymal distortion were the first factors to be assessed in explaining PH in COPD. Emphysema can be quantified on CT using low attenuation area percent (LAA%) derived from the voxel frequency distribution histogram with a threshold of -950 Hounsfield units most used. No relationship has been shown between LAA% and the presence or degree of PH(223). However, a study by Huang et al (229) did show a relationship with RV dysfunction with significant correlations between percent emphysema and RV end-diastolic volume, stroke volume and CO.

Limited correlation has been seen between PH severity and high-resolution CT fibrosis score(56).

2.6.6.1.4 Airways

Proximal and distal bronchial wall thickening is a common feature in COPD and a correlation between mPAP and bronchial wall thickness has been described(230).

By combining main PA diameter of ≥ 29 mm with artery-to bronchus ratio > 1 in 3 or 4 lobes, Tan et al achieved a specificity of 100% for detecting PH in patients suffering from parenchymal lung diseases(92).

2.6.6.1.5 Small Vessels

Matsuoka et al measured the % cross-sectional area of small pulmonary vessels less than $5mm^2$ normalised by lung area ($\%CSA_{<5}$) using non-contrast enhanced chest CT in patients with severe emphysema and found it inversely correlated with mPAP(231). The mPAP in this study was 25.8 ± 5.0mmHg. A later study by Coste et al using the same CT quantification method showed that $\%CSA_{<5}$ correlated to mPAP in opposite ways in COPD patients with ($r=0.53$, $p=0.01$) and without severe PH ($r=-0.57$, $p<0.001$) suggesting the ability of CT to discriminate COPD phenotypes on a small vessel-basis (232).

Further work derived the “paw” score which combines $\%CSA_{<5}$, bronchial wall thickness and paO_2 to select patients with potentially severe PH (mPAP ≥ 35mmHg) for further investigation with RHC(223,232).

CT derived 3D reconstructions of the pulmonary vasculature with deep learning processing approaches (233) can be used to calculate distal pulmonary arterial blood vessel volume (BV5). In a cohort of COPD patients, this technique demonstrated loss of distal arterial vasculature (pruning) which was associated with right ventricular enlargement and an increased risk of death(234). Both CT based markers of small vessel loss ($\%CSA_{<5}$ and BV5 normalised by lung volume) have been shown to correlate with vascular density changes in corresponding histology samples(235) suggesting they could give a useful imaging insight into the pulmonary vascular changes occurring in-vivo.

With advances in CT image acquisition, reconstruction and post-processing, there is increasing interest in the imaging of the more peripheral/small vessels of the pulmonary circulation to detect and quantify pulmonary vascular disease(236).

2.7 Study Rationale

One of the recommendations from the most recent world symposium on PH with regards to use of PAH specific therapies in CLD was to identify CLD patients with a phenotype more in keeping with PAH based on physiological testing and CT morphology (Figure 3.2) (56). This largely concentrated on parenchymal changes. As discussed previously, there are other CT findings in CLD that correlate with the severity of PH and may show change in response to treatment.

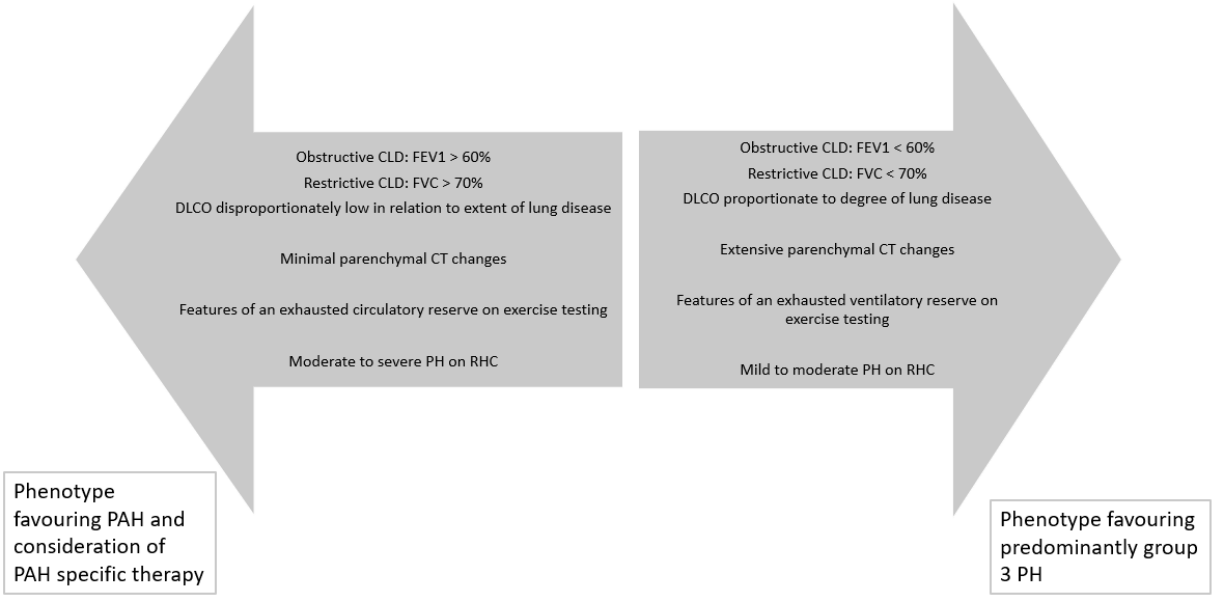


Figure 3.2: Features favouring a pulmonary arterial hypertension versus group 3 pulmonary hypertension phenotype based on physiological testing and computed tomography morphology(56). *[CLD: chronic lung disease, FEV1: forced expiratory volume in 1 second, FVC: forced vital capacity, DLCO: Diffusing capacity of the lung for carbon monoxide, PH: pulmonary hypertension, RHC: right heart catheterisation, PAH: pulmonary arterial hypertension].*

CT is easily accessible in all NHS settings and if there are features on imaging that may suggest response to treatment with PAH specific therapy this would provide a non-invasive tool to help identify patients that may benefit from referral to specialist centres for further work-up.

2.8 Hypothesis, Aims and Objectives:

2.8.1 Hypothesis

CT derived imaging measures in group 3 PH correlate with disease severity, treatment response and mortality:

- Previously documented CT measures of disease severity apply in this cohort of group 3 PH.
- Patients with group 3 PH who show response to PAH specific therapies have a CT phenotype that differs from those who do not respond.

- CT findings associated with group 3 PH demonstrate improvement following treatment.
- Markers of severity and treatment response predict mortality.

2.8.2 Aims:

To identify which CT measures are most able to predict disease severity, treatment response and mortality in patients with group 3 PH.

2.8.3 Objectives:

- Document baseline CT findings in a cohort of group 3 PH patients treated with sildenafil.
- Document CT findings following treatment with sildenafil in the same cohort.
- Identify whether there are any differences between baseline CT findings in responders to sildenafil treatment and non-responders that may predict response.
- Demonstrate if there were any improvements in CT parameters in those patients who showed response to treatment.
- Identify whether these CT measures are associated with mortality.

2.9 Methods

A retrospective study of patients with severe group 3 PH (defined as mPAP ≥ 35mmHg at RHC) treated with sildenafil at Royal Brompton Hospital between March 2015 and May 2019 was conducted. Sildenafil was initiated at 12.5-25mg TDS.

Eligible patients were identified by performing searches on the trust's electronic patient records system (Infoflex® digital healthcare system). Patients with a diagnosis of sarcoidosis or connective tissue disease were excluded to maintain a "pure" group 3 cohort.

Inclusion Criteria:
Diagnosis of severe group 3 PH (with mPAP ≥ 35mmHg)
Treatment with Sildenafil
Baseline CT imaging
Exclusion Criteria:
Concurrent treatment with another PH specific therapy
Diagnosis of sarcoidosis or connective tissue disease

Table 3.4: Eligibility Criteria. [PH: pulmonary hypertension, mPAP: mean pulmonary arterial pressure, CT: computed tomography].

In addition to patient demographics and diagnoses, the following variables were documented at baseline (pre-treatment initiation) and follow up:

- Haemodynamics from RHC
- Echocardiography parameters
- Serum BNP levels
- WHO functional class
- 6MWD
- E-10 scores

The below CT measurements were recorded by a cardiothoracic radiologist (blinded to patient's clinical outcomes) from imaging at baseline and follow-up where available (as described in Chapter 2: Methods):

- PA diameter
- PA:Ao
- RV diameter
- RV:LV
- Distribution, extent and pattern of emphysema or fibrosis where applicable

Patients were defined as "responders" or "non-responders" to treatment with sildenafil based on achieving one or more of the criteria below (based on cut-offs from previous studies in similar populations(177,205):

1. Improvement in PVR ≥ 20%

2. Improvement in 6MWD ≥ 30m
3. Improvement in WHO FC

Mortality data was also collected. Follow up time for mortality analysis was from the date of sildenafil initiation, until either the primary outcome (death) occurred, or the patients were censored at last data review (date of last screen 08/10/2019).

Data are mean ± SD or median (range). Statistical analysis was carried out using paired t and Wilcoxon signed rank tests for continuous data, Fisher's exact test for categorical data, Spearman's rank correlation and logistic regression.

2.10 Results

2.10.1 Patient demographics and Baseline variables

A total of 24 patients were included in this study with mean age 65.3 ± 10.0 years; 54.2% were male. The underlying categories of CLD diagnoses were ILD (n=9, 37%), COPD (n=5, 21%), CPFE (n=7, 27%) and other (n=3, 13%). "Other" CLD diagnoses consisted of bronchiectasis, congenital scoliosis, and obesity hypoventilation syndrome. Sub-types of ILD included IPF (n=4), chronic hypersensitivity pneumonitis (n=3) and fibrotic cryptogenic organising pneumonia (n=2). Patients with underlying COPD were GOLD grade 1-3. Table 3.5 and Figure 3.3 demonstrate patient demographics and underlying CLD.

Mean lung function was FEV1 65.5 ± 27.7% predicted, FVC 76.4 ± 32.7% predicted and TLCO 23 ± 6.0% predicted. At RHC, mPAP was 45.6 ± 9.5 mmHg and PVR 10.8 ± 4.3 wood units. Patients were predominantly in WHO functional class III.

Baseline Patient Demographics (n=24)	
Age	65.3 ± 10.0 years
Gender	54.2% males
WHO Functional Class: II,III,IV	8.3, 79.2, 12.5 %
E-10	38 (17-50)
6MWD	192.0 ± 78.7 m
BNP	427.0 (52.2-2022.0) ng/L
Lung Function:	
FEV1 % Pred	65.5 ± 27.7 %
FVC % Pred	76.4 ± 32.7%
TLCO % Pred	23.0 ± 6.0%
KCO % Pred	43.1 ± 21.8%
RHC:	
mPAP	45.6 ± 9.5mmHg
PVR	10.8 ± 4.3 wood units
CO	3.7 ± 0.6 L/min
PCWP	8.8 ± 3.5 mmHg
RAP	5.9 ± 4.3 mmHg
ECHO:	
TRV	4.2 ± 0.6 m/s
RVSP	80.5 (41.0-148.0) mmHg
RAA	30.0 (22.0-97.0) cm^2
Pulmonary acceleration time	74.0 (32.0-108.0) ms
TAPSE	1.7 (0.4-2.7) mm
RV base	5.2 (3.2-6.2) cm
RV FAC	18.0 (6.0-39.0) %

Table 3.5: Baseline patient demographics (n=24). [WHO: World Health Organisation, E-10: emphasis 10, 6MWD: 6 minute walk distance, BNP: B-type natriuretic peptide, FEV1: forced expiratory volume in 1 second, FVC: Forced vital capacity, TLCO: transfer factor for carbon monoxide, KCO: carbon monoxide transfer co-efficient, mPAP: mean pulmonary arterial pressure, PVR: pulmonary vascular resistance, CO: cardiac output, PCWP: pulmonary capillary wedge pressure, RAP: right atrial pressure, TRV: tricuspid regurgitation velocity, RVSP: right ventricle systolic pressure, RAA: right atrial area, TAPSE: tricuspid annular plane systolic excursion, RV: right ventricle, FAC: fractional area change].

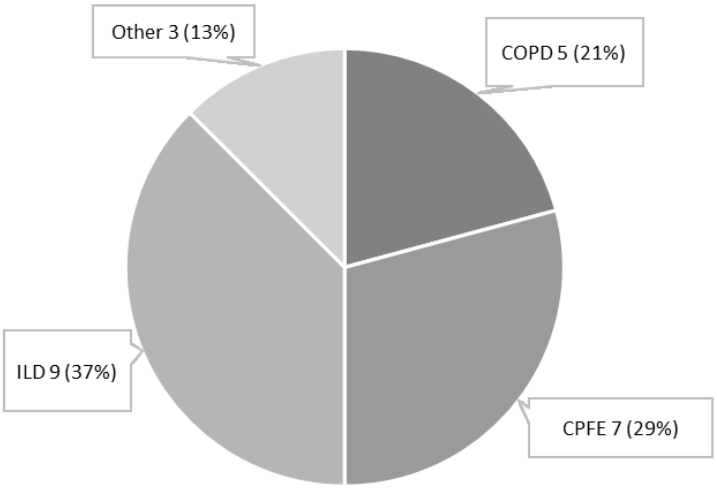


Figure 3.3: Underlying Chronic Lung Disease Diagnosis (n=24). "Other" (n=3) – bronchiectasis, congenital scoliosis, and obesity hypoventilation syndrome. Sub-types of ILD - IPF (n=4), chronic hypersensitivity pneumonitis (n=3) and fibrotic cryptogenic organising pneumonia (n=2). [COPD: chronic obstructive pulmonary disease, ILD: interstitial lung disease, CPFE: combined pulmonary fibrosis and emphysema, IPF: idiopathic pulmonary fibrosis].

2.10.2 Baseline CT Measurements

Table 3.6 summarises the CT measurements pre-treatment.

Baseline CT Characteristics	
Mean PA Diameter (n=24)	36.3 ± 5.4mm
PA:Aorta (n=24)	1.0 (0.9-1.7)
RV Diameter (Mid Ventricle) (n=17)	45.8 (29.4-58.7)mm
RV:LV (n=17)	1.4 (0.9-2.0)
% Emphysema (n=14)	30.0 (5.0-55.0)%
% Fibrosis (n=16)	30.0 (5.0-50.0)%

Table 3.6: Baseline CT characteristics. [PA: pulmonary artery, RV: right ventricle, RV:LV: right ventricle to left ventricle ratio].

The mean PA diameter was 36.3 ± 5.4mm. The RV:LV ratio (1.4[0.9-2.0]) and PA:Ao ratio (1.0[0.9-1.7]) were both ≥ 1.0. RV (45.8 [29.4-58.7]mm) diameter was enlarged. Patients with emphysema present were quantified as having 30.0 (5.0-55.0) % emphysema changes in the lungs and equally those with ILD had 30.0 (5.0-50.0) % fibrotic change.

2.10.3 Post treatment analysis

Median follow-up between initiation of Sildenafil and re-assessment was 4.0 (1.0-7.0) months. 9 (37.5%) patients had post treatment RHCs, and 10 (41.6%) patients had repeat CT scans.

There were no statistically significant improvements in haemodynamics (mPAP, cardiac output or pulmonary vascular resistance [Table 3.7]) in those who underwent repeat RHCs, CT (Table 3.8), echo or BNP measurements following treatment with sildenafil.

RHC Variable	Pre- Treatment	Post -Treatment	P value
mPAP (mmHg)	44.6 ± 10.1	44.9 ± 10.7	0.888
CO (L/min)	3.4 ± 0.5	3.6 ± 0.7	0.375
PVR (WU)	11.0 ± 2.8	10.2 ± 4.6	0.436

Table 3.7: Change in haemodynamics at right heart catheterisation following treatment with Sildenafil (n=9, median time from treatment initiation to reassessment = 4.0 [1.0-7.0] months). [RHC: right heart catheterisation, mPAP: mean pulmonary arterial pressure, CO: cardiac output, PVR: pulmonary vascular resistance].

There was a reduction in BNP of 21.6 ng/L, but this was not statistically significant (p=0.85).

An improvement in 6MWD was seen (in n=7 patients where paired values were available), from 230.7 ± 61.4m to 300.6 ± 61.0m (p=0.009) (Figure 3.4).

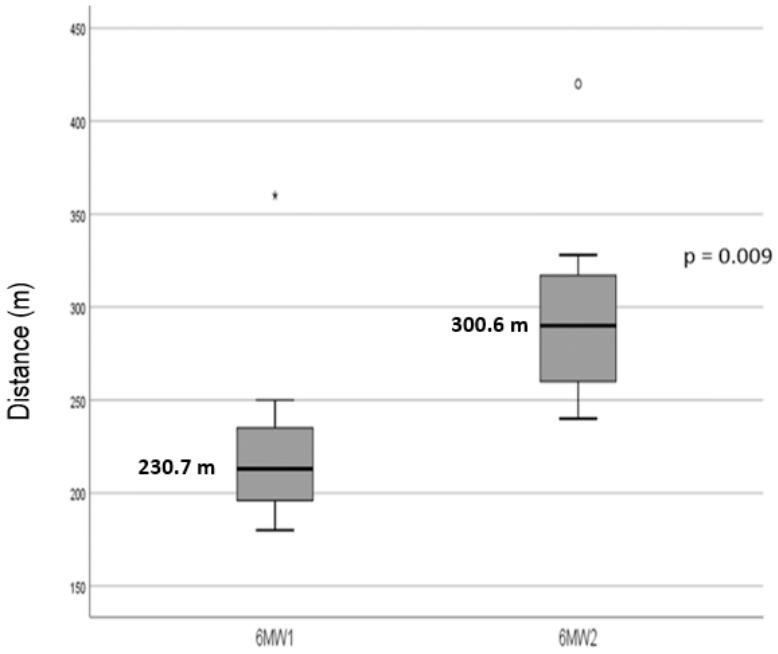


Figure 3.4: Boxplot of change in 6-minute walk distance following treatment with Sildenafil (n=7, median time from treatment initiation to reassessment = 4.0 [1.0-7.0] months). An improvement in 6-minute walk distance from 230.7 ± 61.4m to 300.6 ± 61.0m was seen with a significance value of p=0.009. [6MW1: baseline 6-minute walk distance, 6MW2: 6-minute walk distance post treatment].

2.10.4 CT Measurements

No significant correlations were found between previously documented CT markers of disease severity (PA diameter, Pa:Ao ratio, RV:LV ratio and % emphysema) (63,64,68,69,70,71) and standard RHC measures of disease severity (mPAP, PVR and CO) in this cohort (Table 3.8).

		CT measurements			
		PA diameter (n=24)	**PA:Ao (n=24)**	**RV:LV (n=17)**	**% emphysema (n=14)**
RHC measurements	**mPAP**	0.4 (0.136)	0.4 (0.107)	0.2 (0.577)	0.17 (0.648)
	PVR	0.1 (0.680)	0.1 (0.701)	-0.2 (0.615)	0.3 (0.374)
	CO	0.05 (0.863)	0.03 (0.903)	-0.1 (0.851)	-0.1 (0.749)

Table 3.8: Spearman's rank correlation of baseline CT and RHC variables - displayed as R_s (p value). [CT: computed tomography, PA: pulmonary artery, PA:Ao: pulmonary artery to aorta ratio, RV:LV: right ventricle to left ventricle ratio, RHC: right heart catheterisation, mPAP: mean pulmonary arterial pressure, PVR: pulmonary vascular resistance, CO: cardiac output, R_s: spearman's rank correlation coefficient].

There were no statistically significant improvements in CT measures following treatment (in n=10 patients who had paired CT scans). There was a significant worsening of PA:Ao ratio (Z=-2.2, p=0.028) and % fibrosis (Z= -2.4, p=0.016).

CT Measurement	Pre-Treatment	Post-Treatment	P value
Mean PA Diameter, mm (n=10)	35.9 (27.7-51.0)	39.9 (29.7-49.6)	0.074
PA:Aorta (n=10)	1.0 (0.9-1.7)	1.1 (0.9-1.6)	**0.028***
RV Diameter (Mid Ventricle), mm (n=4)	45.8 (29.4-58.7)	42.7 (27.6-47.9)	0.655
RV:LV (n=4)	1.4 (0.9-2.0)	1.5(0.8-2.1)	0.180
% Emphysema (n=5)	30.0 (5.0-55.0)	25.0 (5.0-45.0)	0.257
% Fibrosis (n=8)	30.0 (5.0-50.0)	50.0 (5.0-60.0)	**0.016***

Table 3.9: Pre versus post-treatment CT measurements. (Median time from treatment initiation to reassessment = 4.0 [1.0-7.0] months). There was a significant decline in PA:Ao ratio and % fibrosis. [CT: computed tomography, PA: pulmonary artery, PA:AO: pulmonary artery to aorta ratio, RV: right ventricle, RV:LV: right ventricle to left ventricle ratio].

2.10.5 Responders versus Non- Responders

12 patients were classed as responders (50%, 95% CI: 31.4-68.6) based on meeting ≥ 1 of the pre-defined criteria of improvement in PVR, WHO functional class or 6MWD. There were no

significant differences in baseline variables between the responder and non-responder groups (Table 3.10).

Baseline Variable	Responder	Non-Responder	p-value
Lung Function:			
FEV1 % Pred	55.1±26.8	75.1±26.1	0.077
FVC % Pred	66.0±29.4	85.9±33.8	0.229
TLCO % Pred	23.4±6.8	23.1±5.4	0.959
KCO % Pred	48.0±26.2	47.6±36.7	0.397
Haemodynamics:			
mPAP (mmHg)	45.0±10.8	46.6±8.1	0.651
PVR	10.2±5.2	11.6±2.7	0.219

Table 3.10: Comparison of baseline variables in responders (Meeting ≥ 1 of criteria, n=12) versus non-responders (n=12). There were no statistically significant differences between the 2 groups. [FEV1: forced expiratory volume in 1 second, FVC: forced vital capacity, TLCO: transfer factor for carbon monoxide, KCO: carbon monoxide transfer co-efficient, mPAP: mean pulmonary arterial pressure, PVR: pulmonary vascular resistance].

Table 3.11 shows the breakdown of the patients defined as responders. Of the 2 that responded by > 1 criteria, one patient saw an improvement in WHO functional class and 6MWD and the other in PVR and 6MWD. Further sub-group analysis of the group that achieved an improvement in WHO FC (Table 3.12 and Figure 3.5) showed lower baseline % predicted FEV1 (31.3±11.8 in responders vs 70.6±25.8 in non-responders, p=0.008) and FVC (39.3±9.0 in responders vs 81.9±31.2 in non-responders, p=0.049). mPAP and PVR were higher in the responder group but did not reach statistical significance.

Response Criteria	Total
Improvement in 6MWD ≥ 30m	4
Improvement in WHO Functional class	3
Improvement in PVR ≥ 20%	3
Responder by > 1 of above criteria	2
Grand Total	**12**

Table 3.11: Breakdown of criteria met by responders to treatment with sildenafil (n=12). Of the 2 that responded by > 1 criteria, one patient saw an improvement in WHO functional class and 6MWD and the other in PVR and 6MWD. [6MWD: 6-minute walk distance, WHO: World Health Organisation, PVR: pulmonary vascular resistance].

Variable	Responder	Non Responder	p-value
Lung Function:			
FEV1 % Pred	31.3±11.8	70.6±25.7	**0.008***
FVC % Pred	39.2±9.0	81.9±31.2	**0.046***
TLCO % Pred	24.5±9.1	23.1±5.9	0.752
KCO % Pred	73.1±47.8	45.1±29.7	0.233
Haemodynamics:			
mPAP	58.0±5.7	43.9±8.7	0.052
PVR	14.9±11.2	10.2±3.1	0.602

Table 3.12: Comparison of baseline variables in responders (n=4) versus non-responders (n=20) to sildenafil treatment by WHO functional class criteria. Baseline FEV1 and FVC % predicted were significantly lower in the responder group. [FEV1: forced expiratory volume in 1 second, FVC: forced vital capacity, TLCO: transfer factor for carbon monoxide, KCO: carbon monoxide transfer co-efficient, mPAP: mean pulmonary arterial pressure, PVR: pulmonary vascular resistance].

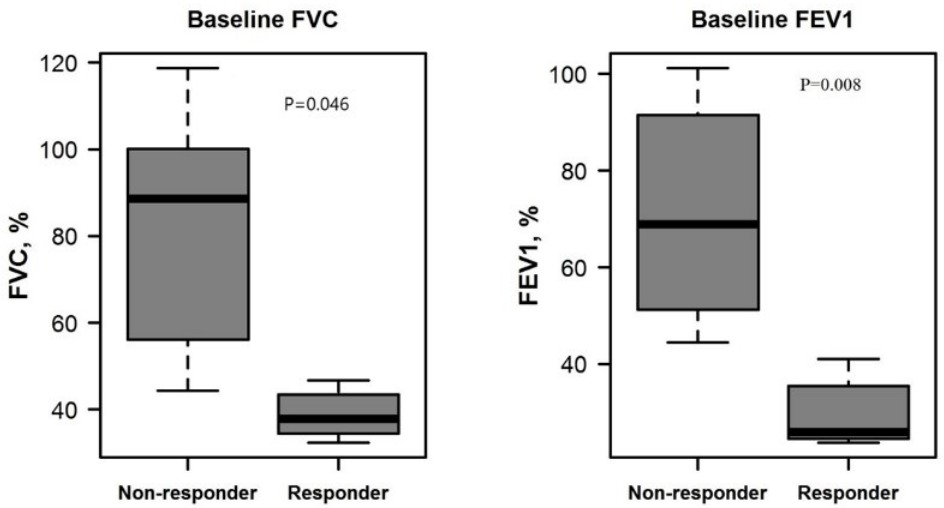


Figure 3.5: Boxplot of baseline % predicted FEV1 and FVC in responders (n=4) vs non-responders (n=20) by World Health Organisation functional class criteria. Both % predicted FEV1 and FVC were significantly lower in the responder group. [FEV1: Forced expiratory volume in 1 second FVC: forced vital capacity].

There were no significant differences between baseline CT measurements in responders compared to non-responders when analysed as meeting ≥ 1 response criteria (Table 3.13) or on sub-group analysis based on individual response criteria (PVR, WHO functional class, 6MWD). No significant improvements in CT measurements were seen post-treatment when sub-group analysis was carried out in the responder group.

Logistic regression to analyse the effect of the CT variables on response to treatment did not yield a statistically significant model.

CT Measurement	Responder	Non-Responder	p value
Mean PA Diameter, mm	35.9 (27.7-51.0)	32.2 (27.7-37.7)	0.326
PA:Aorta	1.0 (0.9-1.7)	1.0 (0.9-1.2)	0.729
RV Diameter (Mid Ventricle), mm	45.8 (29.4-58.7)	49.4 (43.3-58.7)	0.149
RV:LV	1.4 (0.9-2.0)	1.5 (1.3-1.9)	0.773
% Emphysema	30.0 (5.0-55.0)	15.0 (5.0-30.0)	0.158
% Fibrosis	30.0 (5.0-50.0)	20.0 (10.0-50.0)	0.423

Table 3.13: Comparison of baseline CT measurements in responders versus non-responders based on meeting ≥ 1 response criteria. There were no statistically significant differences. [CT: computed tomography, PA: pulmonary artery, RV: right ventricle, RV:LV: right ventricle to left ventricle ratio].

2.10.6 Symptomatic benefit and Adverse effects

3 (12.5%) patients experienced adverse effects (deterioration of oxygenation [n=2]) and hypotension [n=1]).

14 (58.3%) patients reported an improvement in symptoms, however there was no significant improvement in E-10 scores or WHO functional class. The predominant improvement reported was reduced shortness of breath. 2 patients stated they had less syncopal symptoms and 1 demonstrated a reduction in peripheral oedema (without any concomitant medication changes).

2.10.7 Mortality

7 (29%) patients had died at the point of censorship. Mortality was lower in the responder group; however, this did not reach statistical significance (1 versus 6, 2-sided p-value = 0.069). There were no significant differences in baseline CT measurements between the alive and dead patients and the logistic regression model was not statistically significant.

2.11 Discussion

The baseline variables of our cohort were in keeping with those previously described for CLD associated with a PAH or vascular phenotype(56). In that, FEV1 and FVC % predicted were relatively preserved and both greater than 60% and 70% predicted respectively with a disproportionately low TLCO % predicted (23.0±6%). 30.0% emphysema (5.0-55.0%) and fibrosis (5.0-50.0%) changes were seen on baseline CT, in keeping with the theory that severe PH in CLD may occur independently to the underlying CLD. It is estimated that a loss of > 80% normal lung structure is required to provoke PH(164), supporting a separate vascular phenotype.

This study examined the short-term effects of sildenafil treatment with a median time to follow up of 4 months. Unfortunately, less than 50% of patients had follow-up CT scans and RHC which limited the data available for analysis at follow-up.

No statistically significant improvements in haemodynamics were seen at repeat RHC. However, 3 patients (33.3% of those that had a repeat RHC) did show a ≥20% improvement in PVR following treatment. Of these, 1, also had an improvement in 6MWD from 203m to 270m.

In this cohort of patients, a significant improvement was seen in 6MWD from 230.7 ± 61.4m to 300.6 ± 61.0m (p=0.009) following treatment. Less mortality was seen in the responder group however this was not statistically significant. Similar trends with survival were seen in responders to vasodilator therapy in previous studies(177,205).

Sub-group analysis of patients who showed improved WHO functional class with treatment showed a lower baseline FEV1 (31.3 ± 11.8 in responders versus 70.6 ± 25.7 in non-responders) and FVC (39.2 ± 9.0 versus 81.9 ± 31.2) % predicted which is not in keeping with the preserved lung function group 3 PH phenotype that is thought to be more responsive to PAH specific treatment. A higher mPAP was seen in responders (58.0 ± 5.7mmHg) versus non-responders (43.9 ± 8.7mmHg) but this did not quite reach statistical significance (p=0.052).

Previous work by Ando et al(225) showed an improvement in PA:Ao with vasodilator therapy in COPD with PH. This was not replicated in this study where no improvements were seen in CT parameters measured post treatment and there were no significant differences in CT

findings between responders and non-responders. PA:Ao ratio and % fibrosis were significantly worse at follow-up CT.

None of the CT variables examined showed strong or statistically significant correlations with mPAP, PVR or CO in this cohort.

Increases in PA diameter, PA:Ao, RV diameter and RV:LV ratio (the predominant CT variables assessed) are right-heart associated structural changes which occur secondary to increased mPAP(95). Therefore, whilst they can suggest the presence of PH, they are unlikely to be sensitive enough to recognise the vascular phenotype which may be associated with treatment response. Equally, they are less likely to be responsive to short term haemodynamic improvements with treatment and show less reversibility.

Vascular alteration of small pulmonary vessels is one of the characteristic features of PH in COPD(231) and other CLD. Histological studies suggest that vascular remodelling leads to reduced distensibility of small pulmonary vessels with a resultant increase in PVR and PH(237). Concentrating on imaging of the smaller, more distal pulmonary vessels where these changes occur and where pulmonary vasodilators primarily act is therefore more likely to yield associations with response to treatment than the macroscopic findings discussed in this chapter which occur further downstream in the disease process.

Novel CT based measurements are already being explored. CT quantification of small pulmonary vessels (%$CSA_{<5}$) has been shown to predict mPAP (231,232) in COPD and when combined with measures of bronchial wall thickness and paO2 can predict severe PH(232). Automated vessel segmentation on non-contrast CT scans has been used to examine arterial, venous, and lobar circulation in the lung as a measure of the loss of distal vasculature(238). Measures derived from these techniques are related to changes of vascular density as assessed by histology(235).

A study be Iyer et al (104) looking at perfused blood volume (PBV [as a surrogate for blood flow]) and PBV coefficients of variation (measures of spatial blood flow heterogeneity) on DECT in patients with emphysema was able to demonstrate changes in these variables following treatment with sildenafil. These changes reflected an improvement in peripheral perfusion and support the ability of CT based measurements of peripheral blood flow to show response to vasodilator treatment.

Preliminary work by Rahaghi et al showed quantitative changes in pulmonary vascular calibre and volume in response to inhaled nitric oxide using automated methods on non-contrast CT scans(236).

These CT based techniques could provide novel ways of predicting and assessing response to PAH specific therapy by providing imaging-based biomarkers of pulmonary vascular disease. The use of a cardiac MRI derived PA/RV model has also been proposed as a means of accurate (sensitivity 92%, specificity 80%, positive predictive value 96% and negative predictive value 63%, AUC 0.93, $p<0.0001$), non-invasive estimation of mPAP and the presence of PH in COPD(239).

2.11.1 Study Limitations

This was a single-centre, retrospective, observational study and therefore had several limitations including a small and heterogenous study population with in-complete data available at follow-up. The number of patients in each lung disease phenotype was small so it was not possible to tease out differences between the underlying CLD types. Meaningful regression analyses were also prevented by small numbers. Any statistically significant results should be interpreted with caution. Improvements seen, particularly with subjective outcomes, may be confounded by placebo effect.

2.12 Conclusion

The CT measurements assessed in this study did not correlate with standard markers of PH severity at RHC, predict response, show improvement with treatment, or relate to mortality.

Sildenafil appears well tolerated and safe in most patients with an improvement in 6MWD observed. There are signals that some patients do respond to treatment and that this may improve prognosis, but larger, prospective, RCTs with longer follow up are required.

Larger, prospective, longitudinal studies concentrating on CT imaging of the smaller vessels in different CLD groups is also needed to gain a better understanding of which CT derived imaging biomarkers may be useful in the assessment and follow-up of patients with PH.

Chapter 4: Pulmonary artery morphology and calcification on Computed Tomography in Eisenmenger Syndrome

2.13 Introduction

2.13.1 Eisenmenger syndrome

Eisenmenger syndrome (ES) is an advanced form of pulmonary arterial hypertension (PAH) associated with congenital heart disease (CHD). It occurs when a large congenital left-to-right shunt causes increased flow through the pulmonary vasculature resulting in severe pulmonary vascular disease and reversal of the shunt (27,240). Figure 4.1 summarises the development of ES.

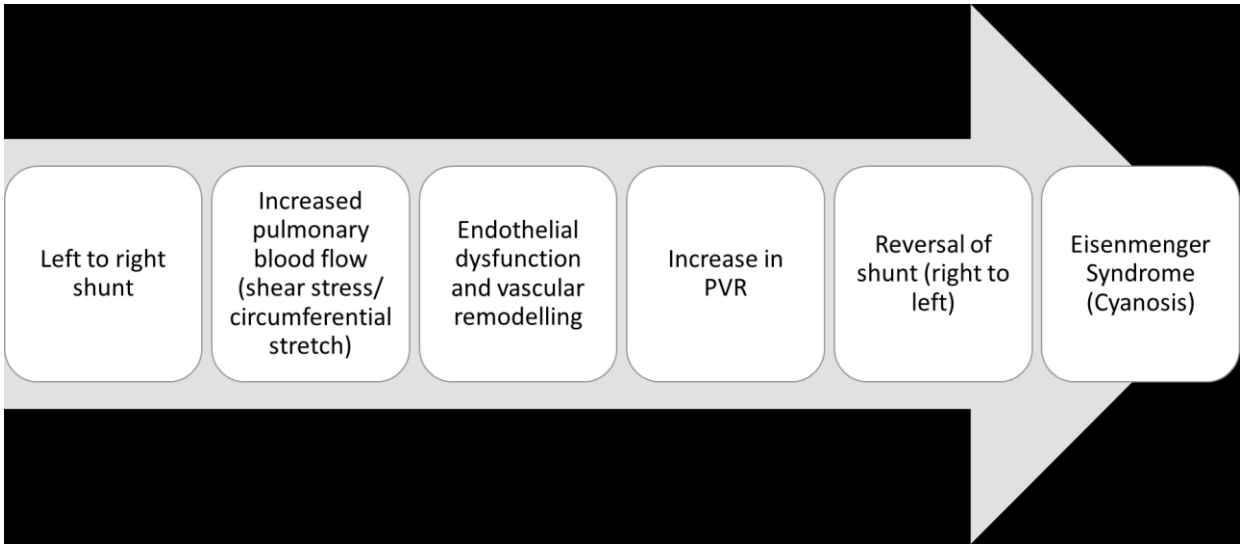


Figure 4.1: Mechanisms involved in the development of Eisenmenger Syndrome(27,241)*. A systemic to pulmonary circulation connection leads to a left to right shunt with increased*

pulmonary blood flow and pulmonary vascular injury. This results in increased PVR and a reversal of the shunt (Eisenmenger Syndrome). [PVR: pulmonary vascular resistance].

The shunting associated with PAH can occur at different levels and the risk of developing PAH and ES depends on the location and size of the shunt lesion as well as other factors such as the presence of Down's syndrome(242). The cardiac defects most common to ES are ventricular septal defects (VSD), atrial septal defects (ASD), atrioventricular septal defects (AVSD) and patent ductus arteriosus(240,243). The underlying CHD defects can be classified anatomically as pre-tricuspid (e.g., ASD), post-tricuspid (e.g., VSD) or complex (e.g., AVSD)(25,242).

The increased volume of blood flowing from the CHD defect through the pulmonary circulation overloads it and leads to increased PVR and pulmonary artery pressure (PAP)(244). If the shunt is significant and persistent, there is progressive pulmonary vessel disease and an irreversible PAH develops(245).

The pulmonary vascular disease in CHD demonstrates similar pulmonary histology to other types of PAH(50). Endothelial damage is associated with degeneration of the extracellular matrix, release of growth factors, activation of coagulation pathway, increased production of vasoconstrictors and decreased production of vasodilators(246,247). If PAP exceeds systemic pressure, there is reversal of blood flow through the CHD defect producing a bidirectional or pulmonary-to-systemic shunt with resultant hypoxaemia and central cyanosis(245,247). This represents the final stage of CHD with PAH and is called ES(248).

Development of ES in patients with complex CHD is associated with a 10 to 12 fold increase in mortality(249). However, patients with ES exhibit a more favourable haemodynamic profile and prognosis compared to patients with idiopathic PAH(250) through initial preservation of right ventricular (RV) function and alleviation of raised PA pressure via the right to left shunt(96).

With post-tricuspid shunts, the RV may not remodel at birth and remains hypertrophied, preserving the foetal-like phenotype and sustaining elevated PAP better and longer compared with IPAH(251). The prognosis is worse in ES patients with pre-tricuspid defects where the

RV response appears to resemble that of IPAH with dilatation and progressive RV dysfunction(252).

2.13.2 CT findings in Eisenmenger syndrome

Some CT features of ES are similar to those seen in idiopathic and other forms of PAH(244). Commonly encountered CT findings can be divided into vascular, cardiac, and pulmonary parenchymal.

2.13.2.1 Vascular

Severe dilatation of the main pulmonary arteries is characteristic of ES and the result of chronically high volume and pressure and intrinsic PA wall abnormalities relating to the CHD (244,253). Dilatation of the main PAs is often out of proportion to PAP at right heart catheterisation and may be due to inherent medial abnormalities of elastin and smooth muscle which can also lead to aneurysmal PAs(254). PA diameters can reach 6 to 7 cm in patients with ES(255).

Secondary to the severe dilatation and turbulent blood flow within the PAs, ES patients are prone to the development of in-situ thrombosis and intramural calcification(253). Other mechanisms thought to contribute to thrombus formation include damage to the endothelium with activation of procoagulants and impairment in the fibrinolytic system(244,253). The endothelium can be damaged by the increased shear stress on the vessel walls, increased blood viscosity and chronic hypoxaemia(256). The prevalence of PA in-situ thrombosis in ES has previously been documented as 20%(257,258).

Intramural calcification is mostly seen in the proximal pulmonary arteries and involves the tunica media rather than the intima, which is more affected by atherosclerosis(254).

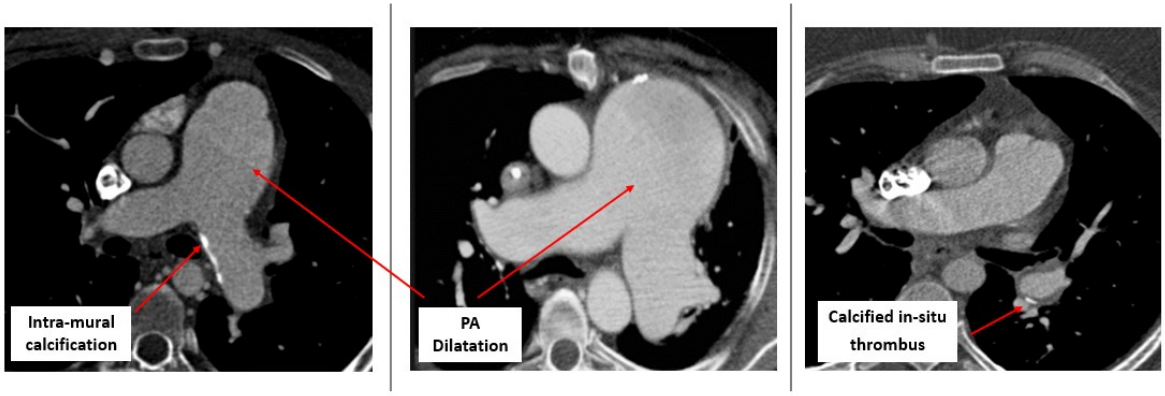


Figure 4.2: Trans-axial CT sections demonstrating PA dilatation, intra-mural calcification, and calcified in-situ thrombus. [PA: pulmonary artery, CT: computed tomography].

Pulmonary neovascularisation (proliferation of small, serpiginous, subpleural vessels, often arising from centrilobular arterioles(96)) is significantly more common in ES than other aetiologies of PAH, particularly in patients with post-tricuspid defects where pulmonary vascular disease develops early in life(259).

Hypertrophic bronchial arteries (appearing as curvilinear mediastinal vessels greater than 2mm diameter(244)) are often found in ES and occur as a result of hypoxia causing increased blood flow through the bronchial arteries to contribute to increasing blood oxygenation(244). Reversal of the shunt in ES reduces blood flow in the pulmonary arteries and stimulates the formation of collateral vessels(260). Bleeding from hypertrophic bronchial arteries may be associated with alveolar haemorrhage and haemoptysis which is often recurrent and can be life-threatening(244).

2.13.2.2 Cardiac

Chronic pressure overload leads to remodelling of the RV, characterised by chamber dilatation and hypertrophy of the free wall (wall thickness > 5 mm)(261). Bowing of the interventricular septum towards the left ventricle (D-shape interventricular septum, as seen in the short axis view in echocardiography) is seen with further increases in pressure in the RV(262).

Some left-to-right shunts such as sinus venosus defects, partial anomalous pulmonary venous return, and patent ductus arteriosus may be detected on CT whilst missed with echocardiography(244).

2.13.2.3 Pulmonary Parenchymal

Centrilobular ground glass nodules are a well-known feature of PAH(263). In PAH associated with CHD, ground glass nodules have characteristic high attenuation at the lobular core and normal attenuation at the lobular margin with a relatively diffuse distribution(264). Infarction, caused by emboli from proximal thrombosis, presents as peripheral areas of parenchymal consolidation and both it and associated pleural effusions may be haemorrhagic because of the haemostatic defects(244).

2.14 Study Rationale

CT is often utilised in the clinical assessment of patients with ES and is low risk and minimally invasive. It can provide detailed information on the anatomy of the PAs, and the presence, distribution, and quantification of calcium. Whilst common CT pulmonary vascular findings and their prognostic significance are well documented in other forms of PH, there is limited literature regarding their significance in ES. PA calcification, in particular, has limited data published about it, with most publications being historic case reports and series(265–268). Coronary artery calcification is a known risk factor for adverse outcomes in the general population and in patients with coronary artery disease(269) and its causes and pathogenesis are well documented. The finding of PA calcification is quite unique to ES, but little is known about which patients develop it and whether this finding is associated with clinical outcome.

2.15 Hypothesis, Aims and Objectives:

2.15.1 Hypothesis

Quantitative CT markers of PA morphology, including the presence and extent of PA calcification, correlate with disease severity and predict mortality in ES.

2.15.2 Aims

Investigate relationships between CT measures of PA morphology (including PA calcification) and markers of disease severity and mortality.

2.15.3 Objectives

- Identify cohort of ES patients with CT scans.
- To document previously described and novel measures of PA morphology and calcification in this cohort.
- To determine whether these measures relate to mortality.

2.16 Methods

A single-centre retrospective analysis of CT scans in ES patients was performed. All patients known to the PH service with a diagnosis of ES and an adequate quality CT scan were included. Where patients had more than 1 CT scan available, the most recent was used.

The following measurements were documented (as described in the Methods chapter): PA diameter, PA trunk volume, presence of PA thrombus and calcification. The degree of PA calcification was further evaluated using a modified Agatston score (as used in assessing coronary artery calcification)(152). The distance between the pulmonary bifurcation and the most distal calcification was measured on curved planar reformatted images using the

Intuition Viewer 3D workstation and the most distal generation of PA affected by calcification was recorded.

Mortality data was also collected. Follow up time for mortality analysis was from the date of CT, until either the primary outcome (death) occurred, or the patients were censored at date of last review (04/02/2019).

A sample of 15 patients had measurements taken by both reviewers to look for reliability of novel CT measurements (PA trunk volume and measures of PA calcification).

Data are mean ± SD or median (range). Spearman's rank correlation, intraclass correlation coefficient, logistic and Cox regression were used for analysis of data.

2.17 Results

2.17.1 Patient demographics

A total of 104 ES patients with adequate quality CT imaging were included: 39 (37.5%) male, median age 33.0 [14.3 - 69.5] years. 35 (33.7%) patients had Down syndrome. The underlying cardiac defect was defined as pre-tricuspid in 4 (3.8%) patients, post-tricuspid in 65 (62.5%) patients and complex in 35 (33.7%) patients. Most patients (96.2%) were in WHO functional class 3 at the time of their CT scan. Median 6MWD was 290.0m (80.0 - 540.0m) and oxygen saturations at rest were 85% (62 - 98%).

Patient Demographics (n=104)	
Age (years)	33.0 (14.3-69.5)
Male	39 (37.5%)
Down Syndrome	35 (33.7%)
Underlying Cardiac Defect:	
Pre-tricuspid	4 (3.8%)
Post-tricuspid	65 (62.5%)
Complex	35 (33.7%)

Table 4.1: Summary of Patient Demographics (n=104).

2.17.2 PA diameter and trunk volume

Dilatation of the main PA (>30mm) was present in 84 (82.4%), and this was severe (>50mm) in 5(4.9%). Median PA diameter was 35.0mm (19.0 - 60.0mm). Median pulmonary trunk volume was 81.5mm^3 (26.0 – 400.0mm^3).

A small correlation was seen between age and PA diameter ($r_s = 0.3$, $p = 0.006$) and a moderate correlation with PA trunk volume ($r_s = 0.5$, $p < 0.001$) (Table 4.2 and Figure 4.3).

	Correlation of Age (years) with PA Diameter and Trunk Volume	
	PA diameter (mm)	**PA trunk volume (mm^3)**
$r_{(s)}$	0.3**	0.5**
P value	0.006	<0.001

*Table 4.2: Spearman's rank correlation of age with measures of PA dilatation (** denotes a significant result at the p < 0.01 level). Both PA diameter and trunk volume showed significant correlations. [PA: pulmonary artery, r_s: Spearman's rank correlation coefficient].*

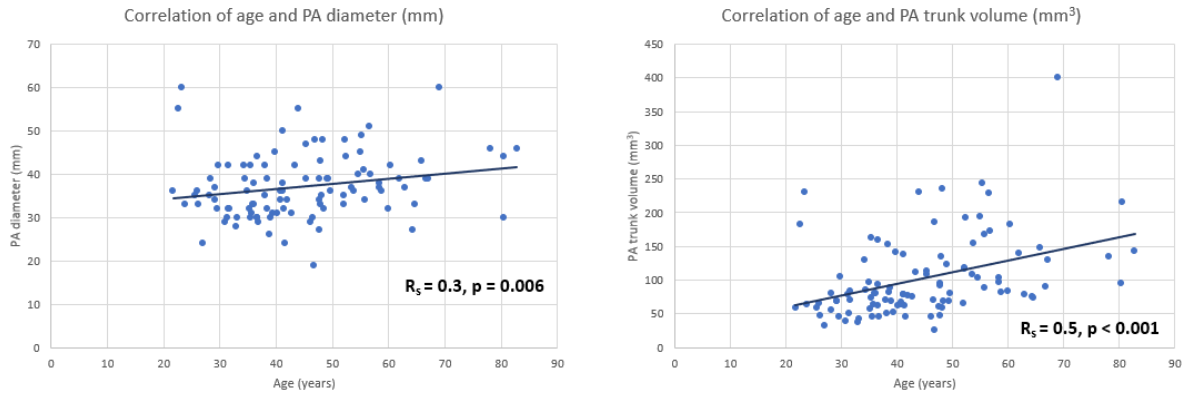


Figure 4.3: Scatter plots to show correlation of age with PA diameter and trunk volume. [PA: pulmonary artery, r_s: Spearman's rank correlation coefficient].

2.17.3 PA Thombosis and calcification

PA thrombosis was present in 22 (21.4%) and pulmonary artery calcification was present in 29 (27.9%). PA calcification was present within an area of thrombosis in 16 (15.4%).

The median number of calcifications was 6 (1 - 218) and calcification was seen from the main PA down to 4th generation PAs. The majority of the most distal calcium lesions were found in 3rd generation PAs (71%) with a preponderance for the right lower lobe PA (75% of 3rd generation lesions). Median calcium score was 218.0 [2.0 - 56097.0], median volume 120.0mm^3 [2.0 - 41594.0mm^3] and mass 68.0mg [1.0 - 42835.0mg]. The median distance from the pulmonary bifurcation to the most distal calcification was 94.0mm (44.0 – 157.0mm). No significant correlations were seen between PA diameter or trunk volume and calcification measurements.

	No calcfication	Calcification	P value
Age at scan (years)*	29[14-69]	44[18-68]	<0.001
Female	42	22	0.094
Male	32	7	NA
Down Syndrome*	32	3	0.003
Underlying Cardiac Defect:			
Complex	33	2	NA
Post tricuspid*	41	24	<0.001
Pre tricuspid	0	4	NA
WHO FC 2	4	0	0.462
WHO FC 3	70	30	NA
6MWD (m)	300[75-540]	285[115-425]	0.734
log.BNP	1.07[0.3-2.15]	1.28[0.48-2.26]	0.279
PA diameter (mm)*	35[19-60]	38.5[27-60]	0.039

*Table 4.3: Comparison of patient demographics in those with PA calcification (n=29) and those without (n=75) (*denotes statistically significant differences). [WHO FC: World Health Organisation functional class, 6MWD: 6-minute walk distance, BNP: brain natriuretic peptide, PA: pulmonary artery].*

On univariable logistic regression analysis the following parameters were related to the presence of PA calcification: age (per 10 years OR 3.01, 95% CI: 1.91 - 5.19, p<0.0001), Down syndrome (OR 0.16, 95% CI: 0.03 - 0.49, p=0.004), post-tricuspid shunt (OR 3.01, 95% CI: 1.16 - 8.92, p=0.03), a PA diameter above the median for this population (>35mm, OR 2.57, 95% CI: 1.03 - 6.91, p=0.049) and presence of PA thrombus (OR 21.64, 95% CI: 7.08 - 77.7, p<0.0001).

On further analysis of age with measures of PA calcification, a small but significant correlation was seen between age and the distance from the pulmonary artery bifurcation to the most distal calcification (r_s = 0.4, p = 0.041) (Table 4.4 and Figure 4.4).

	Correlation of Age (years) with measures of PA calcification				
	Number of calcifications	Calcium score	Calcium volume (mm^3)	Calcium mass (mg)	Most distal length from pulmonary bifurcation (mm)
$r_{(s)}$	0.2	0.04	0.01	0.1	0.4*
P value	0.225	0.827	0.943	0.746	0.041

*Table 4.4: Spearman's rank correlation of age (years) with measures of PA calcification (*denotes a statistically significant result at the p <0.05 level). A small, significant correlation was seen between age and distance from pulmonary bifurcation to the most distal calcification (r_s = 0.4, p = 0.041). [PA: pulmonary artery, $r_{(s)}$: Spearman's rank correlation coefficient].*

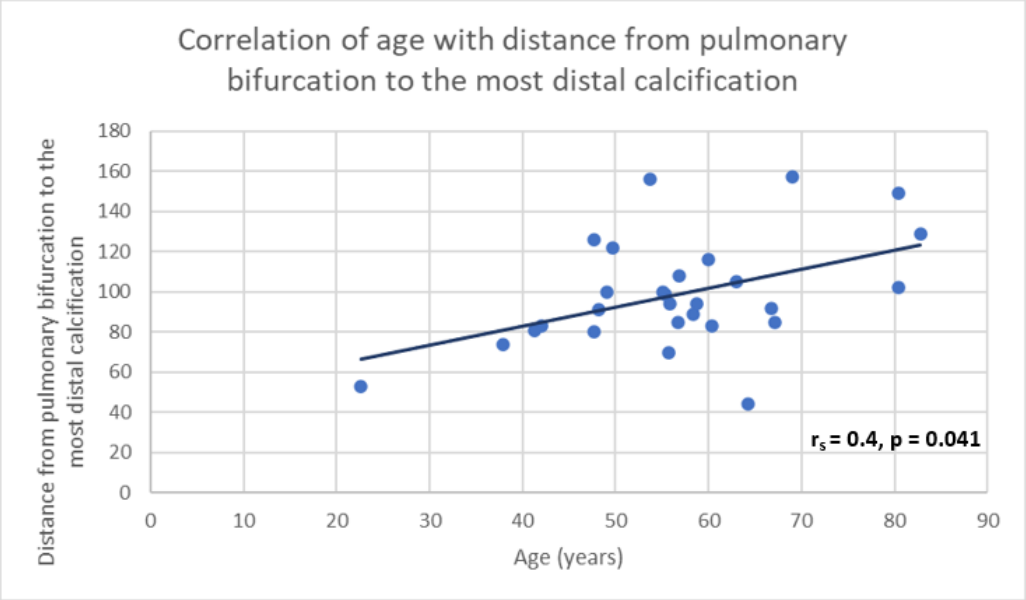


Figure 4.4: Scatter plot showing correlation of age with distance from pulmonary bifurcation to most distal pulmonary artery calcification. [r_s = Spearman's rank correlation coefficient].

2.17.4 Prognosis

During a median follow-up of 9.5 [0.2-20.8] years from the index CT, 22 (21.2%) patients died. On univariable Cox regression analysis, only age was predictive of death (per 10 years HR 1.39, 95% CI: 1.03 - 1.88, p=0.03). PA diameter, trunk volume and the presence of calcification or thrombosis did not affect prognosis.

2.17.5 Inter- reviewer agreement for novel CT measurements: Pulmonary trunk volume and measures of PA calcification

The intraclass correlation coefficient (ICC) between the 2 independent reviewers (SS and BR) was calculated for pulmonary trunk volume and PA calcification measures which are not routinely used in the assessment of PH patients on a sample of 15 patients. Table 4.5 summarises the results. There was evidence to support good reliability of the measurement of pulmonary trunk volume (ICC = 0.88 [95% CI 0.71 – 0.96, p = < 0.0001]) and distance from the pulmonary bifurcation to the most distal calcification (ICC = 0.83 [95% CI 0.57 – 0.94, p = <0.001]) between reviewers (Figure 4.5). Evidence to support inter-reviewer reliability of

number of calcifications, calcium score, volume and mass was lacking with p values > 0.05 and confidence intervals crossing '0'.

Measurement	Intraclass correlation coefficient	95% Confidence Interval (lower bound – upper bound)	P value
PA Trunk Volume	0.88*	0.71 – 0.96	<0.001
Distance from pulmonary bifurcation to the most distal calcification	0.83*	0.57 - 0.94	<0.001
Number of calcifications	0.43	-0.51 – 0.75	0.038
Calcium score	0.14	-0.35 – 0.57	0.292
Calcium volume	0.12	-0.38 – 0.55	0.337
Calcium mass	0.12	-0.37 – 0.56	0.315

Table 4.5: Intraclass correlation coefficient to assess reliability of novel CT measurements (n=15). PA trunk volume (ICC = 0.88 [95% CI 0.71 – 0.96, p = < 0.001]) and distance from pulmonary bifurcation to the most distal calcification (ICC = 0.83 [95% CI 0.57 – 0.94, p = <0.001]) showed good reliability. [PA: pulmonary artery].

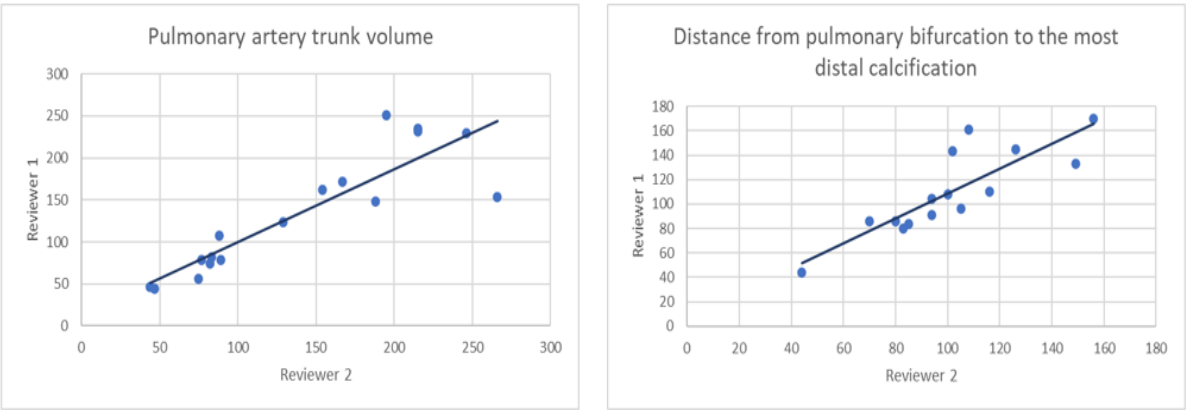


Figure 4.5: Scatter plots to show degree of agreement in measurement of pulmonary artery trunk volume and distance from pulmonary bifurcation to the most distal calcification between 2 independent reviewers (n=15).

2.18 Discussion

This chapter retrospectively examined the CT findings in a heterogenous cohort of patients with ES. Dilatation of the main PA on CT (PA diameter >30mm) was present in most patients (84, 82.4%). Pulmonary trunk volume ranged between 26.0 – 400.0mm^3 (with a median of 81.5mm^3). Both PA diameter and trunk volume significantly correlated with age.

PA calcification was a common finding in this cohort with a prevalence (27.9%) similar to that previously quoted by Perloff et al (26%)(254).

In 55.2% of patients, PA calcification was present within an area of thrombus. This was lower than that demonstrated by Silversides et al (257), where PA calcification was seen more frequently (71%) in patients with thrombosis versus those without (19%).

The development of PA thrombus is thought to occur in the context of low pulmonary flow associated with severe microvascular obstruction, hypoxia, endothelial dysfunction and blood hyperviscosity(270).

The presence of extensive calcification within PAs in those with thrombus(253,271) supports the hypothesis that thrombi may arise from local vascular injury from progressive pulmonary hypertension. The presence of PA thrombus in ES has been observed to be associated with increasing age(270). This age related risk of PA thrombosis may be explained by endothelial dysfunction becoming more extensive over time (257,270).

Inherent medial abnormalities of the main PAs in CHD(272) may predispose to dilatation that is out of proportion to haemodynamic expectations(254). Perloff et al(254) noted that aneurysmal PAs were significantly less calcified than non-aneurysmal PAs and therefore hypothesised that extensive mural calcification may limit dilatation. In this study, a PA diameter above the median for this population (>35mm, OR 2.57, 95% CI: 1.03 - 6.91, p=0.049) was associated with the presence of calcification but no significant correlation was found between PA diameter or trunk volume and measures of calcification.

The hypothesis for this study that quantitative CT measures of PA calcification would correlate with disease severity and predict mortality in ES was based on the rationale that abnormal flow properties associated with more severe PH may predispose to the deposition of calcium in the PAs. This has already been suggested as a possible contributor to thrombogenesis(271).

In situ thrombosis in the PAs of patients with ES has been demonstrated to be associated with older age, biventricular dysfunction, dilatation of the pulmonary arteries, and concomitantly decreased pulmonary flow velocity(271). In this study, age, and PA diameter >35mm were also associated with PA calcification. A correlation was seen between age and the distance from the pulmonary artery bifurcation to the most distal calcification (r_s = 0.4, p = 0.041).

The presence of PA thrombus was strongly associated with PA calcification (OR 21.64, 95% CI: 7.08 - 77.7, p<0.0001) which may suggest that the two are inter-related and/or share a similar pathogenesis.

PA calcification was less common in Down syndrome (OR 0.16, 95% CI: 0.03 - 0.49, p=0.004) and more common in patients with post-tricuspid shunt (OR 3.01, 95% CI: 1.16 - 8.92, p=0.03). Patients with post-tricuspid shunt and Down Syndrome both have a tendency to develop ES earlier(245) therefore it is not clear why these groups showed opposite associations with PA calcification.

Age was the only factor found to be predictive of death (per 10 years HR 1.39, 95% CI: 1.03 - 1.88, p=0.03). PA diameter, trunk volume and the presence of calcification or thrombosis did not affect prognosis.

The presence and extent of coronary artery calcification is well recognised as having prognostic implications. Vascular calcification can be classified depending on its location as intimal (the predominant type seen in coronary arteries) or medial (as seen in PAs)(273). This distinction may explain why the prognostic significance of calcification varies between its presence in the coronary and pulmonary arteries. Medial calcification is most commonly found in peripheral arterial disease and results in loss of elasticity(273). Arterial medial calcification has also been documented in chronic renal failure and its progression is reported to be associated with hypercalcaemia, hyperphosphatemia and parathyroid abnormalities(273–275). In chronic renal failure, local tissue injury and alteration in intracellular pH may also predispose to calcium precipitation(275) and excess parathyroid hormone levels have been shown to induce pulmonary calcification, pulmonary hypertension and right ventricular hypertrophy(274). It has also previously been proposed that pulmonary artery obstruction alters the microchemical environment of the lung, favouring tissue

alkalosis and augmenting calcification(276). The exact mechanisms leading to pulmonary artery calcification remain unclear.

In this cohort, novel CT measures of pulmonary trunk volume and distance from pulmonary bifurcation to most distal calcification were able to be measured with good reliability between 2 independent reviewers.

2.18.1 Study limitations

Due to the retrospective nature of this study, it was not possible to include all patients with ES presenting to the hospital (as not all had a CT scan as part of their care), standardise the point at which CT imaging was carried out or allow for the time from diagnosis to CT in analysis of results. All potential factors that might play a role in PA calcification were not assessed (e.g., serum calcium, phosphate, and parathyroid levels). There was only limited RHC data available for this cohort of patients, therefore associations between haemodynamic parameters and calcification were not assessed. Further work is required to understand the pathogenesis of pulmonary artery calcification better.

2.19 Conclusion

The commonly described radiological findings of dilated PA, PA calcification and in-situ thrombus in ES do not appear to be markers of prognosis but more likely reflect the longstanding severe pulmonary hypertension in these patients.

Chapter 5: A novel quantitative MRI derived biomarker: Dynamic Oxygen Enhanced MRI. Is there a role for it in the assessment of Pulmonary Hypertension?

2.20 Introduction

The pathophysiology of group 1 and 4 PH involves vascular remodelling of small and medium sized pulmonary arteries and pulmonary arterioles, with a subsequent increase in pulmonary vascular resistance (PVR) and right ventricular (RV) afterload(1). Pulmonary perfusion, particularly in the peripheries, may therefore represent the severity of PH(94). Reduced efficiency of gas exchange is also seen as a result of vascular remodelling and progressive loss of pulmonary arterial vasculature with decreased capillary blood volume available for gas exchange(65).

Group 1 (including IPAH and CTD-PAH) and 4 PH (predominantly CTEPH in clinical practice) are characterised by pre-capillary PH on RHC (mPAP ≥ 25mmHg, PAWP ≤ 15mmHg and PVR > 3 WU) which remains the gold-standard investigation for diagnosis, risk stratification and assessment of response to treatment(17,18).

RHCs are invasive in nature, and this can sometimes preclude more intensive monitoring of patients. Monitoring via CT is limited by ionising radiation and the use of intra-venous contrast agents with their associated risks to renal function and does not provide functional information. There is therefore a need for new techniques, which can be used in the assessment of these patients.

2.20.1 Role of MRI in PH

The role of MRI in PH has been expanding and is a promising one. Cardiac MRI is widely used in PH for assessment of RV size, morphology, and function. It allows non-invasive assessment of blood-flow (including stroke volume, CO, pulmonary arterial distensibility) and RV mass and therefore provides useful prognostic information both at baseline and at follow-up (17).

The use of MRI in pulmonary imaging is more challenging due to the inherent limitations of low proton density, multiple air-tissue interfaces and reduced signal secondary to cardiac and respiratory motion and blood flow(109)(110). However, advances in MRI technology are beginning to overcome this.

In the research setting, novel techniques are emerging that would allow quantitative analysis of lung perfusion, without IV contrast administration, and could be repeated pre and post treatment as frequently as practicable to allow assessment of therapeutic response (131). In this study, the role of one of these novel techniques is investigated (Dynamic Oxygen Enhanced MRI).

2.20.2 Dynamic oxygen enhanced MRI (OE-MRI)

Dissolved molecular oxygen is weakly paramagnetic and results in regional shortening of T1 relaxation time(134). T1 relaxation time varies in proportion to dissolved oxygen concentration and measurement of local T1 relaxation therefore allows calculation (or at least approximation) of the local oxygen partial pressure (PaO_2)(148). Whilst static measures of enhancement can be achieved via two acquisitions, one before and one after a period of time breathing 100% oxygen, repeated measurements are possible at short, regular intervals allowing the assessment of oxygen dynamics across the lung (136,277).

As the change in T1 results from oxygen in its dissolved state (as opposed to from the gas itself), signal change on administration of inhaled oxygen reflects a combined measure of efficiency of alveolar oxygenation, diffusion and ventilation-perfusion matching, presented both spatially and temporally (149). The highest volume of fluid per unit of normal lung resides within the pulmonary vascular system, so OE-MRI outputs are inherently reliant on

pulmonary perfusion and represent promising imaging biomarkers of pulmonary vascular disease (149).

2.21 Study Rationale

Dynamic OE- MRI represents an imaging technique that may provide a novel set of imaging biomarkers for the assessment of PH with the advantages of:

1. Being non-invasive
2. Not requiring exposure to ionising radiation or contrast media
3. Having an imaging protocol that can be carried out on standard clinical scanners (the only additional equipment required is a simple gas mixing system)
4. Data acquisition not requiring long breath-holds (an advantage in patients with cardio-respiratory disease and symptoms of breathlessness)
5. Being repeatable at as high a frequency as is practicable.

Combining this novel technique with existing cardiac MRI protocols could provide an alternative, non-invasive tool for monitoring pulmonary perfusion and right heart function in PH.

2.22 Hypothesis, Aims and Objectives:

2.22.1 Hypothesis

Quantitative measures of pulmonary perfusion, derived from dynamic OE-MRI, correlate with standard markers of disease severity and demonstrate response to treatment.

2.22.2 Aims

To investigate the feasibility of dynamic OE-MRI in a cohort of PH patients and whether the imaging biomarkers correlate with standard clinical measures of disease severity and treatment response.

2.22.3 Objectives

- To prospectively recruit and study the feasibility of dynamic OE-MRI in patients with a new diagnosis of IPAH, CTD-PAH and CTEPH pre-treatment and again following treatment initiation
- Describe pre-treatment imaging phenotypes based on quantitative measures derived from OE-MRI
- To assess whether quantitative measures derived from OE-MRI correlate with standard clinical measures of PH severity
- Evaluate if these new quantitative MRI measurements are sensitive to change related to treatment over a short period of time (3-6 months).

2.23 Methods

Patients were prospectively recruited between November 2018 and January 2020 from the RBH PH Service as per criteria defined in Chapter 2: Methods. Written consent was obtained (Appendix II). In addition to standard of care investigations, participants underwent a research MRI scan at baseline (pre-initiation of treatment). This was then repeated 3-6 months later following treatment initiation and timed to correspond with standard of care repeat investigations. Treatment was commenced as per current clinical guidelines and following discussion at a PH multi-disciplinary team meeting. The post-processing of the MRI scans has been in collaboration with researchers from Bioxydyn Ltd.

Further details of the MRI protocol and post processing can be found in Chapter 2: Methods.

Data are expressed as mean ± standard deviation or median (range). Correlations between MRI derived measures and standard clinical measurements were assessed by Spearman's rank correlation analysis. Changes in variables pre and post treatment were assessed using paired-samples T-test or Wilcoxon and Sign tests.

2.24 Results

2.24.1 Patient demographics and clinical characteristics

12 patients were recruited and underwent baseline study MRI scans. Of these, 5 went on to have a follow up scan post-treatment initiation. Median time to follow-up was 3.7 months (range 2.7-3.9 months). Table 5.1 demonstrates patient's baseline characteristics.

2 normal subjects with no underlying cardio-pulmonary disease were scanned as part of protocol set up and formed a small reference cohort.

Patient Baseline Demographics and Clinical Information (n=12)	
Age (years)	54.9 ± 16.6
Sex	75% Female, 25% Male
WHO FC	75% WHO FC 2
	25% WHO FC 3
6MWD (m)	312 ± 135.7
BNP (ng/L)	56.5 (7-555)
Haemodynamics	
MPAP (mmHg)	41.3 ± 13.9
PCWP (mmHg)	8.5 ± 4.3
PVR (WU)	9.9 ± 5.0
CO (L/min)	3.7 ± 1.0
Lung Function (% predicted)	
FEV1	100.6 ± 22.7
FVC	108.5 ± 19.2
TLCO	56.8 ± 26.5
KCO	62.0 ± 26.5
Cardiac MRI	
SV (ml)	85.0 (56-100)
RV EF (%)	43.5 ± 10.9
Cardio Pulmonary Exercise Test	
Peak VO2 (% predicted)	51.5 ±7.1
VE/VCO2 slope	51.9 ± 14.8

Table 5.1: Baseline patient demographics and clinical information (n=12). [WHO FC: World Health Organisation functional class, 6MWD: 6 minute walk distance, BNP: brain natriuretic

peptide, mPAP: mean pulmonary arterial pressure, PCWP: pulmonary capillary wedge pressure, PVR: pulmonary vascular resistance, CO: cardiac output, FEV1: forced expiratory volume in 1 second, FVC: forced vital capacity, TLCO: Transfer factor for carbon monoxide, KCO: Carbon monoxide transfer co-efficient, SV: stroke volume, RV EF: right ventricle ejection fraction, VO2: oxygen consumption, VE/VCO2: ventilatory equivalent for carbon dioxide].

The mean age was 54.9 ± 16.6 years, with a female preponderance (n=9, 75.0% female). Most patients were in WHO functional class 2 at diagnosis (n=9, 75.0%), with reduced mean 6MWD (312 ± 135.7m).

Baseline RHC data demonstrated severe PH with mPAP of 41.3 ± 13.9mmHg and mean PVR 9.9 ± 5.0 WU. One patient with group 1 PH showed a positive vasoreactivity test with a reduction in mPAP of 17mmHg following inhalation of nitric oxide.

Lung function showed preserved spirometry (FEV1 100.6 ± 22.7 % predicted and FVC 108.5 ± 19.2% predicted) with impaired TLCO (56.8 ± 26.5% predicted) and KCO (62.0 ± 26.5 predicted).

6 (50.0%) patients had a diagnosis of group 1 PAH and 6 (50.0%) had CTEPH. Further break down of group 1 diagnoses are shown in Figure 5.1.

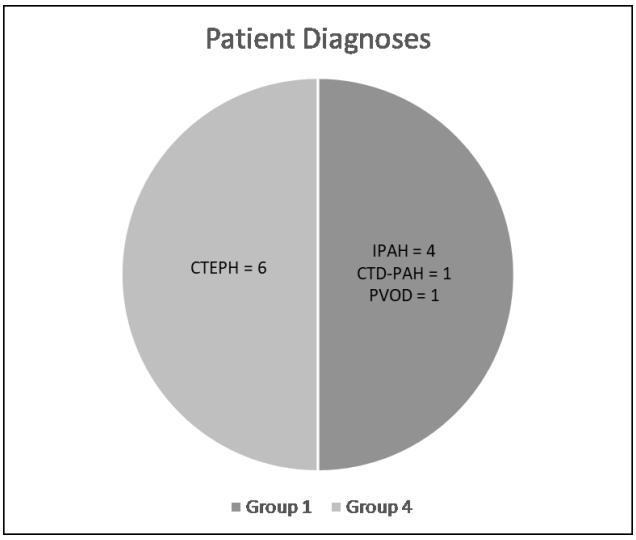


Figure 5.1: Classification of patient's pulmonary hypertension diagnosis. (n=12). [CTEPH: chronic thromboembolic disease. IPAH: idiopathic pulmonary arterial hypertension, CTD-PAH: PAH associated with CTD, PVOD: pulmonary veno-occlusive disease].

Patients were treated as per current clinical guidelines and following discussion at a PH multi-disciplinary team meeting. Those with CTEPH were initiated on 25mg Sildenafil three times daily whilst awaiting further review regarding suitability for PEA or BPA. Those with group 1 PH and no vasoreactivity demonstrated at RHC were started on dual therapy with a PDE5i and ERA. The patient demonstrating positive vasoreactivity was started on Nifedipine 30mg twice daily but later stepped up to treatment with dual vasodilators due to clinical progression.

In the cohort of patients who had follow-up study MRIs (n=5), significant improvement was seen in haemodynamic parameters at RHC following treatment with a decrease in mPAP from 50 ± 10.1mmHg to 36.8 ± 3.7mmHg (p = 0.022) and PVR from 13.9 ± 3.8WU to 8.5 ± 4.1 WU (p = 0.046) (Figure 5.2).

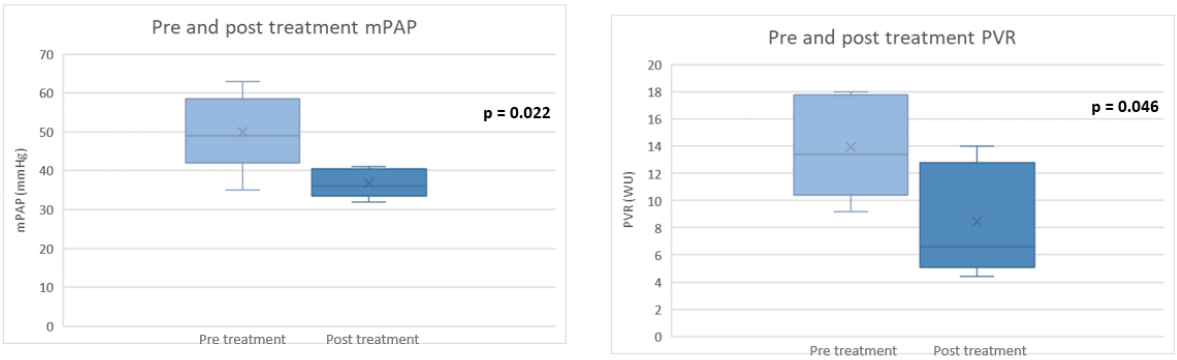


Figure 5.2: Haemodynamic measurements at right heart catheterisation pre and post treatment. (n = 5, median time to follow up = 3.7 [2.7 – 3.9] months). A significant improvement was seen in both mPAP (50 ± 10.1mmHg to 36.8 ± 3.7mmHg [p = 0.022]) and PVR (13.9 ± 3.8 WU to 8.5 ± 4.1 WU [p = 0.046]). [mPAP: mean pulmonary arterial pressure, PVR: pulmonary vascular resistance].

2.24.2 OE-MRI

All recruited patients completed the full OE-MRI protocol, including T1 mapping and dynamic oxygen enhancement.

The following quantitative measures were obtained over the entire lungs in the field of view in addition to parameter maps:

1. Enhancement fraction (EF) – fraction of the lung presenting with oxygen enhancement (max 1, min 0).
2. Baseline T1 (ms) – longitudinal relaxation time.
3. ΔPO_2 - oxygen enhancement as change in partial pressure of oxygen (mmHg).
4. Wash in time [WIT] (s) – the lung PO_2 curves of the enhancing pixels fitted using exponential functions for the oxygen wash in portion of the dynamic enhancement curve.

2.24.2.1 Enhancement Fraction (EF)

Figure 5.3 demonstrates the EF maps for a normal subject and representative scans for patients with IPAH and CTEPH. The EFs for these 3 participants are 0.992, 0.960 and 0.949 respectively. Visually, the normal individual demonstrates homogenous enhancement across both lungs, whilst both subjects with PH demonstrate non-enhancing regions. The CTEPH patient demonstrates more widespread enhancement heterogeneity, as might be expected given the heterogenous distribution of embolic disease in this participant (Figure 5.6).

EF showed a moderate negative correlation (r_s = -0.6, p = 0.029) with age (Figure 5.4). In the IPAH patient, the non-enhancing regions are predominantly peripheral. In the CTEPH patient there is some visual agreement with where areas of perfusion defects were seen on VQ scan (Figure 5.6).

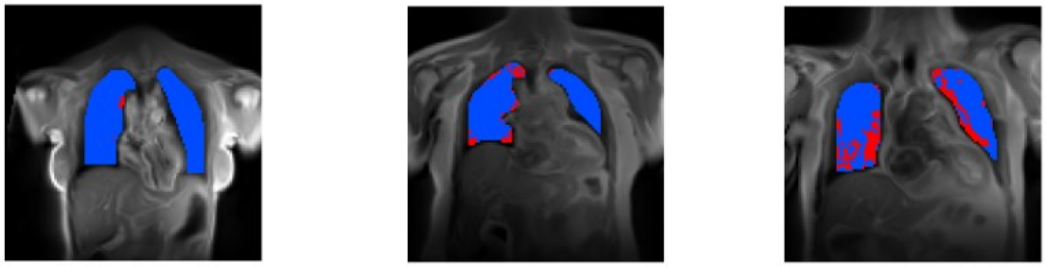


Figure 5.3: Enhancement fraction (EF) maps for a normal subject, patient with IPAH and CTEPH. Blue areas represent enhancing regions of lung and red areas represent non enhancing regions. The EFs are 0.992, 0.960 and 0.949 respectively. [IPAH: idiopathic pulmonary arterial hypertension, CTPEH: chronic thromboembolic pulmonary hypertension, EF: enhancement fraction].

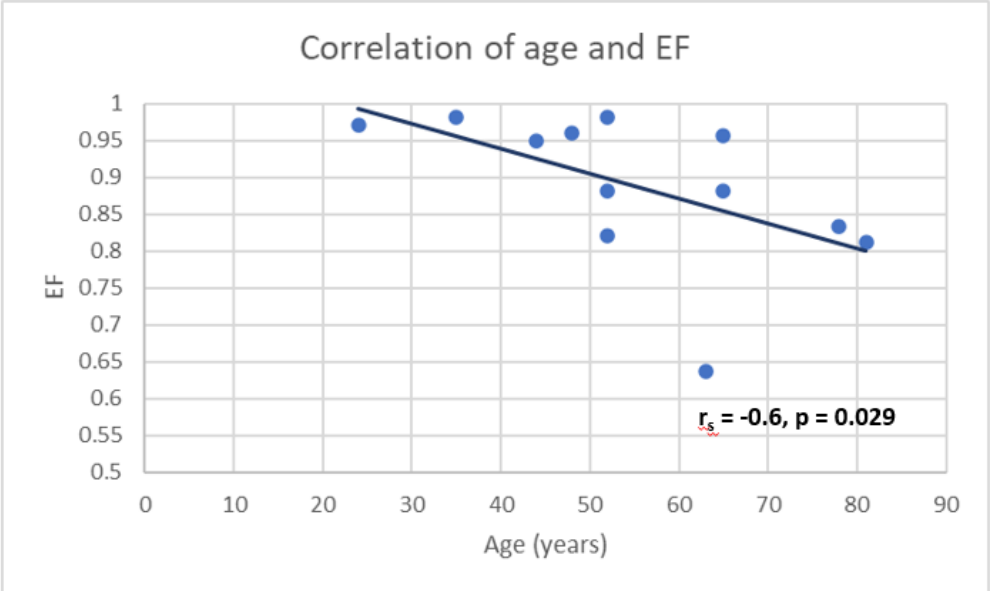


Figure 5.4: Scatter plot of age and EF. (n= 12). A moderate, negative correlation was seen (r_s =-0.6, p = 0.029). [EF: enhancement fraction, R_s: Spearman's rank correlation coefficient].

2.24.2.2 *Baseline T1, ΔPO_2 and WIT*

Figure 5.5 shows example imaging parameter maps for the remaining quantitative measurements (baseline T1, ΔPO_2 and WIT) in a normal subject and patients with IPAH and CTEPH.

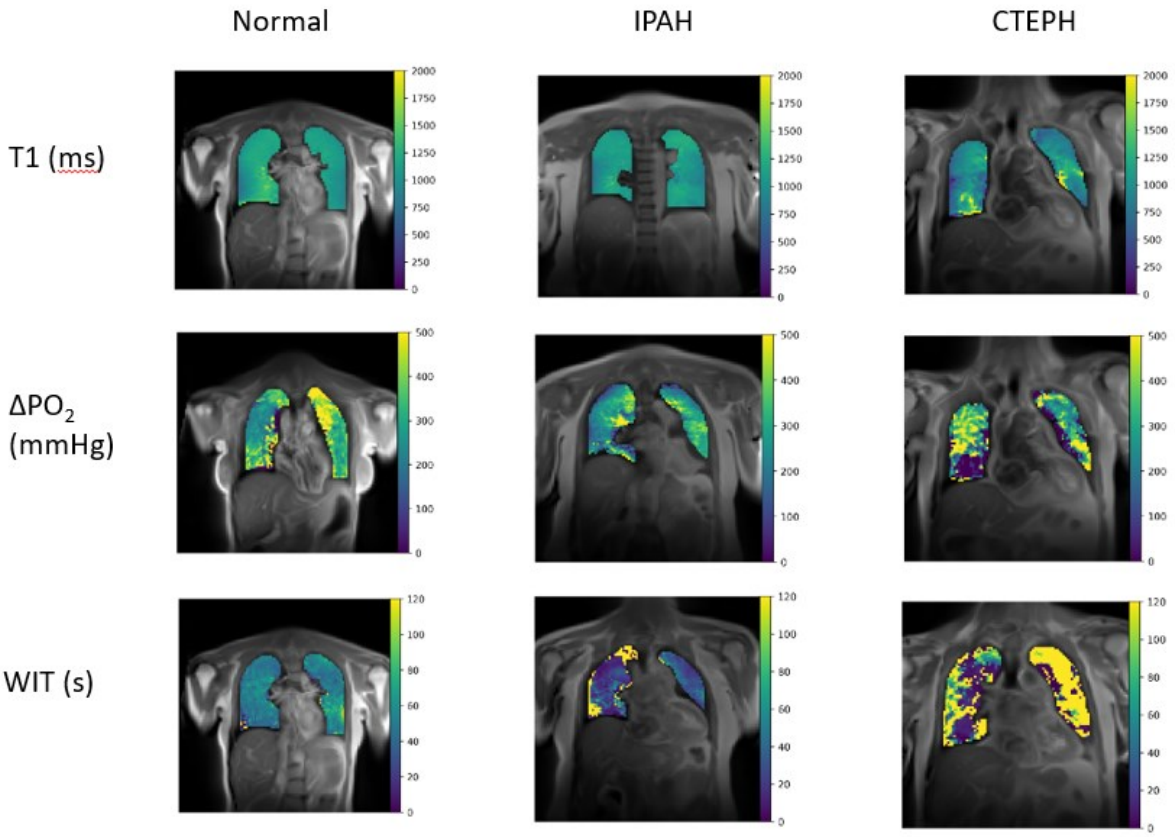


Figure 5.5: Baseline parameter maps for T1, ΔPO2 and WIT in a normal subject, patient with IPAH and patient with CTEPH. [IPAH: idiopathic pulmonary arterial hypertension, CTEPH: chronic thromboembolic pulmonary hypertension, T1: longitudinal relaxation time, ΔPO2: oxygen enhancement as change in partial pressure of oxygen, WIT: wash in time].

The CTPEH patient shows the greatest degree of heterogeneity in baseline T1. All 3 ΔPO_2 maps show a degree of heterogeneity. The areas of lower ΔPO_2 appear more peripheral in the IPAH patient and there is some visual agreement with areas of known thromboembolic disease (figure 5.6) in the CTEPH patient. Compared to the normal WIT map, the IPAH and CTEPH

patients show more areas of longer WIT with areas of WIT prolongation again appearing to be predominantly peripheral in the IPAH patient and more widespread in the CTEPH patient.

Figure 5.6 demonstrates the parameter maps from a patient with extensive, bilateral chronic thromboembolic disease causing severe PH. All 3 OE- MRI parameter maps (Figure 5.6a-c) show a heterogenous distribution with particularly low ΔPO_2 in the right lower zone. Conversely, WIT in the right lower zone remained low despite multiple other confluent regions of longer WIT. This perhaps represents an area of such marked hypoperfusion that time to peak enhancement is artificially reduced by the low peak enhancement obtained.

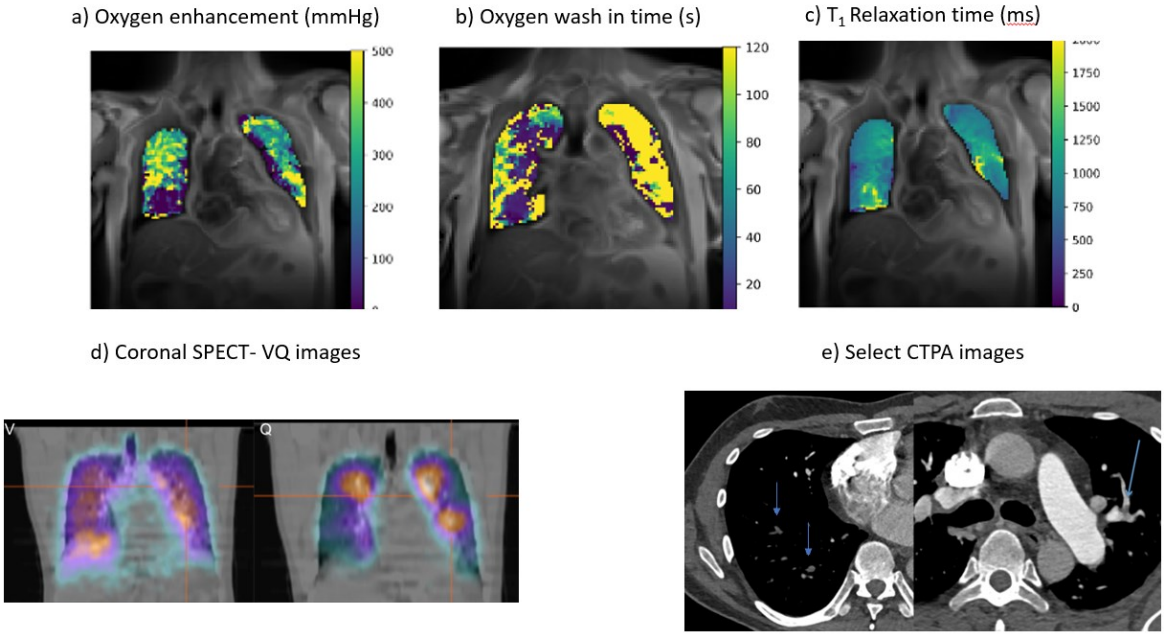


Figure 5.6: Parameter maps from a participant with CTEPH. a) oxygen enhancement, b) oxygen wash in time, c) T1 relaxation time d) coronal SPECT-VQ images at the same slice position and e) select images from CTPA. The SPECT-VQ image demonstrates marked perfusion abnormality at the right lung base, base of the right upper lobe and in the left upper lobe. Corresponding areas of reduced oxygen enhancement are well demonstrated on the oxygen enhancement map. These regions also demonstrate more heterogeneous T1 relaxation times. Wash-in time is harder to interpret with reduced wash in times within the right sided perfusion defects and prolonged times on the left. This could be because the left perfusion abnormality involves slow perfusion, compared to absent perfusion on the right. In support of this, select images from a contemporaneous CTPA demonstrate non-occlusive webs in the left upper lobe and occlusive thrombi in the right lower lobe. [SPECT - VQ: single photon

emission computed tomography- ventilation perfusion, CTPA: computed tomography pulmonary angiogram].

2.24.2.3 Comparison of OE-MRI measurements in group 1 and 4 PH

Baseline EF, ΔPO_2 and WIT measurements showed a tendency to be worse and more heterogenous in distribution in patients with group 4 PH (CTEPH) compared to those with group 1 PH, however this difference did not reach statistical significance (Table 5.2).

	Group 1	Group 4	p value
EF	0.930	0.848	0.132
ΔPO2 median (mmHg)	240.5	227.8	1.000
ΔPO2 IQR (mmHg)	170.6	210.3	1.000
WIT median (s)	19.4	40.6	0.310
WIT IQR (s)	35.8	92.0	0.24
T1 median (ms)	1030.3	1017.8	1.000
T1 IQR (ms)	192.4	177.5	0.485

Table 5.2: Comparison of baseline Oxygen Enhanced - MRI measurements in patients with group 1 and 4 PH. (n=12). [EF: enhancement fraction, T1: T1 longitudinal relaxation time, ΔPO2: oxygen enhancement as change in partial pressure of oxygen, WIT: wash in time, IQR: interquartile range].

2.24.2.4 Correlation between quantitative dynamic OE-MRI and standard clinical measurements

Table 5.3 shows the correlations between the quantitative dynamic OE-MRI measurements and standard clinical measurements in the PH patients.

	EF	ΔPO2 median (mmHg)	ΔPO2 IQR (mmHg)	WIT median (s)	WIT IQR (s)	T1 median (ms)	T1 IQR (ms)
Age (years)	**-0.6* (0.029)**	-0.5 (0.134)	-0.2 (0.524)	-0.2 (0.630)	-0.05 (0.887)	-0.1 (0.662)	0.4 (0.151)
MPAP (mmHg)	-0.2 (0.563)	-0.1 (0.712)	0.03 (0.940)	-0.56 (0.136)	-0.2 (0.455)	0.1 (0.828)	-0.3 (0.364)
PVR (WU)	-0.05 (0.880)	0.1 (0.863)	0.2 (0.542)	-0.3 (0.331)	-0.2 (0.471)	-0.1 (0.729)	-0.04 (0.914)
CO (L/min)	0.03 (0.937)	-0.1 (0.853)	-0.2 (0.537)	0.1 (0.832)	0.3 (0.450)	0.2 (0.612)	-0.6 (0.071)
FEV1 (% predicted)	-0.6 (0.119)	-0.3 (0.535)	-0.04 (0.939)	0.00 (1.000)	0.00 (1.000)	0.3 (0.482)	0.2 (0.645)
FVC (% predicted)	-0.6 (0.180)	-0.4 (0.337)	-0.3 (0.535)	-0.2 (0.702)	0.7 (0.071)	0.3 (0.535)	0.5 (0.294)
TLCO (% predicted)	-0.1 (0.867)	0.02 (0.955)	0.1 (0.779)	-0.2 (0.867)	0.02 (0.955)	-0.3 (0.651)	**-0.8* (0.015)**
RV EDV (ml)	0.02 (0.955)	0.3 (0.456)	0.3 (0.456)	**0.8* (0.015)**	**0.9** (0.001)**	0.1 (0.867)	-0.2 (0.610)
SV (ml)	0.5 (0.294)	0.2 (0.702)	0.04 (0.939)	0.2 (0.645)	0.00 (1.000)	0.3 (0.482)	-0.3 (0.482)
RV EF %	0.1 (0.778)	-0.6 (0.146)	-0.7 (0.069)	-0.6 (0.083)	**-0.8* (0.023)**	0.3 (0.471)	0.04 (0.933)

Table 5.3: Spearman's rank correlation coefficients between dynamic OE-MRI imaging parameters and standard clinical measurements (n=12). [Data are presented as correlation coefficient (p value) with significant results in bold. '' indicates correlation is significant at the p < 0.05 level and '**' at the p < 0.01 level. [EF: enhancement fraction, T1: longitudinal relaxation time, ΔPO2: oxygen enhancement as change in partial pressure of oxygen, WIT: wash in time, IQR: interquartile range, mPAP: mean pulmonary arterial pressure, PVR: pulmonary vascular resistance, CO: cardiac output, FEV1: forced expiratory volume in 1 second, FVC: forced vital capacity, TLCO: Transfer factor for carbon monoxide, SV: stroke volume, RV EF: right ventricle ejection fraction].*

Median WIT and WIT IQR showed strong positive correlations with RV end diastolic volume (RV EDV) (r_s= 0.8, p = 0.015 and r_s = 0.9, p=0.001 respectively). The WIT IQR also showed a strong, negative association (r_s = -0.8, p = 0.023) with RV ejection fraction (RV EF). T1 IQR showed a strong negative correlation with % predicted TLCO (r_s = -0. 8, p = 0.015).

No significant correlations were seen between ΔPO_2 parameters and clinical measurements.

2.24.2.5 Comparison between pre and post treatment OE-MRI measurements

	Pre - Treatment	Post Treatment	p value
EF	0.889	0.925	1.000
ΔPO2 median (mmHg)	234.2	202.4	0.715
ΔPO2 IQR (mmHg)	190.5	142.1	0.465
WIT median (s)	30.0	38.1	0.273
WIT IQR (s)	63.9	50.8	0.465
T1 median (ms)	1024.0	1112.6	0.068
T1 IQR (ms)	184.9	181.9	0.715

Table 5.4: Comparison of baseline and post-treatment dynamic Oxygen Enhanced - MRI parameters (n=5). Median time to follow-up 3.7 months (range 2.7-3.9 months). [EF: enhancement fraction, T1: T1 longitudinal relaxation time, ΔPO2: oxygen enhancement as change in partial pressure of oxygen, WIT: wash in time, IQR: interquartile range].

The comparison between the pre and post treatment OE- MRI measurements is shown in Table 5.4. 5 patients underwent follow-up OE-MRI scans with a median follow-up time of 3.7 months (2.7 – 3.9 months). Given the small numbers recruited, statistical significance was not met, but there were trends in treatment response with follow up scans demonstrating increased enhancement fraction (i.e., more widespread perfusion) and more homogeneous enhancement and wash in times across the lung as a whole. Figure 5.7 shows the parameter maps for a patient with CTEPH at baseline and following treatment. Visually, there is reduced heterogeneity in the post-treatment maps and a diffuse reduction in WIT post treatment.

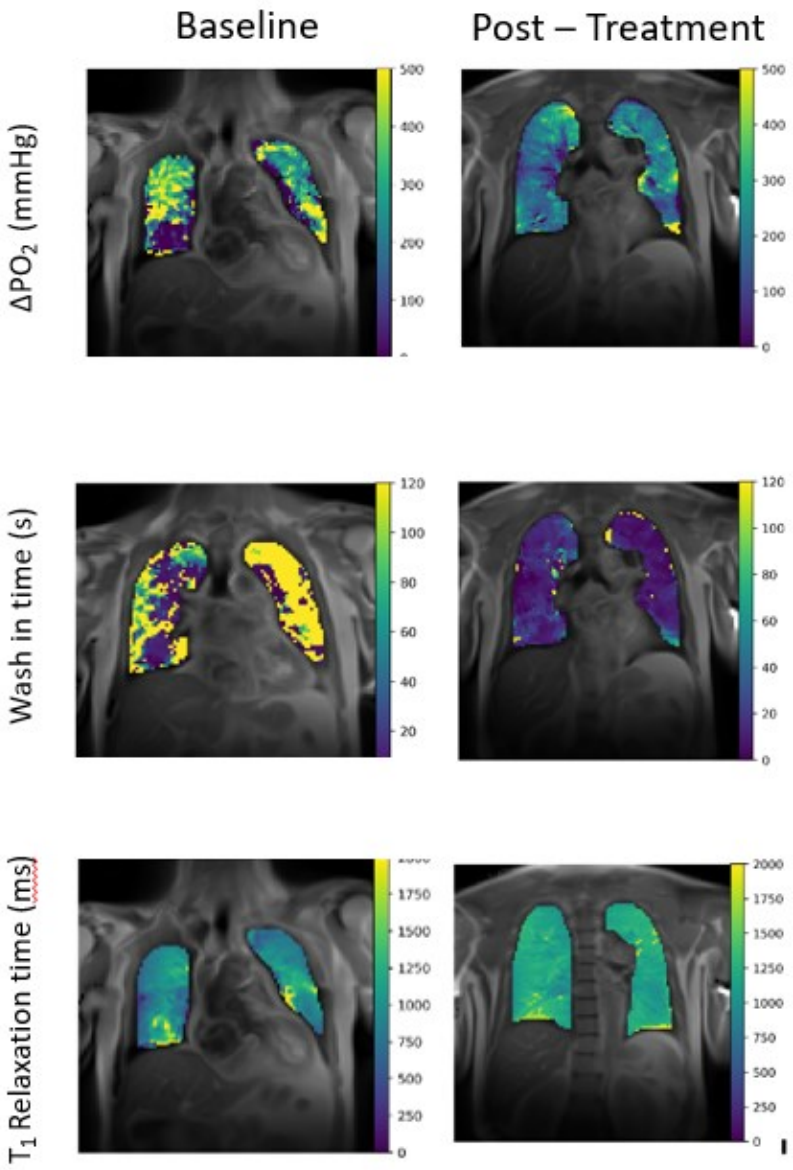


Figure 5.7: Dynamic Oxygen Enhanced - MRI parameter maps for a patient with chronic thromboembolic pulmonary hypertension at baseline and post-treatment. Time between baseline [and treatment initiation] and follow-up scan = 2.7 months. [ΔPO2: oxygen enhancement as change in partial pressure of oxygen].

2.24.3 Patient questionnaires

All 12 patients undergoing the study MRIs completed a questionnaire (Appendix III) regarding their experience of the OE-MRI scan.

2.24.3.1 Anxiety around the scan

7 patients experienced no anxiety related to the scan. The remaining 5 had “some” anxiety and none expressed “a lot” of anxiety. For those experiencing anxiety, this was related to not having previously been involved in research, the “unknown” and being in a new clinical setting/ organisation.

2.24.3.2 Wearing a non-rebreather oxygen mask

9 patients found wearing a non-rebreather mask for the scan “acceptable”. 2 patients found it “a bit uncomfortable” and 1 patient found the mask “very uncomfortable”. Issues regarding comfort were largely due to feeling the mask was not sitting comfortably on their face either from the beginning of the scan or part way through the scan.

2.24.3.3 Discomfort during the scan

4 patients experienced “some” discomfort during the scan with the remaining 8 experiencing no discomfort. The causes of discomfort included feeling hot and back ache after a period in the scanner.

2.24.3.4 Breath holds

Whilst the lung T1 mapping and dynamic OE-MRI images are acquired during free breathing, breath-hold imaging was required for some of the cardiac acquisitions. 9 patients found the breath holds “acceptable”. 3 patients found them “difficult”, and comments made regarding this included “leaving more time between each breath hold” and that “a lot of breath holding over an extended period was difficult”.

2.24.3.5 Length of scan

All patients found the length of the scan acceptable.

2.24.3.6 Overall experience

Figure 5.8 demonstrates patient's rating of their experience from 1-10 with all patients rating their experience ≥ 5 and 5 patients rating their scan experience 10 out of 10. One patient commented that they "found the breath holds much easier than previous MRI at hospital 'X'".

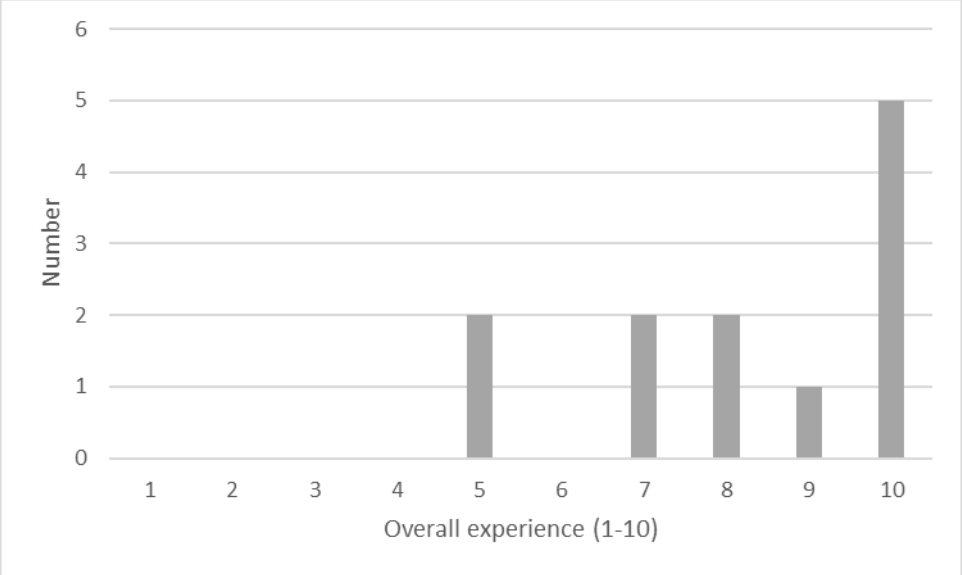


Figure 5.8: Overall patient experience of study MRI scan (as rated from 1-10).

2.24.3.7 Repeat scans and intervals

All 12 patients stated they would have the scan again and Figure 5.9 demonstrates the interval at which they would be happy to have it repeated. Most patients (8) were willing to have the scan at 3-6 monthly intervals.

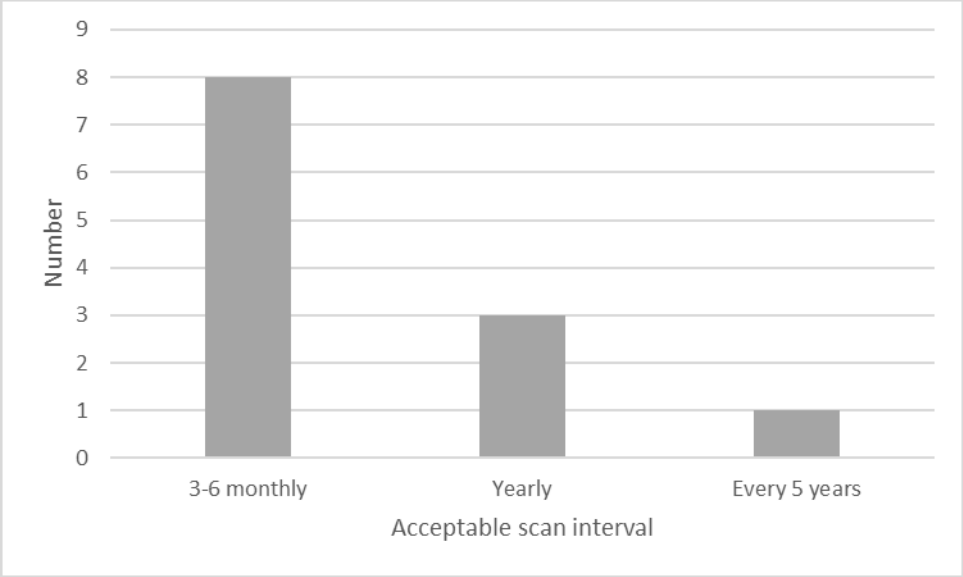


Figure 5.9: Interval at which patients would be happy to have scan repeated.

2.25 Discussion

This prospective pilot study provides evidence of the feasibility and tolerability of dynamic OE-MRI in patients with group 1 and 4 PH.

Baseline haemodynamic measurements derived from RHC were in keeping with severe, pre-capillary PH (mPAP 41.3 ± 13.9 mmHg, PCWP 8.5 ± 4.3 mmHg, PVR 9.9 ± 5.0 WU). Patients with any suggestion of co-existent lung disease were excluded to prevent any compounding of results, as demonstrated by preserved spirometry at diagnosis (FEV1 100.6 ± 22.7% predicted, FVC 108.5 ± 19.2% predicted). TLCO was disproportionately low as is typically seen in patients with PAH (56.8 ± 26.5% precited).

Following a median treatment time of 3.7 months (range 2.7-3.9 months), significant improvement was seen in haemodynamic parameters at follow-up RHC with a decrease in mPAP from 50 ± 10.1mmHg to 36.8 ± 3.7mmHg ($p = 0.022$) and PVR from 13.9 ± 3.8WU to 8.5 ± 4.1 WU ($p = 0.046$).

In this study, dynamic OE-MRI demonstrated an ability to visualise abnormalities in patients with PH. Imaging parameter maps in the PH patients tended to show visually more heterogeneous values supported by wider parameter IQRs (a quantitative marker of spatial heterogeneity). These differences were more marked in the CTEPH group. EF, ΔPO_2 and WIT

parameter maps in an IPAH patient visually suggested more marked peripheral abnormalities. These findings are in keeping with what is often seen on VQ scintigraphy for patients with IPAH and CTEPH. In IPAH the perfusion scintigraphy often demonstrates more homogenous, subsegmental areas of reduced perfusion; in CTEPH a more heterogenous pattern is seen with both patchy areas of perfusion defects and larger embolic type defects (wedge shaped, pleural based and sharply marginated areas affecting part of or a whole segment)(278,279).

Signal changes observed in OE-MRI are related to a combination of ventilation, diffusion, and perfusion effects. In this study population, patients with ventilatory impairment were excluded as evidenced by normal to supranormal lung spirometry at study enrolment. Therefore, in this group, any changes seen should predominantly be due to diffusion and/or perfusion abnormalities. Disentangling the contribution of each of these processes is not possible, however, both diffusion and perfusion abnormalities are known to play a part in the pathophysiology of PH. Changes in pulmonary blood volume and distribution that occur in PH may have a measurable effect on OE-MRI parameters as the blood plasma is the largest fluid compartment within the lungs, providing substrate for MRI signal change on delivery of oxygen.

Non-enhancing regions observed in the lungs on the EF maps may indicate areas of most severe diffusion/perfusion defects. A statistically significant, moderate, negative correlation was seen between EF and age (r_s = -0.628, p = 0.029). This may be secondary to a combination of the following documented age-related pulmonary changes:

- Decline in lung expiratory flow and volumes(280,281) affecting ventilation
- Remodelling of the pulmonary vasculature that is characterised by an increase in pulmonary vascular stiffness, pressures, and resistance
- Decrease in gas exchange efficiency with reduced TLCO (282,283) resulting from a reduction in pulmonary capillary blood volume(283,284), decrease in number of capillaries perfusing the lungs(285) and a decrease in alveolar surface area(284,286).

The signal change characterised with dynamic OE-MRI is given by a change in regional oxygen concentration within the fluid compartments of the lung (predominantly plasma). The increase is exponential and so the speed at which this change occurs over time can be

characterised as the WIT parameter. A prolonged WIT suggests less efficient gas exchange and a larger WIT IQR suggests more spatial heterogeneity in gas exchange across the whole of the imaged lung.

WIT related parameters (median WIT and WIT IQR) showed the most significant correlation with recognised measures of PH severity in this study. With a strong positive correlation seen between RV end diastolic volume and median WIT (r_s= 0.8, p = 0.015) and WIT IQR (r_s = 0.9, p=0.001). WIT IQR also showed a strong, negative association (r_s = -0.778, p = 0.023) with RV ejection fraction.

In PH, a chronically raised mPAP and PVR lead to remodelling of the RV. The RV compensates for the increased afterload with RV enlargement and hypertrophy. Progressive RV dilatation and an increased RV EDV are predictors of poor survival(127); as is reduced RVEF with a 1% decrease in RVEF demonstrated to be associated with a 4.9% increase in the risk of clinical worsening and a 2.1% increase in risk of mortality(287).

In airways disease, WIT has been shown to relate to severity of ventilatory impairment (141,149). In this study, this should not be the case as patients had normal lung spirometry and patients with any co-existent lung disease were excluded. Therefore, it can be hypothesised that the longer median WIT with increased RV EDV and increased heterogeneity in WIT (as demonstrated by larger WIT IQR) as RVEF decreases are due to the more marked and heterogenous diffusion and perfusion impairment in those patients with more severe PH.

Mapping of T1 (longitudinal relaxation times) has been evaluated as a promising technique in the assessment of pulmonary diseases(288). Preliminary studies in cystic fibrosis have demonstrated that T1 imaging can visualise and quantify areas of diseased lung (with lower T1 within fibrotic areas) and correlates with blood volume fraction(146). In COPD, T1 mapping at room air correlated with perfusion deficits and severity of COPD(288).

In this study, T1 IQR showed a strong negative correlation with % predicted TLCO (r_s = -0. 810, p = 0.015) suggesting more heterogeneity in T1 in PH patients with more marked diffusion abnormalities. The variation in T1 may also be related to perfusion defects as demonstrated in both COPD and cystic fibrosis (146,288).

Whilst ΔPO_2 has been shown to correlate with lung function in asthma, with a lower ΔPO_2 seen in severe versus mild asthma (149), it did not show any significant correlations in this study.

Visually, there appeared to be less heterogeneity in the parameter maps following treatment and suggestion of an improvement in some OE-MRI parameters, however this was not statistically significant.

Based on the results of this study, looking at degree of heterogeneity in the OE-MRI parameters (as represented by parameter IQRs) and parameter maps, may prove more useful than absolute values.

2.25.1 Patient questionnaires

The scan protocol was well tolerated by PH patients with most willing to have the scan at 3-12 monthly intervals which is the general interval at which PH patients are reviewed.

To improve patient experience of the scan, the following should be addressed:

1. Reduce anxiety around the scan by more detailed, step-by-step discussion of what to expect.
2. Ensure mask on comfortably at beginning of scan and empower patients to highlight if it is not or becomes uncomfortable during the scan.
3. Allow longer pause between breath holds.

2.25.2 Study limitations

The main limitation was the small study number which precluded more definitive analysis of these novel imaging parameters in PH. Incorporating imaging of more healthy volunteers into the study design will have allowed further analysis and may have provided a better understanding of the changes being seen in the PH patients.

The small cohort without normal controls may affect the impact of the statistical analysis and therefore results should not be over-interpreted. In addition, age was found to correlate with enhancement fraction in the OE-MRI analysis and hence is potentially a confounding factor.

A specific drawback of OE-MRI to consider is the possible alteration of pulmonary pathophysiology as a result of oxygen administration(137).

Comparison of the parameter maps obtained with perfusion scintigraphy or dynamic contrast enhanced perfusion maps may have helped further assess these techniques. Unfortunately, not all patients had these as part of their standard work up.

Due to the post-processing occurring remotely through collaboration with an external organisation, there was some limitation in what results were obtainable, their format and when they were available.

2.26 Conclusion

This pilot study demonstrates the feasibility of OE-MRI in patients with group 1 and 4 PH. Correlations have been demonstrated between OE-MRI measures and established markers of PH severity and changes in parameter maps were observed post-treatment. The degree of heterogeneity in OE-MRI measures (IQRs) and on visual inspection of parameter maps may be more sensitive to severity of PH and treatment response than absolute values. Whilst the small sample size limits statistical analysis at this time, this preliminary data adds significant weight to the argument for further work to validate these findings and continue exploration of the role of OE-MRI in PH.

Chapter 6: Final Discussion and Conclusion

2.27 Discussion

CT and MRI based imaging is playing an increasing role in the screening and monitoring of pulmonary vascular disease and is used in a complementary manner with RHC which remains the current gold standard. This thesis sought to examine the role of existing and novel CT and MRI derived imaging biomarkers in the assessment of disease severity, treatment response and prognosis in PH.

CT is a readily available tool and used frequently in the clinical assessment of patients. It can simultaneously assess the pulmonary vasculature, parenchyma, cardiac and mediastinal structures. Relevant CT findings may provide the initial suggestions of PH. In chapters 3 and 4 of this thesis, the role of both known and novel CT markers of PH presence and disease severity were examined in 2 separate groups of PH (1 and 3).

The role of MRI in PH has been expanding with cardiac MRI widely used for assessment of RV size, morphology, and function. Advances in MRI technology are providing promise for its use in pulmonary and pulmonary vascular imaging by overcoming the intrinsic limitations of low proton density, multiple air-tissue interfaces and reduced signal secondary to cardiac and respiratory motion and blood flow (109)(110)(69). Emerging MRI techniques are demonstrating the ability to quantify lung perfusion and be sensitive to post treatment changes (131). In chapter 5 of this thesis, the potential role of a novel MRI technique (OE-MRI) was investigated.

2.27.1 Chapter 3: Quantitative CT findings in Group 3 PH treated with Sildenafil

In chapter 3, the role of CT in predicting severity of PH and treatment response to Sildenafil in group 3 PH was examined. The baseline demographics of this cohort were similar to those

previously described for CLD associated with a PAH or vascular phenotype(56) with a preserved FEV1 and FVC % predicted (of greater than 60% and 70% respectively) and a disproportionately low TLCO % predicted. The average extent of parenchymal disease was also mild to moderate with a maximum % extent of 55% and median 30%. These findings are in line with the theory that severe PH in CLD may occur independently to the underlying CLD and supports the existence of a separate vascular phenotype.

No improvement in CT vascular or cardiac measurements were observed following treatment and there was a significant deterioration in PA:Ao ratio and %fibrosis. The results in this chapter are therefore possibly confounded by the effects of progressing lung disease.

This raises the question of whether in the absence of established guidelines on the use of vasodilator treatment in group 3 patients at the time of this study, patients with more advanced disease were being selected where the potential benefits of a controversial treatment were considered greater than the risks.

The vascular and cardiac CT measurements used in this chapter are a reflection of the downstream effects of an increased mPAP and may therefore not be the most sensitive markers for predicting and measuring response to short term treatment with vasodilator therapies which primarily act on the smaller, distal PAs (vascular alteration of which are thought to be a characteristic feature of PH in COPD(74, 83) and other CLD). Therefore, quantitative imaging biomarkers of these smaller, distal PAs may be more likely to predict a vascular phenotype, the severity of PH and response to treatment.

2.27.2 Chapter 4: Pulmonary artery morphology and calcification on CT in Eisenmenger Syndrome

Chapter 4 concentrated on pulmonary vascular changes on CT in patients with ES (part of group 1 of the PH classification). CT is routinely used in the clinical assessment of patients with ES and can provide data about the morphology of the PAs and presence of calcification and thrombus. Despite this, there is limited information in the literature about the prognostic implications of these changes in ES.

In this study, there was unique access to a large cohort of patients with ES, however data collection was limited by the retrospective nature of the research.

The CT measures examined did not predict mortality in this cohort. Age was the only significant predictor of mortality and correlated with PA diameter, trunk volume and distance to the most distal calcification.

ES is known to confer a more favourable haemodynamic profile and prognosis compared to patients with other forms of PAH(250), which may explain why the CT changes that are associated with disease severity and prognosis in other forms of PH do not have the same association in ES and instead appear to relate to chronicity of pulmonary vascular disease.

2.27.3 Chapter 5: A novel quantitative MRI derived biomarker: Dynamic Oxygen Enhanced MRI. Is there a role for it in the assessment of Pulmonary Hypertension?

In chapter 5, a prospective pilot study examined the potential role of dynamic OE- MRI in patients with group 1 and 4 PH. This technique has the advantages of being non-invasive, not requiring ionising radiation exposure and can be carried out on standard clinical scanners. The MRI protocol proved both feasible and acceptable for patients with PH.

Dynamic OE-MRI demonstrated the ability to visualise abnormalities in patients with PH and detect changes following treatment. More heterogeneity was seen in the OE-MRI derived parameter maps of patients with PH with a reduction in heterogeneity seen with treatment. Wider IQRs (a marker of spatial disease heterogeneity) also appear to correlate more significantly with standard measures of PH severity than total or median values derived from OE-MRI, suggesting that concentrating on these in the assessment of PH may be more successful.

The signal changes seen in OE-MRI are related to a combination of ventilation, diffusion, and perfusion effects. In this study population an attempt was made to minimise the effects of ventilatory differences by excluding patients with co-existent lung disease. Beyond this, it is not possible to separate out how much of the signal change may be related to impaired diffusion or perfusion. However, both these processes are known to be impaired in the pathophysiology of PAH (63,64). The reduced membrane diffusion capacity is likely related to

an increase in alveolar capillary membrane thickness caused by remodelling, fibrotic and proliferative changes and the reduction in perfusion secondary to increased PVR, decreased CO and local thrombosis of the vascular bed (65). Some studies suggest that diffusion capacity plays a more significant role (65–67), whereas others show a proportional reduction in both and an interdependence as any change in perfusion and the pulmonary alveolar capillary bed volume available for gas transfer would lead to a reduction in diffusion capacity though loss of surface area available for gas exchange(65). Therefore, in the absence of a ventilatory impairment, OE-MRI derived measures should provide a reasonable reflection of the degree of pulmonary vascular disease.

This technique also has the advantage of not requiring use of ionising radiation or IV contrast agents which most current, pulmonary perfusion imaging techniques utilise.

2.27.4 Future Directions

- Large, prospective, randomised controlled studies with longer follow-up periods are required to evaluate the role of pulmonary vasodilator therapies in group 3 PH.
- Further work on biomarkers derived from CT and MRI based imaging of the smaller, distal PAs may provide insight into the vascular phenotype that is more likely to respond to these treatments.
- Comparing imaging changes with vascular changes seen in histology samples may help guide which imaging techniques are more relevant in the assessment of PH.
- Comparison of OE-MRI derived parameter maps with VQ scintigraphy may help validate this technique in PH.
- Larger studies including controls (with no cardiopulmonary disease) and more post-treatment follow-up scans are required to further assess the repeatability and role of OE-MRI in PH.

2.28 Conclusion

Imaging is recognised as a valuable tool in assessing severity, improving phenotyping, and providing prognostic information in PH. The Pulmonary Vascular Research Institute identified imaging as an important area for international collaboration(88). Advances in CT and MRI acquisition, reconstruction, and post-processing have led to an increasing number of quantitative features that can be used to detect and stratify the severity of PH, define subpopulations with homogeneous characteristics, and monitor response to therapeutics (236). These novel quantitative imaging biomarkers provide exciting prospects for a non-invasive alternative to diagnosis, assessment, and follow-up of patients with PH.

BIBLIOGRAPHY

1. Lai YC, Potoka KC, Champion HC, Mora AL, Gladwin MT. Pulmonary arterial hypertension: The clinical syndrome. Circ Res. 2014;115(1):115–30.
2. Townsley MI. Structure and composition of pulmonary arteries, capillaries, and veins. Compr Physiol. 2012 Jan;2(1):675–709.
3. Boyette L, Burns B. Physiology, Pulmonary Circulation. 2020.
4. Suresh K, Shimoda LA. Lung Circulation. Compr Physiol. 2016 Mar;6(2):897–943.
5. Aggarwal S, Gross CM, Porcelli RJ, Black SM. Chapter 14 - Pulmonary Hemodynamics. In: Parent RABT-CB of the NL (Second E, editor. San Diego: Academic Press; 2015. p. 205–43. Available from: https://www.sciencedirect.com/science/article/pii/B978012404577400014X
6. Clark A, Tawhai M. Pulmonary Vascular Dynamics. Compr Physiol. 2019 Jun;9(3):1081–100.
7. Kovacs G, Berghold A, Scheidl S, Olschewski H. Pulmonary arterial pressure during rest and exercise in healthy subjects: a systematic review. Eur Respir J [Internet]. 2009 Oct 1;34(4):888 LP – 894. Available from: http://erj.ersjournals.com/content/34/4/888.abstract
8. SOBOL BJ, BOTTEX G, EMIRGIL C, GISSEN H. GASEOUS DIFFUSION FROM ALVEOLI TO PULMONARY VESSELS OF CONSIDERABLE SIZE. Circ Res. 1963 Jul;13:71–9.
9. JAMESON AG. Diffusion of gases from alveolus to precapillary arteries. Science. 1963 Mar;139(3557):826–8.
10. Stickland MK, Tedjasaputra V, Fuhr DP, Wagner HE, Collins SÉ, Byers BW, et al. Precapillary pulmonary gas exchange is similar for oxygen and inert gases. J Physiol. 2019 Nov;597(22):5385–97.
11. Tabuchi A, Styp-Rekowska B, Slutsky AS, Wagner PD, Pries AR, Kuebler WM. Precapillary oxygenation contributes relevantly to gas exchange in the intact lung. Am J Respir Crit Care Med. 2013 Aug;188(4):474–81.
12. Gehr P, Bachofen M, Weibel ER. The normal human lung: ultrastructure and morphometric estimation of diffusion capacity. Respir Physiol [Internet]. 1978;32(2):121–40. Available from: https://www.sciencedirect.com/science/article/pii/0034568778901044
13. Weibel ER, Federspiel WJ, Fryder-Doffey F, Hsia CC, König M, Stalder-Navarro V, et al. Morphometric model for pulmonary diffusing capacity. I. Membrane diffusing capacity. Respir Physiol. 1993 Aug;93(2):125–49.
14. Weibel ER. What makes a good lung? Swiss Med Wkly. 2009 Jul;139(27–28):375–86.
15. Dunham-Snary KJ, Wu D, Sykes EA, Thakrar A, Parlow LRG, Mewburn JD, et al. Hypoxic Pulmonary Vasoconstriction: From Molecular Mechanisms to Medicine. Chest. 2017 Jan;151(1):181–92.
16. Hatano, Suichi S. Primary pulmonary hypertension : report on a WHO meeting, Geneva, 15-17 October 1973. 1973.
17. Galiè N, Humbert M, Vachiery J-L, Gibbs S, Lang I, Torbicki A, et al. 2015 ESC/ERS Guidelines

for the diagnosis and treatment of pulmonary hypertension. Eur Respir J [Internet]. 2015 Oct 1;46(4):903 LP – 975. Available from: http://erj.ersjournals.com/content/46/4/903.abstract

18. Simonneau G, Montani D, Celermajer DS, Denton CP, Gatzoulis MA, Krowka M, et al. Haemodynamic definitions and updated clinical classification of pulmonary hypertension. Eur Respir J [Internet]. 2019;53(1). Available from: http://dx.doi.org/10.1183/13993003.01913-2018

19. Simonneau G, Galiè N, Rubin LJ, Langleben D, Seeger W, Domenighetti G, et al. Clinical classification of pulmonary hypertension. J Am Coll Cardiol [Internet]. 2004 Jun 16 [cited 2018 Nov 19];43(12):S5–12. Available from: https://www.sciencedirect.com/science/article/pii/S0735109704004759?via%3Dihub

20. Britain G. NAPH 10th Annual Report National Audit of Pulmonary Hypertension Tenth Annual Report. 2019;(October).

21. Kiely D. National Audit of Pulmonary Hypertension: Eleventh Annual Report. NHS Digit. 2021;v1.1(October):22–5.

22. Zanatta E, Polito P, Famoso G, Larosa M, De Zorzi E, Scarpieri E, et al. Pulmonary arterial hypertension in connective tissue disorders: Pathophysiology and treatment. Exp Biol Med (Maywood). 2019 Feb;244(2):120–31.

23. Fayed H, Coghlan JG. Pulmonary Hypertension Associated with Connective Tissue Disease. Semin Respir Crit Care Med. 2019 Apr;40(2):173–83.

24. Launay D, Sitbon O, Hachulla E, Mouthon L, Gressin V, Rottat L, et al. Survival in systemic sclerosis-associated pulmonary arterial hypertension in the modern management era. Ann Rheum Dis. 2013 Dec;72(12):1940–6.

25. Ramjug S, Hussain N, Hurdman J, Billings C, Charalampopoulos A, Elliot CA, et al. Pulmonary arterial hypertension associated with congenital heart disease: Comparison of clinical and anatomic-pathophysiologic classification. J Hear Lung Transplant [Internet]. 2016;35(5):610–8. Available from: http://dx.doi.org/10.1016/j.healun.2015.12.016

26. Dimopoulos K, Wort SJ, Gatzoulis MA. Pulmonary hypertension related to congenital heart disease: A call for action. Eur Heart J. 2014;35(11):691–700.

27. Beghetti M, Galiè N. Eisenmenger Syndrome. A Clinical Perspective in a New Therapeutic Era of Pulmonary Arterial Hypertension. J Am Coll Cardiol. 2009;53(9):733–40.

28. Tuder RM, Abman SH, Braun T, Capron F, Stevens T, Thistlethwaite PA, et al. Development and pathology of pulmonary hypertension. J Am Coll Cardiol. 2009 Jun;54(1 Suppl):S3–9.

29. Loscalzo J. Endothelial dysfunction in pulmonary hypertension. Vol. 327, The New England journal of medicine. United States; 1992. p. 117–9.

30. Rabinovitch M. Pathobiology of pulmonary hypertension. Annu Rev Pathol. 2007;2:369–99.

31. Schermuly RT, Ghofrani HA, Wilkins MR, Grimminger F. Mechanisms of disease: pulmonary arterial hypertension. Nat Rev Cardiol [Internet]. 2011;8(8):443–55. Available from: https://doi.org/10.1038/nrcardio.2011.87

32. Davie N, Haleen SJ, Upton PD, Polak JM, Yacoub MH, Morrell NW, et al. ET(A) and ET(B) receptors modulate the proliferation of human pulmonary artery smooth muscle cells. Am J Respir Crit Care Med. 2002 Feb;165(3):398–405.

33. Geiger R, Berger RM, Hess J, Bogers AJ, Sharma HS, Mooi WJ. Enhanced expression of

vascular endothelial growth factor in pulmonary plexogenic arteriopathy due to congenital heart disease. J Pathol. 2000 Jun;191(2):202–7.

34. Benisty JI, McLaughlin V V, Landzberg MJ, Rich JD, Newburger JW, Rich S, et al. Elevated basic fibroblast growth factor levels in patients with pulmonary arterial hypertension. Chest. 2004 Oct;126(4):1255–61.

35. Le Cras TD, Hardie WD, Fagan K, Whitsett JA, Korfhagen TR. Disrupted pulmonary vascular development and pulmonary hypertension in transgenic mice overexpressing transforming growth factor-alpha. Am J Physiol Lung Cell Mol Physiol. 2003 Nov;285(5):L1046-54.

36. Machado RD, Eickelberg O, Elliott CG, Geraci MW, Hanaoka M, Loyd JE, et al. Genetics and genomics of pulmonary arterial hypertension. J Am Coll Cardiol. 2009 Jun;54(1 Suppl):S32–42.

37. Grimminger F, Schermuly RT. PDGF receptor and its antagonists: role in treatment of PAH. Adv Exp Med Biol. 2010;661:435–46.

38. Perros F, Montani D, Dorfmüller P, Durand-Gasselin I, Tcherakian C, Le Pavec J, et al. Platelet-derived growth factor expression and function in idiopathic pulmonary arterial hypertension. Am J Respir Crit Care Med. 2008 Jul;178(1):81–8.

39. Hassoun PM, Mouthon L, Barberà JA, Eddahibi S, Flores SC, Grimminger F, et al. Inflammation, growth factors, and pulmonary vascular remodeling. J Am Coll Cardiol. 2009 Jun;54(1 Suppl):S10–9.

40. Cool CD, Kennedy D, Voelkel NF, Tuder RM. Pathogenesis and evolution of plexiform lesions in pulmonary hypertension associated with scleroderma and human immunodeficiency virus infection. Hum Pathol. 1997 Apr;28(4):434–42.

41. Tuder RM, Groves B, Badesch DB, Voelkel NF. Exuberant endothelial cell growth and elements of inflammation are present in plexiform lesions of pulmonary hypertension. Am J Pathol. 1994 Feb;144(2):275–85.

42. Humbert M, Monti G, Brenot F, Sitbon O, Portier A, Grangeot-Keros L, et al. Increased interleukin-1 and interleukin-6 serum concentrations in severe primary pulmonary hypertension. Am J Respir Crit Care Med. 1995 May;151(5):1628–31.

43. Tournier A, Wahl D, Chaouat A, Max J-P, Regnault V, Lecompte T, et al. Calibrated automated thrombography demonstrates hypercoagulability in patients with idiopathic pulmonary arterial hypertension. Thromb Res. 2010 Dec;126(6):e418-22.

44. Johnson SR, Granton JT, Mehta S. Thrombotic arteriopathy and anticoagulation in pulmonary hypertension. Chest. 2006 Aug;130(2):545–52.

45. Christman BW, McPherson CD, Newman JH, King GA, Bernard GR, Groves BM, et al. An imbalance between the excretion of thromboxane and prostacyclin metabolites in pulmonary hypertension. N Engl J Med. 1992 Jul;327(2):70–5.

46. Bourgeois A, Omura J, Habbout K, Bonnet S, Boucherat O. Pulmonary arterial hypertension: New pathophysiological insights and emerging therapeutic targets. Int J Biochem Cell Biol [Internet]. 2018;104(April):9–13. Available from: https://doi.org/10.1016/j.biocel.2018.08.015

47. Kiely DG, Elliot CA. Pulmonary hypertension : diagnosis and management. 2013;2028(April):1–12.

48. Bogaard HJ, Abe K, Vonk Noordegraaf A, Voelkel NF. The right ventricle under pressure: cellular and molecular mechanisms of right-heart failure in pulmonary hypertension. Chest.

2009 Mar;135(3):794–804.

49. Ryan JJ, Huston J, Kutty S, Hatton ND, Bowman L, Tian L, et al. Right Ventricular Adaptation and Failure in Pulmonary Arterial Hypertension. Can J Cardiol [Internet]. 2015 Apr 1 [cited 2020 Mar 11];31(4):391–406. Available from: https://www.sciencedirect.com/science/article/pii/S0828282X15000586?via%3Dihub#fig1

50. Dimopoulos K, Giannakoulas G, Wort SJ, Gatzoulis MA. Pulmonary arterial hypertension in adults with congenital heart disease: Distinct differences from other causes of pulmonary arterial hypertension and management implications. Curr Opin Cardiol. 2008;23(6):545–54.

51. Soubrier F, Chung WK, Machado R, Grünig E, Aldred M, Geraci M, et al. Genetics and Genomics of Pulmonary Arterial Hypertension. J Am Coll Cardiol [Internet]. 2013 Dec 24 [cited 2019 Nov 25];62(25):D13–21. Available from: https://www.sciencedirect.com/science/article/pii/S0735109713058786?via%3Dihub

52. Austin ED, Loyd JE. Genetics and Mediators in Pulmonary Arterial Hypertension. Clin Chest Med [Internet]. 2007;28(1):43–57. Available from: https://www.sciencedirect.com/science/article/pii/S0272523106001213

53. Machado RD, Aldred MA, James V, Harrison RE, Patel B, Schwalbe EC, et al. Mutations of the TGF-beta type II receptor BMPR2 in pulmonary arterial hypertension. Hum Mutat. 2006 Feb;27(2):121–32.

54. Teichert-Kuliszewska K, Kutryk MJB, Kuliszewski MA, Karoubi G, Courtman DW, Zucco L, et al. Bone morphogenetic protein receptor-2 signaling promotes pulmonary arterial endothelial cell survival: implications for loss-of-function mutations in the pathogenesis of pulmonary hypertension. Circ Res. 2006 Feb;98(2):209–17.

55. Morrell NW, Aldred MA, Chung WK, Elliott CG, Nichols WC, Soubrier F, et al. Genetics and genomics of pulmonary arterial hypertension. Eur Respir J [Internet]. 2019 Jan 1;53(1):1801899. Available from: http://erj.ersjournals.com/content/53/1/1801899.abstract

56. Nathan SD, Barbera JA, Gaine SP, Harari S, Martinez FJ, Olschewski H, et al. Pulmonary hypertension in chronic lung disease and hypoxia. Eur Respir J [Internet]. 2019;53(1). Available from: http://dx.doi.org/10.1183/13993003.01914-2018

57. Medrek S, Safdar Z. Epidemiology and Pathophysiology of Chronic Thromboembolic Pulmonary Hypertension: Risk Factors and Mechanisms. Methodist Debakey Cardiovasc J. 2016;12(4):195–8.

58. Wilkens H, Konstantinides S, Lang IM, Bunck AC, Gerges M, Gerhardt F, et al. Chronic thromboembolic pulmonary hypertension (CTEPH): Updated Recommendations from the Cologne Consensus Conference 2018. Int J Cardiol [Internet]. 2018;272:69–78. Available from: https://doi.org/10.1016/j.ijcard.2018.08.079

59. Peacock AJ, Murphy NF, McMurray JJ V, Caballero L, Stewart S. An epidemiological study of pulmonary arterial hypertension. Eur Respir J [Internet]. 2007 Jul 1;30(1):104 LP – 109. Available from: http://erj.ersjournals.com/content/30/1/104.abstract

60. Hoeper MM, Humbert M, Souza R, Idrees M, Kawut SM, Sliwa-Hahnle K, et al. A global view of pulmonary hypertension. Lancet Respir Med. 2016 Apr;4(4):306–22.

61. Macintyre N, Crapo RO, Viegi G, Johnson DC, van der Grinten CPM, Brusasco V, et al. Standardisation of the single-breath determination of carbon monoxide uptake in the lung. Eur Respir J. 2005 Oct;26(4):720–35.

62. ROUGHTON FJ, FORSTER RE. Relative importance of diffusion and chemical reaction rates in determining rate of exchange of gases in the human lung, with special reference to true diffusing capacity of pulmonary membrane and volume of blood in the lung capillaries. J Appl Physiol. 1957 Sep;11(2):290–302.

63. Nadel JA, Gold WM, Burgess JH. Early diagnosis of chronic pulmonary vascular obstruction. Value of pulmonary function tests. Am J Med. 1968 Jan;44(1):16–25.

64. Borland C, Cox Y, Higenbottam T. Reduction of pulmonary capillary blood volume in patients with severe unexplained pulmonary hypertension. Thorax. 1996 Aug;51(8):855–6.

65. Farha S, Laskowski D, George D, Park MM, Tang WHW, Dweik RA, et al. Loss of alveolar membrane diffusing capacity and pulmonary capillary blood volume in pulmonary arterial hypertension. Respir Res. 2013 Jan;14(1):6.

66. Bernstein RJ, Ford RL, Clausen JL, Moser KM. Membrane diffusion and capillary blood volume in chronic thromboembolic pulmonary hypertension. Chest. 1996 Dec;110(6):1430–6.

67. Steenhuis LH, Groen HJ, Koëter GH, van der Mark TW. Diffusion capacity and haemodynamics in primary and chronic thromboembolic pulmonary hypertension. Eur Respir J. 2000 Aug;16(2):276–81.

68. Frost A, Badesch D, Gibbs JSR, Gopalan D, Khanna D, Manes A, et al. Diagnosis of pulmonary hypertension. Eur Respir J. 2019 Jan;53(1).

69. Ley S, Kreitner KF, Fink C, Heussel CP, Borst MM, Kauczor HU. Assessment of pulmonary hypertension by CT and MR imaging. Eur Radiol. 2004;14(3):359–68.

70. Yasunobu Y, Oudiz RJ, Sun X-G, Hansen JE, Wasserman K. End-tidal PCO2 abnormality and exercise limitation in patients with primary pulmonary hypertension. Chest. 2005 May;127(5):1637–46.

71. Oudiz RJ. The role of exercise testing in the management of pulmonary arterial hypertension. Semin Respir Crit Care Med. 2005 Aug;26(4):379–84.

72. Sitbon O, Humbert M, Jaïs X, Ioos V, Hamid AM, Provencher S, et al. Long-Term Response to Calcium Channel Blockers in Idiopathic Pulmonary Arterial Hypertension. Circulation [Internet]. 2005 Jun 14 [cited 2018 Nov 26];111(23):3105–11. Available from: https://www.ahajournals.org/doi/10.1161/CIRCULATIONAHA.104.488486

73. Seferian A, Simonneau G. Therapies for pulmonary arterial hypertension: Where are we today, where do we go tomorrow? Eur Respir Rev. 2013;22(129):217–26.

74. Galie N, Olschewski H, Oudiz RJ, Torres F, Frost A, Ghofrani HA, et al. Ambrisentan for the treatment of pulmonary arterial hypertension: results of the ambrisentan in pulmonary arterial hypertension, randomized, double-blind, placebo-controlled, multicenter, efficacy (ARIES) study 1 and 2. Circulation. 2008 Jun;117(23):3010–9.

75. Ahmadi-Simab K, Lamprecht P, Hellmisch B, Gross WL. [Treatment of pulmonary arterial hypertension (PAH) with oral endothelin-receptor antagonist bosentan in systemic sclerosis: BREATHE-1 trial and clinical experience]. Z Rheumatol. 2004 Dec;63(6):495–7.

76. Galie N, Rubin L, Hoeper M, Jansa P, Al-Hiti H, Meyer G, et al. Treatment of patients with mildly symptomatic pulmonary arterial hypertension with bosentan (EARLY study): a double-blind, randomised controlled trial. Lancet (London, England). 2008 Jun;371(9630):2093–100.

77. McGoon MD, Frost AE, Oudiz RJ, Badesch DB, Galie N, Olschewski H, et al. Ambrisentan therapy in patients with pulmonary arterial hypertension who discontinued bosentan or

sitaxsentan due to liver function test abnormalities. Chest. 2009 Jan;135(1):122–9.

78. D'Alto M, Vitulo P. [The SERAPHIN study]. G Ital Cardiol (Rome). 2015 Jan;16(1):6–10.

79. Galie N, Ghofrani HA, Torbicki A, Barst RJ, Rubin LJ, Badesch D, et al. Sildenafil citrate therapy for pulmonary arterial hypertension. N Engl J Med. 2005 Nov;353(20):2148–57.

80. Rubin LJ, Badesch DB, Fleming TR, Galie N, Simonneau G, Ghofrani HA, et al. Long-term treatment with sildenafil citrate in pulmonary arterial hypertension: the SUPER-2 study. Chest. 2011 Nov;140(5):1274–83.

81. Lian T-Y, Jiang X, Jing Z-C. Riociguat: a soluble guanylate cyclase stimulator for the treatment of pulmonary hypertension. Drug Des Devel Ther. 2017;11:1195–207.

82. Ghofrani H-A, Galie N, Grimminger F, Grunig E, Humbert M, Jing Z-C, et al. Riociguat for the treatment of pulmonary arterial hypertension. N Engl J Med. 2013 Jul;369(4):330–40.

83. Simonneau G, Torbicki A, Hoeper MM, Delcroix M, Karlocai K, Galie N, et al. Selexipag: an oral, selective prostacyclin receptor agonist for the treatment of pulmonary arterial hypertension. Eur Respir J. 2012 Oct;40(4):874–80.

84. Sitbon O, Channick R, Chin KM, Frey A, Gaine S, Galie N, et al. Selexipag for the Treatment of Pulmonary Arterial Hypertension. N Engl J Med. 2015 Dec;373(26):2522–33.

85. Galie N, Barbera JA, Frost AE, Ghofrani H-A, Hoeper MM, McLaughlin V V, et al. Initial Use of Ambrisentan plus Tadalafil in Pulmonary Arterial Hypertension. N Engl J Med. 2015 Aug;373(9):834–44.

86. McGoon MD, Miller DP. REVEAL: A contemporary US pulmonary arterial hypertension registry. Eur Respir Rev. 2012;21(123):8–18.

87. Rich S, Kaufmann E, Levy PS. The Effect of High Doses of Calcium-Channel Blockers on Survival in Primary Pulmonary Hypertension. N Engl J Med [Internet]. 1992 Jul 9;327(2):76–81. Available from: https://doi.org/10.1056/NEJM199207093270203

88. Kiely DG, Levin D, Hassoun P, Ivy DD, Jone P-N, Bwika J, et al. EXPRESS: Statement on imaging and pulmonary hypertension from the Pulmonary Vascular Research Institute (PVRI). Pulm Circ. 2019 Mar;9(3):2045894019841990.

89. Lange, Sebastian. Walsh G. Radiology of Chest Diseases.

90. Radiation Dose in X-Ray and CT Exams [Internet]. Available from: https://www.radiologyinfo.org/en/info/safety-xray

91. Rajaram S, Swift AJ, Condliffe R, Johns C, Elliot CA, Hill C, et al. CT features of pulmonary arterial hypertension and its major subtypes: A systematic CT evaluation of 292 patients from the ASPIRE Registry. Thorax. 2015;70(4):382–7.

92. Tan RT, Kuzo R, Goodman LR, Siegel R, Haasler GB, Presberg KW. Utility of CT scan evaluation for predicting pulmonary hypertension in patients with parenchymal lung disease. Medical College of Wisconsin Lung Transplant Group. Chest. 1998 May;113(5):1250–6.

93. Edwards PD, Bull RK, Coulden R. CT measurement of main pulmonary artery diameter. Br J Radiol. 1998 Oct;71(850):1018–20.

94. Okajima Y, Ohno Y, Washko GR, Hatabu H. Assessment of Pulmonary Hypertension : What CT and MRI Can Povide. Acad Radiol [Internet]. 2011;18(4):437–53. Available from: http://dx.doi.org/10.1016/j.acra.2011.01.003

95. Ng CS, Wells AU, Padley SP. A CT sign of chronic pulmonary arterial hypertension: the ratio of main pulmonary artery to aortic diameter. J Thorac Imaging. 1999 Oct;14(4):270–8.

96. Sheehan R, Perloff JK, Fishbein MC, Gjertson D, Aberle DR. Pulmonary neovascularity: A distinctive radiographic finding in Eisenmenger syndrome. Circulation. 2005;112(18):2778–85.

97. Johns CS, Wild JM, Rajaram S, Swift AJ, Kiely DG. Current and emerging imaging techniques in the diagnosis and assessment of pulmonary hypertension. Expert Rev Respir Med [Internet]. 2018;12(2):145–60. Available from: https://doi.org/10.1080/17476348.2018.1420478

98. Revel M-P, Faivre J-B, Remy-Jardin M, Delannoy-Deken V, Duhamel A, Remy J. Pulmonary hypertension: ECG-gated 64-section CT angiographic evaluation of new functional parameters as diagnostic criteria. Radiology. 2009 Feb;250(2):558–66.

99. Bax S, Jacob J, Ahmed R, Bredy C, Dimopoulos K, Kempny A, et al. Right Ventricular to Left Ventricular Ratio at CT Pulmonary Angiogram Predicts Mortality in Interstitial Lung Disease. Chest [Internet]. 2019;1–10. Available from: https://doi.org/10.1016/j.chest.2019.06.033

100. Groves AM, Win T, Charman SC, Wisbey C, Pepke-Zaba J, Coulden RA. Semi-quantitative assessment of tricuspid regurgitation on contrast-enhanced multidetector CT. Clin Radiol. 2004 Aug;59(8):715–9.

101. Ali N, Loughborough WW, Rodrigues JCL, Suntharalingam J, Hudson B, Hall T, et al. Computed tomographic and clinical features of pulmonary veno-occlusive disease: raising the radiologist's awareness. Clin Radiol. 2019 Sep;74(9):655–62.

102. Resten A, Maitre S, Humbert M, Rabiller A, Sitbon O, Capron F, et al. Pulmonary hypertension: CT of the chest in pulmonary venoocclusive disease. AJR Am J Roentgenol. 2004 Jul;183(1):65–70.

103. Resten A, Maitre S, Humbert M, Sitbon O, Capron F, Simoneau G, et al. Pulmonary arterial hypertension: thin-section CT predictors of epoprostenol therapy failure. Radiology. 2002 Mar;222(3):782–8.

104. Iyer KS, Newell JDJ, Jin D, Fuld MK, Saha PK, Hansdottir S, et al. Quantitative Dual-Energy Computed Tomography Supports a Vascular Etiology of Smoking-induced Inflammatory Lung Disease. Am J Respir Crit Care Med. 2016 Mar;193(6):652–61.

105. Thieme SF, Becker CR, Hacker M, Nikolaou K, Reiser MF, Johnson TRC. Dual energy CT for the assessment of lung perfusion--correlation to scintigraphy. Eur J Radiol. 2008 Dec;68(3):369–74.

106. Pontana F, Faivre J-B, Remy-Jardin M, Flohr T, Schmidt B, Tacelli N, et al. Lung perfusion with dual-energy multidetector-row CT (MDCT): feasibility for the evaluation of acute pulmonary embolism in 117 consecutive patients. Acad Radiol. 2008 Dec;15(12):1494–504.

107. Pienn M, Kovacs G, Tscherner M, Johnson TR, Kullnig P, Stollberger R, et al. Determination of cardiac output with dynamic contrast-enhanced computed tomography. Int J Cardiovasc Imaging. 2013 Dec;29(8):1871–8.

108. Pienn M, Kovacs G, Tscherner M, Avian A, Johnson TR, Kullnig P, et al. Non-invasive determination of pulmonary hypertension with dynamic contrast-enhanced computed tomography: a pilot study. Eur Radiol. 2014 Mar;24(3):668–76.

109. Biederer J, Heussel CP, Puderbach M, Wielpuetz MO. Functional Magnetic Resonance Imaging of the Lung. 2014;c:74–82.

110. IWASAWA T. Diagnosis and Management of Pulmonary Arterial Hypertension using MR Imaging. Magn Reson Med Sci [Internet]. 2013;12(1):1–9. Available from: http://jlc.jst.go.jp/DN/JST.JSTAGE/mrms/2012-0040?lang=en&from=CrossRef&type=abstract

111. Swift AJ, Wild JM, Nagle SK, Roldán-Alzate A, François CJ, Fain S, et al. Quantitative magnetic resonance imaging of pulmonary hypertension: A practical approach to the current state of the art. J Thorac Imaging. 2014;29(2):68–79.

112. Saba TS, Foster J, Cockburn M, Cowan M, Peacock AJ. Ventricular mass index using magnetic resonance imaging accurately estimates pulmonary artery pressure. Eur Respir J. 2002 Dec;20(6):1519–24.

113. Freed BH, Collins JD, François CJ, Barker AJ, Cuttica MJ, Chesler NC, et al. MR and CT Imaging for the Evaluation of Pulmonary Hypertension. JACC Cardiovasc Imaging. 2016 Jun;9(6):715–32.

114. Dellegrottaglie S, Sanz J, Poon M, Viles-Gonzalez JF, Sulica R, Goyenechea M, et al. Pulmonary hypertension: accuracy of detection with left ventricular septal-to-free wall curvature ratio measured at cardiac MR. Radiology. 2007 Apr;243(1):63–9.

115. Nayak KS, Nielsen J-F, Bernstein MA, Markl M, D Gatehouse P, M Botnar R, et al. Cardiovascular magnetic resonance phase contrast imaging. J Cardiovasc Magn Reson Off J Soc Cardiovasc Magn Reson. 2015 Aug;17(1):71.

116. Johns CS, Swift AJ, Rajaram S, Hughes PJC, Capener DJ, Kiely DG, et al. Lung perfusion: MRI vs. SPECT for screening in suspected chronic thromboembolic pulmonary hypertension. J Magn Reson Imaging. 2017 Dec;46(6):1693–7.

117. Ley S, Fink C, Zaporozhan J, Borst MM, Meyer FJ, Puderbach M, et al. Value of high spatial and high temporal resolution magnetic resonance angiography for differentiation between idiopathic and thromboembolic pulmonary hypertension: initial results. Eur Radiol. 2005 Nov;15(11):2256–63.

118. Schoenfeld C, Cebotari S, Hinrichs J, Renne J, Kaireit T, Olsson KM, et al. MR Imaging-derived Regional Pulmonary Parenchymal Perfusion and Cardiac Function for Monitoring Patients with Chronic Thromboembolic Pulmonary Hypertension before and after Pulmonary Endarterectomy. Radiology. 2016 Jun;279(3):925–34.

119. Blyth KG, Groenning BA, Martin TN, Foster JE, Mark PB, Dargie HJ, et al. Contrast enhanced-cardiovascular magnetic resonance imaging in patients with pulmonary hypertension. Eur Heart J. 2005 Oct;26(19):1993–9.

120. Saunders LC, Hughes PJC, Alabed S, Capener DJ, Marshall H, Vogel-Claussen J, et al. Integrated Cardiopulmonary MRI Assessment of Pulmonary Hypertension. J Magn Reson Imaging. 2022 Mar;55(3):633–52.

121. Cherubini A, Bifone A. Hyperpolarised xenon in biology. Prog Nucl Magn Reson Spectrosc [Internet]. 2003;42(1):1–30. Available from: https://www.sciencedirect.com/science/article/pii/S0079656502000523

122. Dahhan T, Kaushik SS, He M, Mammarappallil JG, Tapson VF, McAdams HP, et al. Abnormalities in hyperpolarized (129)Xe magnetic resonance imaging and spectroscopy in two patients with pulmonary vascular disease. Vol. 6, Pulmonary circulation. United States; 2016. p. 126–31.

123. Wang Z, Bier EA, Swaminathan A, Parikh K, Nouls J, He M, et al. Diverse cardiopulmonary diseases are associated with distinct xenon magnetic resonance imaging signatures. Eur

Respir J. 2019 Dec;54(6).

124. Bier EA, Alenezi F, Lu J, Wang Z, Mammarappallil JG, O'Sullivan-Murphy B, et al. Noninvasive diagnosis of pulmonary hypertension with hyperpolarised (129)Xe magnetic resonance imaging and spectroscopy. ERJ open Res. 2022 Apr;8(2).

125. Bauman G, Puderbach M, Deimling M, Jellus V, Chefd C, Dinkel J, et al. Non-Contrast-Enhanced Perfusion and Ventilation Assessment of the Human Lung by Means of Fourier Decomposition in Proton MRI. 2009;664:656–64.

126. Van De Veerdonk MC, Kind T, Marcus JT, Mauritz GJ, Heymans MW, Bogaard HJ, et al. Progressive right ventricular dysfunction in patients with pulmonary arterial hypertension responding to therapy. J Am Coll Cardiol [Internet]. 2011;58(24):2511–9. Available from: http://dx.doi.org/10.1016/j.jacc.2011.06.068

127. Van Wolferen SA, Marcus JT, Boonstra A, Marques KMJ, Bronzwaer JGF, Spreeuwenberg MD, et al. Prognostic value of right ventricular mass, volume, and function in idiopathic pulmonary arterial hypertension. Eur Heart J. 2007;28(10):1250–7.

128. Frank H, Globits S, Glogar D, Neuhold A, Kneussl M, Mlczoch J. Detection and quantification of pulmonary artery hypertension with MR imaging: results in 23 patients. AJR Am J Roentgenol. 1993 Jul;161(1):27–31.

129. Swift AJ, Rajaram S, Marshall H, Condliffe R, Capener D, Hill C, et al. Black blood MRI has diagnostic and prognostic value in the assessment of patients with pulmonary hypertension. Eur Radiol. 2012 Mar;22(3):695–702.

130. Johns CS, Swift AJ, Hughes PJC, Ohno Y, Schiebler M, Wild JM. Pulmonary MR angiography and perfusion imaging—A review of methods and applications. Eur J Radiol [Internet]. 2017;86:361–70. Available from: http://dx.doi.org/10.1016/j.ejrad.2016.10.003

131. Nagendran J, Michelakis E. MRI: One-Stop Shop for the Comprehensive Assessment of Pulmonary Arterial Hypertension? Chest [Internet]. 2007 Jul 1 [cited 2018 Nov 19];132(1):2–5. Available from: https://www.sciencedirect.com/science/article/pii/S0012369215356737

132. Maxien D, Dietrich O, Thieme SF, Förster S, Behr J, Reiser MF, et al. Value of oxygen-enhanced MRI of the lungs in patients with pulmonary hypertension: A qualitative and quantitative approach. J Magn Reson Imaging. 2012;35(1):86–94.

133. Edelman RR, Hatabu H, Tadamura E, Li W, Prasad P V. Noninvasive assessment of regional ventilation in the human lung using oxygen-enhanced magnetic resonance imaging. Nat Med. 1996 Nov;2(11):1236–9.

134. Ohno Y, Chen Q, Hatabu H. Oxygen-enhanced magnetic resonance ventilation imaging of lung. Eur J Radiol. 2001;37(3):164–71.

135. Hatabu H, Tadamura E, Chen Q, Stock KW, Li W, Prasad P V, et al. Pulmonary ventilation: dynamic MRI with inhalation of molecular oxygen. Eur J Radiol. 2001 Mar;37(3):172–8.

136. Naish JH, Parker GJM, Beatty PC, Jackson A, Young SS, Waterton JC, et al. Improved quantitative dynamic regional oxygen-enhanced pulmonary imaging using image registration. Magn Reson Med. 2005 Aug;54(2):464–9.

137. Ohno Y, Hatabu H. Basics concepts and clinical applications of oxygen-enhanced MR imaging. Eur J Radiol. 2007;64(3):320–8.

138. Ohno Y, Koyama H, Lee HY, Kishida Y, Seki S, Yoshikawa T, et al. Oxygen-Enhanced MR Imaging for Lung: Basics and Clinical Applications. In: Hyperpolarized and Inert Gas MRI: From

Technology to Application in Research and Medicine. 2016.

139. O'Connor JPB, Boult JKR, Jamin Y, Babur M, Finegan KG, Williams KJ, et al. Oxygen-Enhanced MRI Accurately Identifies, Quantifies, and Maps Tumor Hypoxia in Preclinical Cancer Models. Cancer Res. 2016 Feb;76(4):787–95.

140. Molinari F, Eichinger M, Risse F, Plathow C, Puderbach M, Ley S, et al. Navigator-triggered oxygen-enhanced MRI with simultaneous cardiac and respiratory synchronization for the assessment of interstitial lung disease. J Magn Reson Imaging. 2007;26(6):1523–9.

141. Ohno Y, Koyama H, Nogami M, Takenaka D, Matsumoto S, Obara M, et al. Dynamic oxygen-enhanced MRI versus quantitative CT: pulmonary functional loss assessment and clinical stage classification of smoking-related COPD. AJR Am J Roentgenol. 2008;190(2):8–10.

142. Ohno Y, Hatabu H, Takenaka D, Van Cauteren M, Fujii M, Sugimura K. Dynamic oxygen-enhanced MRI reflects diffusing capacity of the lung. Magn Reson Med. 2002 Jun;47(6):1139–44.

143. Ohno Y, Hatabu H, Takenaka D, Adachi S, Van Cauteren M, Sugimura K. Oxygen-enhanced MR ventilation imaging of the lung: preliminary clinical experience in 25 subjects. AJR Am J Roentgenol. 2001 Jul;177(1):185–94.

144. Müller CJ, Schwaiblmair M, Scheidler J, Deimling M, Weber J, Löffler RB, et al. Pulmonary diffusing capacity: assessment with oxygen-enhanced lung MR imaging preliminary findings. Radiology. 2002 Feb;222(2):499–506.

145. Löffler R, Müller CJ, Peller M, Penzkofer H, Deimling M, Schwaiblmair M, et al. Optimization and evaluation of the signal intensity change in multisection oxygen-enhanced MR lung imaging. Magn Reson Med. 2000 Jun;43(6):860–6.

146. Jakob PM, Wang T, Schultz G, Hebestreit H, Hebestreit A, Hahn D. Assessment of human pulmonary function using oxygen-enhanced T(1) imaging in patients with cystic fibrosis. Magn Reson Med. 2004 May;51(5):1009–16.

147. Morgan AR, Parker GJM, Roberts C, Buonaccorsi GA, Maguire NC, Hubbard Cristinacce PL, et al. Feasibility assessment of using oxygen-enhanced magnetic resonance imaging for evaluating the effect of pharmacological treatment in COPD. Eur J Radiol [Internet]. 2014;83(11):2093–101. Available from: http://dx.doi.org/10.1016/j.ejrad.2014.08.004

148. Zaharchuk G, Busse RF, Rosenthal G, Manley GT, Glenn OA, Dillon WP. Noninvasive Oxygen Partial Pressure Measurement of Human Body Fluids In Vivo Using Magnetic Resonance Imaging. Acad Radiol. 2006;13(8):1016–24.

149. Zhang WJ, Niven RM, Young SS, Liu YZ, Parker GJM, Naish JH. Dynamic oxygen-enhanced magnetic resonance imaging of the lung in asthma - Initial experience. Eur J Radiol [Internet]. 2015;84(2):318–26. Available from: http://dx.doi.org/10.1016/j.ejrad.2014.10.021

150. Martini K, Gygax CM, Benden C, Morgan AR, Parker GJM, Frauenfelder T. Volumetric dynamic oxygen-enhanced MRI (OE-MRI): comparison with CT Brody score and lung function in cystic fibrosis patients (European Radiology, (2018), 28, 10, (4037-4047), 10.1007/s00330-018-5383-5). Eur Radiol. 2018;28(11):4922–3.

151. Corson N, Armato SG 3rd, Labby ZE, Straus C, Starkey A, Gomberg-Maitland M. CT-based pulmonary artery measurements for the assessment of pulmonary hypertension. Acad Radiol. 2014 Apr;21(4):523–30.

152. Agatston AS, Janowitz WR, Hildner FJ, Zusmer NR, Viamonte M, Detrano R. Quantification of

coronary artery calcium using ultrafast computed tomography. J Am Coll Cardiol [Internet]. 1990;15(4):827–32. Available from: http://dx.doi.org/10.1016/0735-1097(90)90282-T

153. Contractor S, Maldjian PD, Sharma VK, Gor DM. Role of helical CT in detecting right ventricular dysfunction secondary to acute pulmonary embolism. J Comput Assist Tomogr. 2002;26(4):587–91.

154. Barr CopdgCTWGRG, Berkowitz EA, Bigazzi F, Bode F, Bon J, Bowler RP, et al. A Combined Pulmonary-Radiology Workshop for Visual Evaluation of COPD: Study Design, Chest CT Findings and Concordance with Quantitative Evaluation. COPD J Chronic Obstr Pulm Dis [Internet]. 2012 Mar 29;9(2):151–9. Available from: https://doi.org/10.3109/15412555.2012.654923

155. Murphy K, Ginneken B van, Reinhardt JM, Kabus S, Ding K, Deng X, et al. Evaluation of Registration Methods on Thoracic CT: The EMPIRE10 Challenge. IEEE Trans Med Imaging. 2011;30(11):1901–20.

156. Wanger J. The ATS Pulmonary Function Laboratory Management and Procedure Manual. 3rd ed.

157. Rudski LG, Lai WW, Afilalo J, Hua L, Handschumacher MD, Chandrasekaran K, et al. Guidelines for the echocardiographic assessment of the right heart in adults: a report from the American Society of Echocardiography endorsed by the European Association of Echocardiography, a registered branch of the European Society of Cardiology, and . J Am Soc Echocardiogr Off Publ Am Soc Echocardiogr. 2010 Jul;23(7):685–8.

158. Picard MH, Adams D, Bierig SM, Dent JM, Douglas PS, Gillam LD, et al. American Society of Echocardiography recommendations for quality echocardiography laboratory operations. J Am Soc Echocardiogr Off Publ Am Soc Echocardiogr. 2011 Jan;24(1):1–10.

159. ATS Statement. Am J Respir Crit Care Med [Internet]. 2002 Jul 1;166(1):111–7. Available from: https://doi.org/10.1164/ajrccm.166.1.at1102

160. Yorke J, Corris P, Gaine S, Gibbs JSR, Kiely DG, Harries C, et al. emPHasis-10: development of a health-related quality of life measure in pulmonary hypertension. Eur Respir J [Internet]. 2014 Apr 1;43(4):1106 LP – 1113. Available from: http://erj.ersjournals.com/content/43/4/1106.abstract

161. Bruce RA, Blackmon JR, Jones JW, Strait G. EXERCISING TESTING IN ADULT NORMAL SUBJECTS AND CARDIAC PATIENTS. Pediatrics [Internet]. 1963 Oct 1;32(4):742 LP – 756. Available from: http://pediatrics.aappublications.org/content/32/4/742.abstract

162. Koo TK, Li MY. A Guideline of Selecting and Reporting Intraclass Correlation Coefficients for Reliability Research. J Chiropr Med. 2016 Jun;15(2):155–63.

163. Brewis MJ, Church AC, Johnson MK, Peacock AJ. Severe pulmonary hypertension in lung disease: Phenotypes and response to treatment. Eur Respir J [Internet]. 2015;46(5):1378–89. Available from: http://dx.doi.org/10.1183/13993003.02307-2014

164. Seeger W, Adir Y, Barberà JA, Champion H, Coghlan JG, Cottin V, et al. Pulmonary hypertension in chronic lung diseases. J Am Coll Cardiol. 2013;62(25 SUPPL.).

165. Boerrigter BG, Bogaard HJ, Trip P, Groepenhoff H, Rietema H, Holverda S, et al. Ventilatory and Cardiocirculatory Exercise Profiles in COPD: The Role of Pulmonary Hypertension. Chest [Internet]. 2012;142(5):1166–74. Available from: https://www.sciencedirect.com/science/article/pii/S0012369212606187

166. Chaouat A, Naeije R, Weitzenblum E. Pulmonary hypertension in COPD. Eur Respir J [Internet]. 2008 Nov 1;32(5):1371 LP – 1385. Available from: http://erj.ersjournals.com/content/32/5/1371.abstract

167. Poms AD, Turner M, Farber HW, Meltzer LA, McGoon MD. Comorbid conditions and outcomes in patients with pulmonary arterial hypertension: a REVEAL registry analysis. Chest. 2013 Jul;144(1):169–76.

168. Weitzenblum E, Chaouat A. Severe pulmonary hypertension in COPD: is it a distinct disease? Vol. 127, Chest. United States; 2005. p. 1480–2.

169. Weitzenblum E, Schrijen F, Mohan-Kumar T, des Francs VC, Lockhart A. Variability of the Pulmonary Vascular Response to Acute Hypoxia in Chronic Bronchitis. Chest [Internet]. 1988;94(4):772–8. Available from: https://www.sciencedirect.com/science/article/pii/S0012369216305785

170. Ashutosh K, Mead G, Dunsky M. Early Effects of Oxygen Administration and Prognosis in Chronic Obstuctive Pulmonary Disease and Cor Pulmonale. Am Rev Respir Dis [Internet]. 1983 Apr 1;127(4):399–404. Available from: https://doi.org/10.1164/arrd.1983.127.4.399

171. Eddahibi S, Chaouat A, Morrell N, Fadel E, Fuhrman C, Bugnet A-S, et al. Polymorphism of the serotonin transporter gene and pulmonary hypertension in chronic obstructive pulmonary disease. Circulation [Internet]. 2003 Oct 14 [cited 2019 Nov 27];108(15):1839–44. Available from: https://www.ahajournals.org/doi/10.1161/01.CIR.0000091409.53101.E8

172. Oswald-Mammosser M, Weitzenblum E, Quoix E, Moser G, Chaouat A, Charpentier C, et al. Prognostic Factors in COPD Patients Receiving Long-term Oxygen Therapy: Importance of Pulmonary Artery Pressure. Chest [Internet]. 1995;107(5):1193–8. Available from: https://www.sciencedirect.com/science/article/pii/S001236921638179X

173. Wright JL, Levy RD, Churg A. Pulmonary hypertension in chronic obstructive pulmonary disease: current theories of pathogenesis and their implications for treatment. Thorax [Internet]. 2005 Jul 1;60(7):605 LP – 609. Available from: http://thorax.bmj.com/content/60/7/605.abstract

174. Teramachi R, Taniguchi H, Kondoh Y, Ando M, Kimura T, Kataoka K, et al. Progression of mean pulmonary arterial pressure in idiopathic pulmonary fibrosis with mild to moderate restriction. Respirology. 2017 Jul;22(5):986–90.

175. Judge EP, Fabre A, Adamali HI, Egan JJ. Acute exacerbations and pulmonary hypertension in advanced idiopathic pulmonary fibrosis. Eur Respir J. 2012 Jul;40(1):93–100.

176. Lettieri CJ, Nathan SD, Barnett SD, Ahmad S, Shorr AF. Prevalence and outcomes of pulmonary arterial hypertension in advanced idiopathic pulmonary fibrosis. Chest. 2006 Mar;129(3):746–52.

177. Hoeper MM, Behr J, Held M, Grunig E, Vizza CD, Vonk-Noordegraaf A, et al. Pulmonary hypertension in patients with chronic fibrosing idiopathic interstitial pneumonias. PLoS One. 2015;10(12):1–13.

178. Lloyd CR, Walsh M SLF, Hansell M. High-resolution CT of complications of idiopathic fibrotic lung disease. Br J Radiol. 2011;84(1003):581–92.

179. Mura M, Anraku M, Yun Z, McRae K, Liu M, Waddell TK, et al. Gene expression profiling in the lungs of patients with pulmonary hypertension associated with pulmonary fibrosis. Chest. 2012 Mar;141(3):661–73.

180. Cottin V, Le Pavec J, Prevot G, Mal H, Humbert M, Simonneau G, et al. Pulmonary hypertension in patients with combined pulmonary fibrosis and emphysema syndrome. Eur Respir J. 2010 Jan;35(1):105–11.

181. Wong HS, Williams AJ, Mok Y. The relationship between pulmonary hypertension and obstructive sleep apnea. Curr Opin Pulm Med [Internet]. 2017;23(6). Available from: https://journals.lww.com/co-pulmonarymedicine/Fulltext/2017/11000/The_relationship_between_pulmonary_hypertension.6.aspx

182. Masa JF, Corral J, Caballero C, Barrot E, Terán-Santos J, Alonso-Álvarez ML, et al. Non-invasive ventilation in obesity hypoventilation syndrome without severe obstructive sleep apnoea. Thorax. 2016 Oct;71(10):899–906.

183. Castro-Añón O, Golpe R, Pérez-de-Llano LA, López González MJ, Escalona Velasquez EJ, Pérez Fernández R, et al. Haemodynamic effects of non-invasive ventilation in patients with obesity-hypoventilation syndrome. Respirology. 2012 Nov;17(8):1269–74.

184. Held M, Walthelm J, Baron S, Roth C, Jany B. Functional impact of pulmonary hypertension due to hypoventilation and changes under noninvasive ventilation. Eur Respir J. 2014 Jan;43(1):156–65.

185. Shorr AF, Helman DL, Davies DB, Nathan SD. Pulmonary hypertension in advanced sarcoidosis: epidemiology and clinical characteristics. Eur Respir J. 2005 May;25(5):783–8.

186. Boucly A, Cottin V, Nunes H, Jaïs X, Tazi A, Prévôt G, et al. Management and long-term outcomes of sarcoidosis-associated pulmonary hypertension. Eur Respir J. 2017 Oct;50(4).

187. Nunes H, Humbert M, Capron F, Brauner M, Sitbon O, Battesti J-P, et al. Pulmonary hypertension associated with sarcoidosis: mechanisms, haemodynamics and prognosis. Thorax. 2006 Jan;61(1):68–74.

188. Emirgil C, Sobol BJ, Herbert WH, Trout K. The lesser circulation in pulmonary fibrosis secondary to sarcoidosis and its relationship to respiratory function. Chest. 1971 Oct;60(4):371–8.

189. Damuth TE, Bower JS, Cho K, Dantzker DR. Major pulmonary artery stenosis causing pulmonary hypertension in sarcoidosis. Chest. 1980 Dec;78(6):888–91.

190. Portier F, Lerebours-Pigeonniere G, Thiberville L, Dominique S, Tayot J, Muir JF, et al. [Sarcoidosis simulating a pulmonary veno-occlusive disease]. Rev Mal Respir. 1991;8(1):101–2.

191. Hoffstein V, Ranganathan N, Mullen JB. Sarcoidosis simulating pulmonary veno-occlusive disease. Am Rev Respir Dis. 1986 Oct;134(4):809–11.

192. Preston IR, Klinger JR, Landzberg MJ, Houtchens J, Nelson D, Hill NS. Vasoresponsiveness of sarcoidosis-associated pulmonary hypertension. Chest. 2001 Sep;120(3):866–72.

193. Salazar A, Mañá J, Sala J, Landoni BR, Manresa F. Combined portal and pulmonary hypertension in sarcoidosis. Respiration. 1994;61(2):117–9.

194. Weatherald J, Savale L, Humbert M. Medical Management of Pulmonary Hypertension with Unclear and/or Multifactorial Mechanisms (Group 5): Is There a Role for Pulmonary Arterial Hypertension Medications? Curr Hypertens Rep. 2017 Oct;19(11):86.

195. Dauriat G, Mal H, Thabut G, Mornex J-F, Bertocchi M, Tronc F, et al. Lung transplantation for pulmonary langerhans' cell histiocytosis: a multicenter analysis. Transplantation. 2006

Mar;81(5):746–50.

196. Fartoukh M, Humbert M, Capron F, Maître S, Parent F, Le Gall C, et al. Severe pulmonary hypertension in histiocytosis X. Am J Respir Crit Care Med. 2000 Jan;161(1):216–23.

197. Hamada K, Teramoto S, Narita N, Yamada E, Teramoto K, Kobzik L. Pulmonary veno-occlusive disease in pulmonary Langerhans' cell granulomatosis. Eur Respir J. 2000 Feb;15(2):421–3.

198. Freitas CSG, Baldi BG, Jardim C, Araujo MS, Sobral JB, Heiden GI, et al. Pulmonary hypertension in lymphangioleiomyomatosis: prevalence, severity and the role of carbon monoxide diffusion capacity as a screening method. Orphanet J Rare Dis. 2017 Apr;12(1):74.

199. Launay D, Montani D, Hassoun PM, Cottin V, Le Pavec J, Clerson P, et al. Clinical phenotypes and survival of pre-capillary pulmonary hypertension in systemic sclerosis. PLoS One. 2018;13(5):e0197112.

200. Bax S, Bredy C, Kempny A, Dimopoulos K, Devaraj A, Walsh S, et al. A stepwise composite echocardiographic score predicts severe pulmonary hypertension in patients with interstitial lung disease. ERJ open Res. 2018 Apr;4(2).

201. Nathan SD, Cottin V. Pulmonary hypertension in patients with idiopathic pulmonary fibrosis [Internet]. Vol. 57, European Respiratory Monograph. 2011. p. 148–60. Available from: https://www.scopus.com/inward/record.uri?eid=2-s2.0-84865588568&doi=10.1183%2F1025448x.10019511&partnerID=40&md5=ba4bf8f4ae8752f05c3d621b3ab08be2

202. Weitzenblum E, Sautegeau A, Ehrhart M, Mammosser M, Pelletier A. Long-term oxygen therapy can reverse the progression of pulmonary hypertension in patients with chronic obstructive pulmonary disease. Am Rev Respir Dis. 1985 Apr;131(4):493–8.

203. Schönhofer B, Barchfeld T, Wenzel M, Köhler D. Long term effects of non-invasive mechanical ventilation on pulmonary haemodynamics in patients with chronic respiratory failure. Thorax. 2001 Jul;56(7):524–8.

204. Rao RS, Singh S, Sharma BB, Agarwal V V, Singh V. Sildenafil improves six-minute walk distance in chronic obstructive pulmonary disease: a randomised, double-blind, placebo-controlled trial. Indian J Chest Dis Allied Sci. 2011;53(2):81–5.

205. Hurdman J, Condliffe R, Elliot CA, Swift A, Rajaram S, Davies C, et al. Pulmonary hypertension in COPD: Results from the ASPIRE registry. Eur Respir J. 2013;41(6):1292–301.

206. Simonneau G, Escourrou P, Duroux P, Lockhart A. Inhibition of Hypoxic Pulmonary Vasoconstriction by Nifedipine. N Engl J Med [Internet]. 1981 Jun 25;304(26):1582–5. Available from: https://doi.org/10.1056/NEJM198106253042606

207. Barberà JA, Roger N, Roca J, Rovira I, Higenbottam TW, Rodriguez-Roisin R. Worsening of pulmonary gas exchange with nitric oxide inhalation in chronic obstructive pulmonary disease. Lancet. 1996;347(8999):436–40.

208. Chaumais MC, Perrin S, Sitbon O, Simonneau G, Humbert M, Montani D. Pharmacokinetic evaluation of sildenafil as a pulmonary hypertension treatment. Expert Opin Drug Metab Toxicol. 2013;9(9):1193–205.

209. Vitulo P, Stanziola A, Confalonieri M, Libertucci D, Oggionni T, Rottoli P, et al. Sildenafil in severe pulmonary hypertension associated with chronic obstructive pulmonary disease: A randomized controlled multicenter clinical trial. J Hear Lung Transplant. 2017;36(2):166–74.

210. Chen X, Tang S, Liu K, Li Q, Kong H, Zeng X, et al. Therapy in stable chronic obstructive

pulmonary disease patients with pulmonary hypertension: a systematic review and meta-analysis. J Thorac Dis. 2015 Mar;7(3):309–19.

211. Prins KW, Duval S, Markowitz J, Pritzker M, Thenappan T. Chronic use of PAH-specific therapy in World Health Organization Group III Pulmonary Hypertension: a systematic review and meta-analysis. Pulm Circ. 2017 Mar;7(1):145–55.

212. A Controlled Trial of Sildenafil in Advanced Idiopathic Pulmonary Fibrosis. N Engl J Med [Internet]. 2010 May 18;363(7):620–8. Available from: https://doi.org/10.1056/NEJMoa1002110

213. Kolb M, Raghu G, Wells AU, Behr J, Richeldi L, Schinzel B, et al. Nintedanib plus Sildenafil in Patients with Idiopathic Pulmonary Fibrosis. N Engl J Med. 2018 Nov;379(18):1722–31.

214. Valerio G, Bracciale P, Grazia D'Agostino A. Effect of bosentan upon pulmonary hypertension in chronic obstructive pulmonary disease. Ther Adv Respir Dis. 2009 Feb;3(1):15–21.

215. Boeck L, Tamm M, Grendelmeier P, Stolz D. Acute effects of aerosolized iloprost in COPD related pulmonary hypertension - a randomized controlled crossover trial. PLoS One. 2012;7(12):e52248.

216. Raghu G, Behr J, Brown KK, Egan JJ, Kawut SM, Flaherty KR, et al. Treatment of idiopathic pulmonary fibrosis with ambrisentan: a parallel, randomized trial. Ann Intern Med. 2013 May;158(9):641–9.

217. Nathan SD, Behr J, Collard HR, Cottin V, Hoeper MM, Martinez FJ, et al. Riociguat for idiopathic interstitial pneumonia-associated pulmonary hypertension (RISE-IIP): a randomised, placebo-controlled phase 2b study. Lancet Respir Med. 2019 Sep;7(9):780–90.

218. King TEJ, Brown KK, Raghu G, du Bois RM, Lynch DA, Martinez F, et al. BUILD-3: a randomized, controlled trial of bosentan in idiopathic pulmonary fibrosis. Am J Respir Crit Care Med. 2011 Jul;184(1):92–9.

219. Raghu G, Million-Rousseau R, Morganti A, Perchenet L, Behr J. Macitentan for the treatment of idiopathic pulmonary fibrosis: the randomised controlled MUSIC trial. Eur Respir J. 2013 Dec;42(6):1622–32.

220. Waxman A, Restrepo-Jaramillo R, Thenappan T, Ravichandran A, Engel P, Bajwa A, et al. Inhaled Treprostinil in Pulmonary Hypertension Due to Interstitial Lung Disease. N Engl J Med. 2021 Jan;384(4):325–34.

221. Baughman RP, Culver DA, Cordova FC, Padilla M, Gibson KF, Lower EE, et al. Bosentan for Sarcoidosis-Associated Pulmonary Hypertension: A Double-Blind Placebo Controlled Randomized Trial. Chest [Internet]. 2014;145(4):810–7. Available from: https://www.sciencedirect.com/science/article/pii/S0012369215359511

222. Le Pavec J, Lorillon G, Jaïs X, Tcherakian C, Feuillet S, Dorfmüller P, et al. Pulmonary Langerhans cell histiocytosis-associated pulmonary hypertension: clinical characteristics and impact of pulmonary arterial hypertension therapies. Chest. 2012 Nov;142(5):1150–7.

223. Coste F, Benlala I, Dournes G, Girodet PO, Laurent F, Berger P. Assessing pulmonary hypertension in COPD. Is there a role for computed tomography? Int J COPD. 2019;14:2065–79.

224. Kuriyama K, Gamsu G, Stern RG, Cann CE, Herfkens RJ, Brundage BH. CT-determined pulmonary artery diameters in predicting pulmonary hypertension. Invest Radiol. 1984;19(1):16–22.

225. Ando K, Kuraishi H, Nagaoka T, Tsutsumi T, Hoshika Y, Kimura T, et al. Potential Role of CT Metrics in Chronic Obstructive Pulmonary Disease with Pulmonary Hypertension. Lung. 2015 Dec;193(6):911–8.

226. Devaraj A, Wells AU, Meister MG, Corte TJ, Wort SJ, Hansell DM. Detection of pulmonary hypertension with multidetector CT and echocardiography alone and in combination. Radiology. 2010 Feb;254(2):609–16.

227. Chan AL, Juarez MM, Shelton DK, MacDonald T, Li C-S, Lin T-C, et al. Novel computed tomographic chest metrics to detect pulmonary hypertension. BMC Med Imaging. 2011 Mar;11:7.

228. Spruijt OA, Bogaard H-J, Heijmans MW, Lely RJ, van de Veerdonk MC, de Man FS, et al. Predicting pulmonary hypertension with standard computed tomography pulmonary angiography. Int J Cardiovasc Imaging [Internet]. 2015;31(4):871–9. Available from: https://doi.org/10.1007/s10554-015-0618-x

229. Huang Y-S, Hsu H-H, Chen J-Y, Tai M-H, Jaw F-S, Chang Y-C. Quantitative computed tomography of pulmonary emphysema and ventricular function in chronic obstructive pulmonary disease patients with pulmonary hypertension. Korean J Radiol. 2014;15(6):871–7.

230. Dournes G, Laurent F, Coste F, Dromer C, Blanchard E, Picard F, et al. Computed tomographic measurement of airway remodeling and emphysema in advanced chronic obstructive pulmonary disease. Correlation with pulmonary hypertension. Am J Respir Crit Care Med. 2015 Jan;191(1):63–70.

231. Matsuoka S, Washko GR, Yamashiro T, Estepar RSJ, Diaz A, Silverman EK, et al. Pulmonary hypertension and computed tomography measurement of small pulmonary vessels in severe emphysema. Am J Respir Crit Care Med. 2010;181(3):218–25.

232. Coste F, Dournes G, Dromer C, Blanchard E, Freund-Michel V, Girodet PO, et al. CT evaluation of small pulmonary vessels area in patients with COPD with severe pulmonary hypertension. Thorax. 2016;71(9):830–7.

233. Nardelli P, Jimenez-Carretero D, Bermejo-Pelaez D, Washko GR, Rahaghi FN, Ledesma-Carbayo MJ, et al. Pulmonary Artery-Vein Classification in CT Images Using Deep Learning. IEEE Trans Med Imaging. 2018 Nov;37(11):2428–40.

234. Washko GR, Nardelli P, Ash SY, Vegas Sanchez-Ferrero G, Rahaghi FN, Come CE, et al. Arterial Vascular Pruning, Right Ventricular Size, and Clinical Outcomes in Chronic Obstructive Pulmonary Disease. A Longitudinal Observational Study. Am J Respir Crit Care Med. 2019 Aug;200(4):454–61.

235. Rahaghi FN, Argemí G, Nardelli P, Domínguez-Fandos D, Arguis P, Peinado VI, et al. Pulmonary vascular density: comparison of findings on computed tomography imaging with histology. Eur Respir J. 2019 Aug;54(2).

236. Rahaghi FN, Winkler T, Kohli P, Nardelli P, Martí-Fuster B, Ross JC, et al. Quantification of the Pulmonary Vascular Response to Inhaled Nitric Oxide Using Noncontrast Computed Tomography Imaging. Vol. 12, Circulation. Cardiovascular imaging. 2019. p. e008338.

237. Kovacs G, Agusti A, Barberà JA, Celli B, Criner G, Humbert M, et al. Pulmonary Vascular Involvement in Chronic Obstructive Pulmonary Disease. Is There a Pulmonary Vascular Phenotype? Am J Respir Crit Care Med. 2018 Oct;198(8):1000–11.

238. Rahaghi FN, Wells JM, Come CE, De La Bruere IA, Bhatt SP, Ross JC, et al. Arterial and Venous Pulmonary Vascular Morphology and Their Relationship to Findings in Cardiac Magnetic

Resonance Imaging in Smokers. J Comput Assist Tomogr [Internet]. 2016;40(6). Available from: https://journals.lww.com/jcat/Fulltext/2016/11000/Arterial_and_Venous_Pulmonary_Vascular_Morphology.19.aspx

239. Johns CS, Rajaram S, Capener DA, Oram C, Elliot C, Condliffe R, et al. Non-invasive methods for estimating mPAP in COPD using cardiovascular magnetic resonance imaging. Eur Radiol. 2018 Apr;28(4):1438–48.

240. Wood P. The Eisenmenger Syndrome or Pulmonary Hypertension With Reversed Central Shunt. Br Med J. 1958;

241. Vongpatanasin W, Brickner ME, Hillis LD, Lange RA. The Eisenmenger syndrome in adults. Ann Intern Med. 1998 May;128(9):745–55.

242. Favoccia C, Constantine AH, Wort SJ, Dimopoulos K. Eisenmenger syndrome and other types of pulmonary arterial hypertension related to adult congenital heart disease. Expert Rev Cardiovasc Ther. 2019 Jun;17(6):449–59.

243. Diller G-P, Gatzoulis MA. Pulmonary vascular disease in adults with congenital heart disease. Circulation. 2007 Feb;115(8):1039–50.

244. Niro F, Garzillo G, Attina D, Lovato L, Galie N. Thoracic Manifestation of Eisenmenger ' s Syndrome in Adult Patients : A MDCT Review. 2015;173–81.

245. D'Alto M, Mahadevan VS. Pulmonary arterial hypertension associated with congenital heart disease. Eur Respir Rev an Off J Eur Respir Soc. 2012 Dec;21(126):328–37.

246. Nashat H, Brida M, Price LS, McCabe C, Alonso-Gonzalez R, Wort SJ, et al. Pulmonary Arterial Hypertension Complicating Congenital Heart Disease: Advances in Therapy. Semin Respir Crit Care Med. 2017 Oct;38(5):636–50.

247. Brida M, Nashat H, Gatzoulis MA. Pulmonary arterial hypertension: closing the gap in congenital heart disease. Curr Opin Pulm Med. 2020 Sep;26(5):422–8.

248. D'Alto M, Diller G-P. Pulmonary hypertension in adults with congenital heart disease and Eisenmenger syndrome: current advanced management strategies. Heart. 2014 Sep;100(17):1322–8.

249. Kidd L, Driscoll DJ, Gersony WM, Hayes CJ, Keane JF, O'Fallon WM, et al. Second natural history study of congenital heart defects. Results of treatment of patients with ventricular septal defects. Circulation. 1993 Feb;87(2 Suppl):I38-51.

250. Hopkins WE, Ochoa LL, Richardson GW, Trulock EP. Comparison of the hemodynamics and survival of adults with severe primary pulmonary hypertension or Eisenmenger syndrome. J Hear lung Transplant Off Publ Int Soc Hear Transplant. 1996 Jan;15(1 Pt 1):100–5.

251. Hopkins WE. The remarkable right ventricle of patients with Eisenmenger syndrome. Coron Artery Dis. 2005 Feb;16(1):19–25.

252. Kempny A, Hjortshøj CS, Gu H, Li W, Opotowsky AR, Landzberg MJ, et al. Predictors of Death in Contemporary Adult Patients With Eisenmenger Syndrome: A Multicenter Study. Circulation. 2017 Apr;135(15):1432–40.

253. Silversides CK, Granton JT, Konen E, Hart MA, Webb GD, Therrien J. Pulmonary thrombosis in adults with Eisenmenger syndrome. J Am Coll Cardiol. 2003 Dec;42(11):1982–7.

254. Perloff JK, Hart EM, Greaves SM, Miner PD, Child JS. Proximal pulmonary arterial and

intrapulmonary radiologic features of Eisenmenger syndrome and primary pulmonary hypertension. Am J Cardiol. 2003 Jul;92(2):182–7.

255. Martínez-Quintana E, Rodríguez-González F, Nieto-Lago V. Pulmonary artery aneurysmal dilatation in adult patients with congenital heart disease. World J Pediatr Congenit Heart Surg. 2011 Jul;2(3):375–9.

256. Reuben SR. Compliance of the human pulmonary arterial system in disease. Circ Res. 1971 Jul;29(1):40–50.

257. Silversides CK, Granton JT, Konen E, Hart MA, Webb GD, Therrien J. Pulmonary thrombosis in adults with Eisenmenger syndrome. J Am Coll Cardiol [Internet]. 2003 Dec 3 [cited 2018 Nov 15];42(11):1982–7. Available from: https://www.sciencedirect.com/science/article/pii/S0735109703012397#BIB9

258. Broberg CS, Ujita M, Prasad S, Li W, Rubens M, Bax BE, et al. Pulmonary Arterial Thrombosis in Eisenmenger Syndrome Is Associated With Biventricular Dysfunction and Decreased Pulmonary Flow Velocity. J Am Coll Cardiol [Internet]. 2007 Aug 14 [cited 2018 Nov 15];50(7):634–42. Available from: https://www.sciencedirect.com/science/article/pii/S0735109707016749?via%3Dihub#fig1

259. Griffin N, Allen D, Wort J, Rubens M, Padley S. Eisenmenger syndrome and idiopathic pulmonary arterial hypertension: do parenchymal lung changes reflect aetiology? Clin Radiol. 2007 Jun;62(6):587–95.

260. Remy-Jardin M, Duhamel A, Deken V, Bouaziz N, Dumont P, Remy J. Systemic collateral supply in patients with chronic thromboembolic and primary pulmonary hypertension: assessment with multi-detector row helical CT angiography. Radiology. 2005 Apr;235(1):274–81.

261. Peña E, Dennie C, Veinot J, Muñiz SH. Pulmonary hypertension: how the radiologist can help. Radiogr a Rev Publ Radiol Soc North Am Inc. 2012;32(1):9–32.

262. McKie SJ, Hardwick DJ, Reid JH, Murchison JT. Features of cardiac disease demonstrated on CT pulmonary angiography. Clin Radiol. 2005 Jan;60(1):31–8.

263. Devaraj A, Hansell DM. Computed tomography signs of pulmonary hypertension: old and new observations. Clin Radiol. 2009 Aug;64(8):751–60.

264. Okada F, Ando Y, Yoshitake S, Ono A, Tanoue S, Matsumoto S, et al. Clinical/pathologic correlations in 553 patients with primary centrilobular findings on high-resolution CT scan of the thorax. Chest. 2007 Dec;132(6):1939–48.

265. Philp T. Pulmonary artery calcification. Scott Med J. 1972 Mar;17(3):104–7.

266. Cohen BA, Gale JT, Mendelson DS, Mitty HA. Computer tomography demonstration of pulmonary artery calcification in Eisenmenger's syndrome. J Comput Tomogr. 1985 Apr;9(2):153–6.

267. RAJASURIYA K, MARKARMA, DE SILVA KM, RATNAIKE VT. Eisenmenger syndrome with radiological calcification of main pulmonary arteries. Postgrad Med J. 1963 Mar;39:155–7.

268. Steinberg I. Calcification of the pulmonary artery and enlargement of the right ventricle: a sign of congenital heart disease. Eisenmenger syndrome--pulmonary hypertension, increased pulmonary resistance, and reversal of blood flow. Am J Roentgenol Radium Ther Nucl Med. 1966 Oct;98(2):369–77.

269. Madhavan M V., Tarigopula M, Mintz GS, Maehara A, Stone GW, Généreux P. Coronary

Artery Calcification: Pathogenesis and Prognostic Implications. J Am Coll Cardiol [Internet]. 2014 May 6 [cited 2019 Aug 12];63(17):1703–14. Available from: https://www.sciencedirect.com/science/article/pii/S0735109714003283?via%3Dihub#bib32

270. Caramuru LH, Maeda NY, Bydlowski SP, Lopes AA. Age-dependent likelihood of in situ thrombosis in secondary pulmonary hypertension. Clin Appl Thromb Off J Int Acad Clin Appl Thromb. 2004 Jul;10(3):217–23.

271. Broberg CS, Ujita M, Prasad S, Li W, Rubens M, Bax BE, et al. Pulmonary arterial thrombosis in eisenmenger syndrome is associated with biventricular dysfunction and decreased pulmonary flow velocity. J Am Coll Cardiol. 2007 Aug;50(7):634–42.

272. Niwa K, Perloff JK, Bhuta SM, Laks H, Drinkwater DC, Child JS, et al. Structural abnormalities of great arterial walls in congenital heart disease: light and electron microscopic analyses. Circulation. 2001 Jan;103(3):393–400.

273. Mori H, Torii S, Kutyna M, Sakamoto A, Finn A V, Virmani R. Coronary Artery Calcification and its Progression: What Does it Really Mean? JACC Cardiovasc Imaging [Internet]. 2018;11(1):127–42. Available from: https://www.sciencedirect.com/science/article/pii/S1936878X1731001X

274. Akmal M, Barndt RR, Ansari AN, Mohler JG, Massry SG. Excess PTH in CRF induces pulmonary calcification, pulmonary hypertension and right ventricular hypertrophy. Kidney Int [Internet]. 1995;47(1):158–63. Available from: https://www.sciencedirect.com/science/article/pii/S0085253815587735

275. Block GA, Port FK. Re-evaluation of risks associated with hyperphosphatemia and hyperparathyroidism in dialysis patients: Recommendations for a change in management. Am J Kidney Dis [Internet]. 2000;35(6):1226–37. Available from: https://www.sciencedirect.com/science/article/pii/S0272638600700643

276. Bloodworth J, Tomashefski Jr JF. Localised pulmonary metastatic calcification associated with pulmonary artery obstruction. Thorax [Internet]. 1992 Mar;47(3):174–8. Available from: https://pubmed.ncbi.nlm.nih.gov/1519194

277. Kershaw LE, Naish JH, McGrath DM, Waterton JC, Parker GJM. Measurement of arterial plasma oxygenation in dynamic oxygen-enhanced MRI. Magn Reson Med. 2010 Dec;64(6):1838–42.

278. Giordano J, Khung S, Duhamel A, Hossein-Foucher C, Bellèvre D, Lamblin N, et al. Lung perfusion characteristics in pulmonary arterial hypertension (PAH) and peripheral forms of chronic thromboembolic pulmonary hypertension (pCTEPH): Dual-energy CT experience in 31 patients. Eur Radiol. 2017 Apr;27(4):1631–9.

279. Gopalan D, McCann C, Sheares K, Screaton N. Imaging in pulmonary hypertension, part 3: small vessel diseases. Postgrad Med J [Internet]. 2012 Jul 1;88(1041):397 LP – 406. Available from: http://pmj.bmj.com/content/88/1041/397.abstract

280. Skloot GS. The Effects of Aging on Lung Structure and Function. Clin Geriatr Med [Internet]. 2017;33(4):447–57. Available from: https://www.sciencedirect.com/science/article/pii/S0749069017300502

281. Sorino C, Battaglia S, Scichilone N, Pedone C, Antonelli-Incalzi R, Sherrill D, et al. Diagnosis of airway obstruction in the elderly: contribution of the SARA study. Int J Chron Obstruct Pulmon Dis. 2012;7:389–95.

282. Crapo RO, Morris AH. Standardized single breath normal values for carbon monoxide

diffusing capacity. Am Rev Respir Dis. 1981 Feb;123(2):185–9.

283. Georges R, Saumon G, Loiseau A. The relationship of age to pulmonary membrane conductance and capillary blood volume. Am Rev Respir Dis. 1978 Jun;117(6):1069–78.

284. Chang SC, Chang HI, Liu SY, Shiao GM, Perng RP. Effects of body position and age on membrane diffusing capacity and pulmonary capillary blood volume. Chest. 1992 Jul;102(1):139–42.

285. Butler C 2nd, Kleinerman J. Capillary density: alveolar diameter, a morphometric approach to ventilation and perfusion. Am Rev Respir Dis. 1970 Dec;102(6):886–94.

286. Gillooly M, Lamb D. Airspace size in lungs of lifelong non-smokers: effect of age and sex. Thorax. 1993 Jan;48(1):39–43.

287. Alabed S, Shahin Y, Garg P, Alandejani F, Johns CS, Lewis RA, et al. Cardiac-MRI Predicts Clinical Worsening and Mortality in Pulmonary Arterial Hypertension: A Systematic Review and Meta-Analysis. JACC Cardiovasc Imaging. 2021 May;14(5):931–42.

288. Jobst BJ, Triphan SMF, Sedlaczek O, Anjorin A, Kauczor HU, Biederer J, et al. Functional lung MRI in chronic obstructive pulmonary disease: comparison of T1 mapping, oxygen-enhanced T1 mapping and dynamic contrast enhanced perfusion. PLoS One. 2015;10(3):e0121520.

APPENDICES

i. Participant Information Sheet

Royal Brompton & Harefield NHS
NHS Foundation Trust

Participant Information Sheet (PIS)

Study Title:

Novel quantitative MRI measures in the assessment and follow- up of patients with Pulmonary Hypertension

Invitation to participate in the above study:

We would like to invite you to take part in a research study. Before you decide we would like you to understand why the research is being done and what it will involve for you. You are under no obligation to take part in the study and if you chose not to participate this will not affect your standard of care in any way. Please take time to read the following carefully and discuss it with others if you wish. We will go through the information sheet with you and answer any questions you have. We'd suggest this should take about 30 minutes.

Part 1 of the PIS tells you the purpose of this study and what will happen to you if you take part.

Part 2 gives you more detailed information about the conduct of the study.

Please ask us if there is anything that is not clear. Take time to decide whether you wish to take part.

What is the purpose of the study?

The purpose of the study is to investigate a new imaging technique using Magnetic Resonance Imaging (MRI) in patients with Pulmonary Hypertension (PH). We believe this technique may provide a new way to assess and follow-up patients with heart and lung disease without the need for radiation or dye (contrast) to be injected. We hope to show that it can be used to predict future response to treatment and for treatment monitoring. This in turn will hopefully save patient time, unnecessary side effects from costly therapies and improve the standard of care we can offer.

Why have I been invited?

You have been invited to participate as you have a confirmed diagnosis of PH. We are aiming to recruit 50 patients with this diagnosis.

Do I have to take part?

It is up to you to decide whether to take part. We will describe the study and go through this information sheet. If you do, you will be given this information sheet to keep and asked to sign a consent form. You are still free to withdraw at any time and without giving a reason. A decision to withdraw at any time or not take part will not affect the standard of care you receive.

What will happen to me if I take part?

You will be asked to have 2 research MRI scans in addition to the standard care you receive. These scans will take place on 2 separate occasions as listed below and each take up to 1 hour:

1. Before starting on treatment/ change to your treatment
2. 3-6 months after starting on treatment/ change to your treatment

The MRI scans will take place at the Royal Brompton MRI scanner in Wimpole Street, London. We will organise transport or reimburse travel costs. The scanning process will take up to 1 hour. During the scan you will be asked to lie on your back in the scanner and stay still whilst images are being taken. We will ask you to wear a mask through which you will be given oxygen to breathe at various points during the scan. You may be asked to perform short breath holding exercises. The scanner is more spacious than conventional ones. You will have headphones to wear to block out the noise of the scanner and can have a choice of music to listen to. We will communicate with you throughout the scan and be able to see you at all times so you can let us know if you are uncomfortable at any point during the scan or have any questions.

We will ask you to fill in a questionnaire about your experience following the ~~1st and 3rd~~ scans. This should only take a few minutes.

We plan to run the study over a 2 year time period. In addition to the images from your scans, we will also be looking at clinical data about you that is collected as standard from diagnosis to the end of the study period.

The only experimental parts of your care are the MRI scans which are in addition to standard care and will not affect your treatment.

Expenses and payments

We will cover the cost of transport to and from the MRI scanner for both scans.

What do I have to do?

The only additional requirements are attending the 2 MRI scans and completing the 2 questionnaires. You should continue any medication prescribed as usual.

If you are involved in any other studies please let us know.

What are the possible disadvantages and risks of taking part?
The risks are those associated with having an MRI scan. We will screen for these prior to recruitment using the NHS MRI safety questionnaire. If you have any of these risk factors, including pregnancy and claustrophobia, you will not be able to take part in the study.

What are the possible benefits of taking part?

The study will not have any immediate benefit for you but the information we get from this study may help improve the care of people with pulmonary hypertension in the future.

What happens when the research study stops?

Your treatment and follow-up will continue as per current guidelines.

What if there is a problem?

Any complaint about the way you have been dealt with will be addressed. The detailed information on this is given in part 2.

Will my taking part in the study be kept confidential?

Yes, we will follow ethical and legal practice and all information about you will be handled in confidence. The details are included in Part 2.

This completes Part 1. If the information in Part 1 has interested you and you are considering participation, please read the additional information in part 2 before making any decision.

Part 2

What will happen if I don't want to carry on with this study?

Your treatment and follow-up will continue as per current guidelines. When we consent you for the study, we will ask whether you are happy for any data captured until that time to be used.

What if there is a problem?

Complaints:

If you have a concern about any aspect of this study you should ask to speak with the researchers who will do their best to answer your questions on 07737978054. If you remain unhappy and wish to complain formally, you can do this. Details can be obtained from the Research Office (please contact Dr Jenny Rivers, Associate Director of Research, Royal Brompton and Harefield NHS Foundation Trust, Research Office, Sydney Street, SW3 6NP; Email: j.rivers@rbht.nhs.uk, Phone: 0207 352 8121 Ext. 2610) or via the hospital Patient and Advice Liaison Service (PALS).

Harm:

In the event that something goes wrong and you are harmed during the research and this is due to someone's negligence then you may have grounds for legal action for compensation against the study Sponsor, Royal Brompton and Harefield NHS Foundation Trust, but you may have to pay your legal costs.

The normal NHS complaints mechanism will still be available to you.

Will my taking part in the study be kept confidential?

All information that is collected about you during the course of the research will be kept strictly confidential. The clinical and questionnaire data will be added to a database, held on a networked drive at The Royal Brompton. All MRI studies will be link- anonymised and stored on The Royal Brompton's Picture Archiving and Communications System (PACS). MRI studies will be sent to our collaborators (Universitatspittal Basel and Bioxydyn Ltd) via the Image Exchange Portal (IEP) – in the same way that NHS studies are sent for review at other NHS hospitals. As your details are not entered onto the MRI console at the time of the research MRI (just a trial ID number), no identifiable information will leave the trust.

Universitatspittal Basel (based in Switzerland) and Bioxydny Ltd (a spin-off company from the University of Manchester) will receive the link anonymised MRI scans only and no identifiable information about you. They will delete the scans from their records at the end of the study period.

The report of your MRI may be shared with other members of your direct care team and if there are any unexpected findings we may need to organise further investigations and/or refer you on to another team. This will be discussed with you.

General Data Protection Regulation (GDPR)

Royal Brompton Hospital is the sponsor for this study based in the United Kingdom. We will be using information from you and your medical records in order to undertake this study and will act as the data controller for this study. This means that we are responsible for looking after your information and using it properly. Royal Brompton Hospital will keep identifiable information about you for up to 1 year after the study has finished.

Your rights to access, change or move your information are limited, as we need to manage your information in specific ways in order for the research to be reliable and accurate. If you withdraw from the study, we will keep the information about you that we have already obtained. To safeguard your rigts, we will use the minimum personally identifiable information possible.

You can find out more about how we use your information at https://www.hra.nhs.uk/information-about-patients or by contacting Dr Jenny Rivers (Associate Director of Research, Royal Brompton and Harefield NHS Foundation Trust, Research Office, Sydney Street, SW3 6NP; Email: j.rivers@rbht.nhs.uk, Phone: 0207 352 8121 Ext. 2610.

The Royal Brompton Hospital will keep your name, NHS number, contact details and any identifiable data confidential. The Royal Brompton will use this information to contact you about the research study, and make sure that relevant information about the study is recorded for your care, and to oversee the quality of the study. Individuals from Royal Brompton Hospital and regulatory organisations may look at your medical and research records to check the accuracy of the research study. The only people in Royal Brompton Hospital who will have access to information that identifies you will be people involved in your clinical care and facilitating this study or who need to audit the data collection process. The people who analyse the information will not be able to identify you and will not be able to find out your name, NHS number or contact details. If you are being recruited from Hammersmith Hospital, they will only retain data that would be kept as part of your routine clinical care.

Consenting to Future Research

With your consent (*no. 6 on consent form), the information collected about your health and care may be provided to researchers running other research studies in this organisation and in other organisations. These organisations may be universities, NHS organisations or companies involved in health and care research in this country or abroad. Your information will only be used by organisations and researchers to conduct research in accordance with the UK Policy Framework for Health and Social Care Research.

Your information could be used for research in any aspect of health or care and could be combined with information about you from other sources held by researchers, the NHS or government.

Where this information could identify you, the information will be held securely with strict arrangements about who can access the information. The information will only be used for the purpose of health and care research, or to contact you about future opportunities to participate in research. It will not be used to make decisions about future services available to you, such as insurance.

Where there is a risk that you can be identified your data will only be used in research that has been independently reviewed by an ethics committee.

What will happen to the results of the research study?

The results of the study may be published in scientific journals and presented at scientific meetings. If you would like us to, we will inform you of the outcome of the study in writing once it is complete. We will not use any identifiable data about you in any report/publication.

Who is organising and funding the research?

The study is being organised by the Pulmonary Hypertension and Radiology departments at the Royal Brompton Hospital. It is funded by a grant from the NIHR Imperial Biomedical Research Centre. There are no conflicts of interest.

Who has reviewed the study?

All research in the NHS is looked at by an independent group of people, called a Research Ethics Committee (REC), to protect your interests. This study has been reviewed and given favourable opinion by London- Bromley Research Ethics Committee (REC).

Thank you for taking the time to read this information sheet. Please let us know if you have any questions. If you agree to take part in this study you will be given a copy of this information sheet and a signed consent form to keep.

ii. Informed Consent Form

Royal Brompton & Harefield NHS
NHS Foundation Trust

Patient Identification Number for this trial: _____

INFORMED CONSENT FORM

Title: Novel Quantitative MRI Measures in the Assessment and Follow-up of Patients with Pulmonary Hypertension

Name of Researcher: Dr. S. Sathianandan, Royal Brompton Hospital

Please initial box

1. I confirm that I have read and understand the information sheet dated 25/02/2019 (Version 3) for the above study and have had the opportunity to consider the information, ask questions and have these answered satisfactorily. ☐

2. I understand that my participation is voluntary and that I am free to withdraw at any time, without giving any reason, without my medical care or legal rights being affected. ☐

   a) If I chose to withdraw at any time, I agree to any of my data collected up to that point in time being used for research. ☐

3. I understand that relevant sections of any of my medical notes and data collected during the study may be looked at by responsible individuals from Royal Brompton and Harefield NHS Foundation Trust. I give permission for these individuals to have access to my records. ☐

4. I consent to link-anonymised copies of my MRI scans being sent outside of the UK (to Universitatspittal Basel in Switzerland) for processing. ☐

5. I agree to take part in the above study. ☐

6. I agree to my data collected during this study being used for future research (as detailed in the information sheet). ☐

7. I would like a written summary of the results of this study to be sent to me at the end of the trial period. ☐

_____	_____	_____
Name of Patient	Date	Signature

Name of person taking consent	Date	Signature

When completed 1 for patient; 1 for researcher; 1 (original) to be kept with hospital notes.

iii. Patient Experience Questionnaire

Royal Brompton & Harefield NHS
NHS Foundation Trust

Oxygen – enhanced MRI Patient Experience Questionnaire:

Scan visit (please circle): 1 or 3

2) Did you experience any anxiety about the MRI scan?

	No	Some	A lot
Before			
During			
After			

If you were anxious, what were you anxious about?

2. **How did you find wearing the mask during the scan?**

Acceptable	A bit uncomfortable	Very uncomfortable

If uncomfortable, what in particular was uncomfortable?

3. How did you find the breath-holding exercises if you were asked to do them?

N/A	Acceptable	Difficult	Very difficult

4. Did you experience any discomfort during the scan?

No	Some	A lot

If yes, what was uncomfortable?

5. How did you find the length of the scan?

Acceptable	Too long	Much too long

If too long, what scan duration would you find acceptable (in minutes)?

6. How would you rate the overall scan experience?

0 1 2 3 4 5 6 7 8 9 10
Very Bad Neutral Very Good

Comments:

8. **Based on your experience of the scan, would you be happy to have it again?**

Yes	No

If yes, and this scan were to become part of routine care, would you be happy to have it?

	3-6 monthly	Yearly	Every 5 years
Yes			
No			

Thank you for taking the time to complete this questionnaire. Your feedback is very valuable.